

The ESO Public Surveys – Review of Milestones and Completion

Magda Arnaboldi¹
 Marina Rejkuba¹
 Jörg Retzlaff¹
 Nausicaa Delmotte¹
 Stephan Geier¹
 Reinhard Hanuschik¹
 Michael Hilker¹
 Wolfgang Hummel¹
 Gaiete Hussain¹
 Valentin D. Ivanov¹
 Alberto Micol¹
 Steffen Mieske¹
 Mark Neeser¹
 Monika Petr-Gotzens¹
 Thomas Szeifert¹

¹ ESO

In 2013 the eleven currently ongoing ESO public surveys successfully completed the submission and publication of their science data products via the ESO Science Archive Facility. An overview of the public survey projects in terms of telescope time allocation, observation progress and expected date of completion is presented. The science data products available in the ESO archive and their usage by the astronomical community are discussed with regard to the legacy value and scientific impact of these projects. This overview represents a natural introduction to the special section of the *Messenger* dedicated to the ESO public survey projects, in which the survey teams present their scientific aims and selected results in a series of dedicated articles.

Introduction

The ESO public surveys are very large programmes that last longer than two years and provide a legacy for the astronomical community at large. The start and implementation of the public surveys is linked to the operational deployment of the dedicated survey telescopes at ESO. The first suite of public survey programmes specifically designed for the VLT Infrared Survey Telescope for Astronomy (VISTA) and the VLT Survey Telescope (VST) started in 2010 and 2011, respectively, as these telescopes entered operations. With the successful start of

these imaging public surveys, ESO also initiated spectroscopic public surveys on two other telescopes at the La Silla Paranal Observatory.

The six near-infrared (NIR) imaging public surveys on VISTA (VHS, UltraVISTA, VIDEO, VVV, VMC and VIKING) and three optical imaging public surveys on VST (KiDS, VST ATLAS and VPHAS+) have strong synergies between their wavelength and area coverage (Arnaboldi et al., 2007). These projects range from shallow whole hemisphere – wide area – to deep pencil beam surveys, and their scientific drivers include a broad range of fundamental astrophysics topics, ranging from the nature of dark energy, the formation and evolution of galaxies, detailed studies of the structure of the Milky Way, to the universality of the stellar initial mass function. Two spectroscopic surveys started in 2012: the Gaia–ESO survey is devoted to the dynamics and chemical evolution of the Milky Way; the PESSTO survey investigates transient objects and, in particular, the physics of supernova explosions. For an overview of the scientific goals of the public surveys, their observing strategies and first results, readers are directed to the following contributions of the survey teams in this issue. (For the survey VISTA Variables in the *Via Lactea* [VVV], a half-way progress report will be presented in the next *Messenger* issue.)

The main difference between the public surveys and the other ESO observing programmes (in particular Large Programmes that may also have observations spanning several years) is that all raw data are immediately public and available worldwide through the ESO Science Archive Facility (SAF) and, even more importantly, the commitment made by the survey teams to deliver science data products and catalogues to ESO with yearly releases. The reduced and calibrated images and/or spectra, as well as catalogues listing physical properties of surveyed targets, are made available to the astronomical community through the SAF. In this article, we present the current status of the surveys and estimate the year of completion for the imaging public surveys that are carried out in service mode. The delivery and publication of data products through the SAF closes

the loop with the community and we present the current status of the Phase 3 delivery for the eleven public surveys. We conclude with an overview of the data downloaded by the community in terms of data volume and data product types.

Telescope time allocation to ESO public surveys

The VISTA surveys started after the end of the dry-run period on 1 April 2010. VISTA has a 4.1-metre diameter primary mirror and is equipped with a near infrared camera VIRCAM (VISTA InfraRed-CAMera) with a 1.65-degree diameter field of view (Emerson et al., 2006). The six VISTA public surveys are well into their fourth year of operation. The overall time allocations for these surveys are comparable, except for the VHS (VISTA Hemisphere Survey), which requires 3400 hrs for completion, according to its survey management plan. The VHS takes up 23% of the telescope time, while about 13% goes on each of the other surveys; in addition up to 5% of the time is allocated to Chilean and 5% to open-time programmes. Figure 1 shows a summary pie chart of the time allocation to the surveys and Chilean and open time as a percentage of the total available VISTA time.

The VST public surveys started on 15 October 2011 in service mode, following the successful commissioning of the VST on Paranal. The VST is a 2.6-metre modified Ritchey–Chrétien alt-azimuth telescope (Arnaboldi et al., 1998) equipped with a 1 × 1 degree optical imager

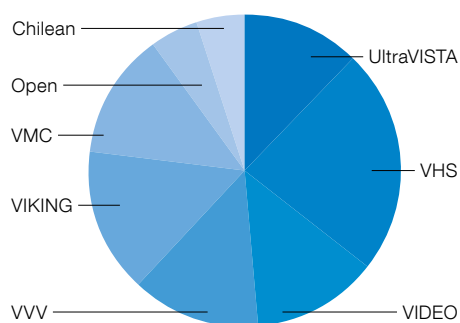


Figure 1. Pie chart showing the time allocation as a percentage of the total available time to the six imaging surveys and open time on VISTA.

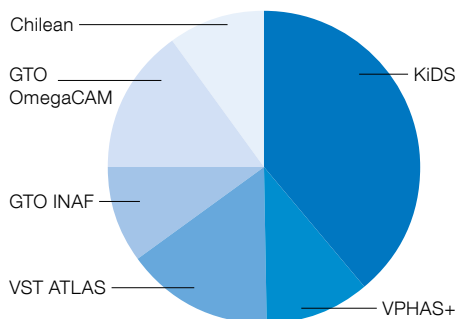


Figure 2. Pie chart showing the time allocation as percentage of the total available time for the VST.

OmegaCAM (Kuijken, 2011). An overview of OmegaCAM's scientific operations is given in Mieske et al. in this issue (p. 12). The VST surveys are starting their third year of operation. KiDS is the largest survey, requiring 3225 hrs to completion, or 39% of the time, followed by 15% for VST ATLAS and 11% for VPHAS+. The time allocated to Chilean programmes (10%), and Guaranteed Time Observations (GTO) of the OmegaCAM consortium (15%) and the Italian National Institute of Astrophysics (INAF; 10%) make up for a sizable fraction of the available telescope time, which has an important impact on the speed of completion. Figure 2 is a summary pie chart of the time allocation of the VST surveys as a percentage of the total available VST time for the public surveys, Chilean and GTO programmes.

The first spectroscopic public survey, the Gaia-ESO survey, started operation on

1 January 2012 on FLAMES at the VLT Unit Telescope 2 (Kueyen) on Paranal. The data acquisition for this survey is carried out in visitor mode and the time allocation of the survey entails 60 nights each year, for an overall assignment over four years initially, with another year pending a review of the survey progress and delivered data. Thus far 105 nights have been allocated to the Gaia-ESO survey. The PESSTO survey started operation on 1 April 2012, on EFOSC and SOFI at the New Technology Telescope (NTT) on La Silla. The data acquisition for this survey is also carried out in visitor mode. The time allocation for the survey includes 90 nights each year, with an allocation of 60/30 nights in odd and even periods respectively, for an overall assignment over four years, also with another year pending a successful review. Thus far 120 nights have been allocated to this project.

Progress and estimated completion time for imaging surveys

An integral part of the approval of public survey projects is the review of their survey management plans (SMPs), which outline the plans for telescope time allocation and observing constraints over the years. Additional information on quality control and pipeline data reduction, survey resource allocation for the survey execution (full-time equivalent [FTE] allocation), the timeline for the delivery and the description of the data products for

publication in the SAF are all part of the SMPs. Hence the SMPs have become the benchmark that is used to compute the progress of the public surveys and they represent the basis for estimating their completion time. In service mode, the basic observation unit is the observation block (OB) and the time charged to the programme is accounted for in terms of the number of successfully completed OBs. This includes the shutter open time (exposure time) and the relevant overheads provided in the execution time reporting module, which is part of the observation preparation software (P2PP3).

Successfully completed OBs are executed observations that fulfil the requested observing constraints according to stringent quality control (QC) criteria that are explained extensively elsewhere¹. Further information on the VST/OmegaCAM QC process, which was designed following the QC for VISTA/VIRCAM observations, is given in the article by Mieske et al. (p. 12). In the following, the fraction of the completion for a survey is computed as a fraction of the total execution time in hours for the completed OBs normalised by the total time in hours requested in the approved SMPs. The cumulative diagrams for the percentage of completion are shown in Figures 3 and 4 for the VISTA and VST surveys, respectively.

VISTA — The six VISTA surveys are progressing at a similar pace. As for any new telescope the start of VISTA operations required some adjustments. After

Figure 3. Graph of the percentage completion for the VISTA surveys as a function of date.

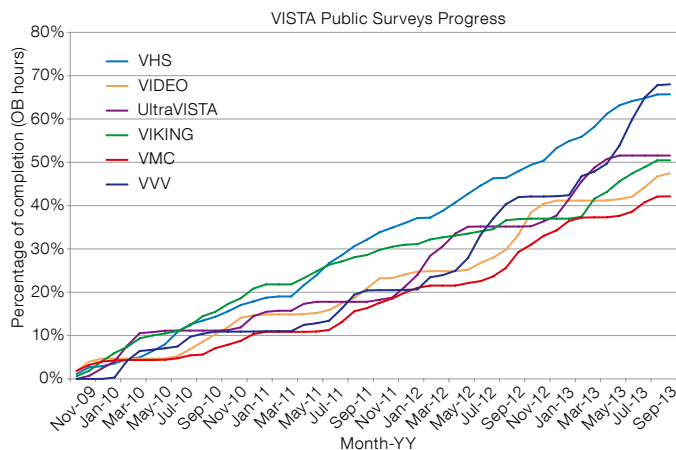
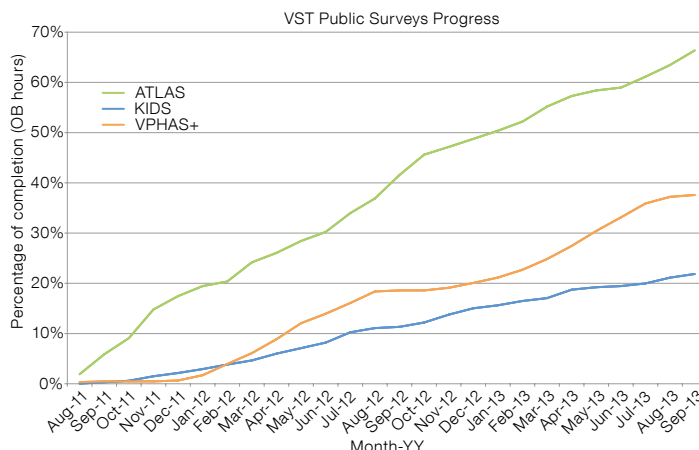


Figure 4. Graph of the percentage completion for the VST surveys as a function of date.



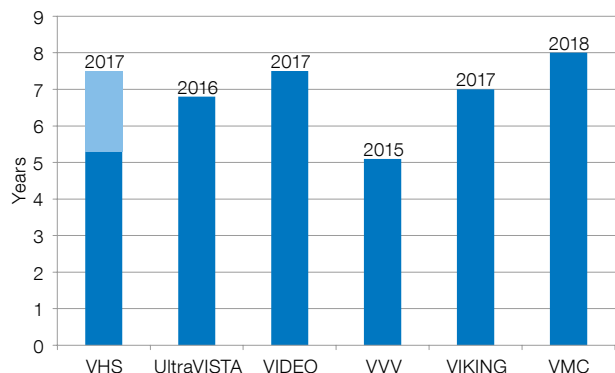


Figure 5. Expected completion time, in years and by year of completion, for the VISTA surveys. For VHS the time to completion for the whole area coverage is indicated in light blue. T = 0 refers to the start of scientific operations, i.e., April 2010.

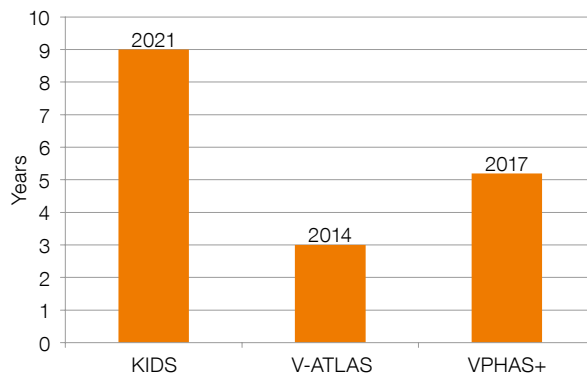


Figure 6. Expected completion time, in years and by year of completion, for the VST surveys. T = 0 refers to the start of scientific operations, i.e., October 2011.

major technical interventions in 2010 (camera shim installation and horizontal re-centring) and 2011 (primary and secondary mirror recoating and extended recovery), operational procedures were adopted to increase the speed of execution and reduce the number of repeated OBs. The current completion rate for the VVV and VHS surveys is more than 67%, while the percentage of completion is in the range 52% to 42% for the other surveys (UltraVISTA, VIKING, VIDEO and VMC).

VST — For the VST surveys, the percentages of completion are 66% for VST ATLAS, 22% for KiDS and 38% for VPHAS+. Of the three VST surveys, KiDS has the tightest requirements in terms of Moon illumination (dark time) and seeing constraints. It is also, by far, the largest survey on the VST and thus, even if it uses a comparable fraction of time per year to the other surveys, its overall completion is much smaller. Furthermore the right ascension/declination distribution of the target fields overlaps with those of approved GTO projects. Strategies are being implemented to mitigate the competition, and speed up the data acquisition for KiDS, and also improve the overall observation progress on the VST. For more details see Mieske et al. (p. 12).

Taking account of the above percentages of completion for each survey and the start of operation of each survey telescope, and assuming the same observation progress as previously, we can evaluate the date of completion for the VST

and VISTA surveys. Figures 5 and 6 show the expected completion time in years and the year of completion for the nine imaging surveys. We expect the VVV, VHS and VST ATLAS to be completed by 2015, with the other surveys coming to completion in the following years, with KiDS completed in 2021. For VHS, two numbers are shown in Figure 5: the completion in 2015 is based on the 3400 hours requested in the SMP, but since the overheads were not known at the time of writing the SMP, this survey will actually need about two years longer to cover the entire southern hemisphere, as shown by the light blue bar. It is important to point out that these projections do not automatically translate into telescope time allocated to these surveys. These estimates are upper limits since, as one survey finishes, the others may progress faster, which is not explicitly taken into account in the simple extrapolation above. The legacy value and the scientific excellence of the survey programmes are considered by the public survey panels organised by ESO and these completion dates are presented at major peer reviews. The public survey panels are

asked to issue informed recommendations on the continuation of survey programmes, or their termination, should they consider any of them not scientifically competitive at the time of the review.

[Publication and download of science data products from ESO public surveys](#)

The ESO policies in place to manage the public survey projects monitor the delivery of data products for ingestion and publication via the SAF. Additional allocation of telescope time is conditional on the submission of data products via Phase 3. Phase 3 concludes the process started with the submission of the letter of intent, followed by Phase 1 (proposal preparation and submission) and the preparation and submission of OBs for observations in service mode, i.e., Phase 2. As a result of Phase 3, the community can access and download the data products from the SAF and is able to carry out independent science projects in addition to those targeted by the survey teams (c.f., Arnaboldi et al., 2011).

Survey	Bands	Sky coverage* (sq.deg)	Data volume (GB)
VHS	YJHKs	4210	8511
VIKING	ZYJHKs	235	288
VVV	ZYJHKs	564	2877
VMC	YJKs	3.6	26
Ultra-VISTA	YJHKs	1.8	86
VIDEO	YJHKs	1.8	24
ATLAS	ugriz	2341	3015
VPHAS+	ugri, H α	375	747
KiDS	ugri	56	701

Table 1. Summary of VISTA and VST public survey products in the ESO science archive (Status: 25 October 2013).

*The quoted sky coverage is the total geometric area of images, which normally differs from the nominal survey area.

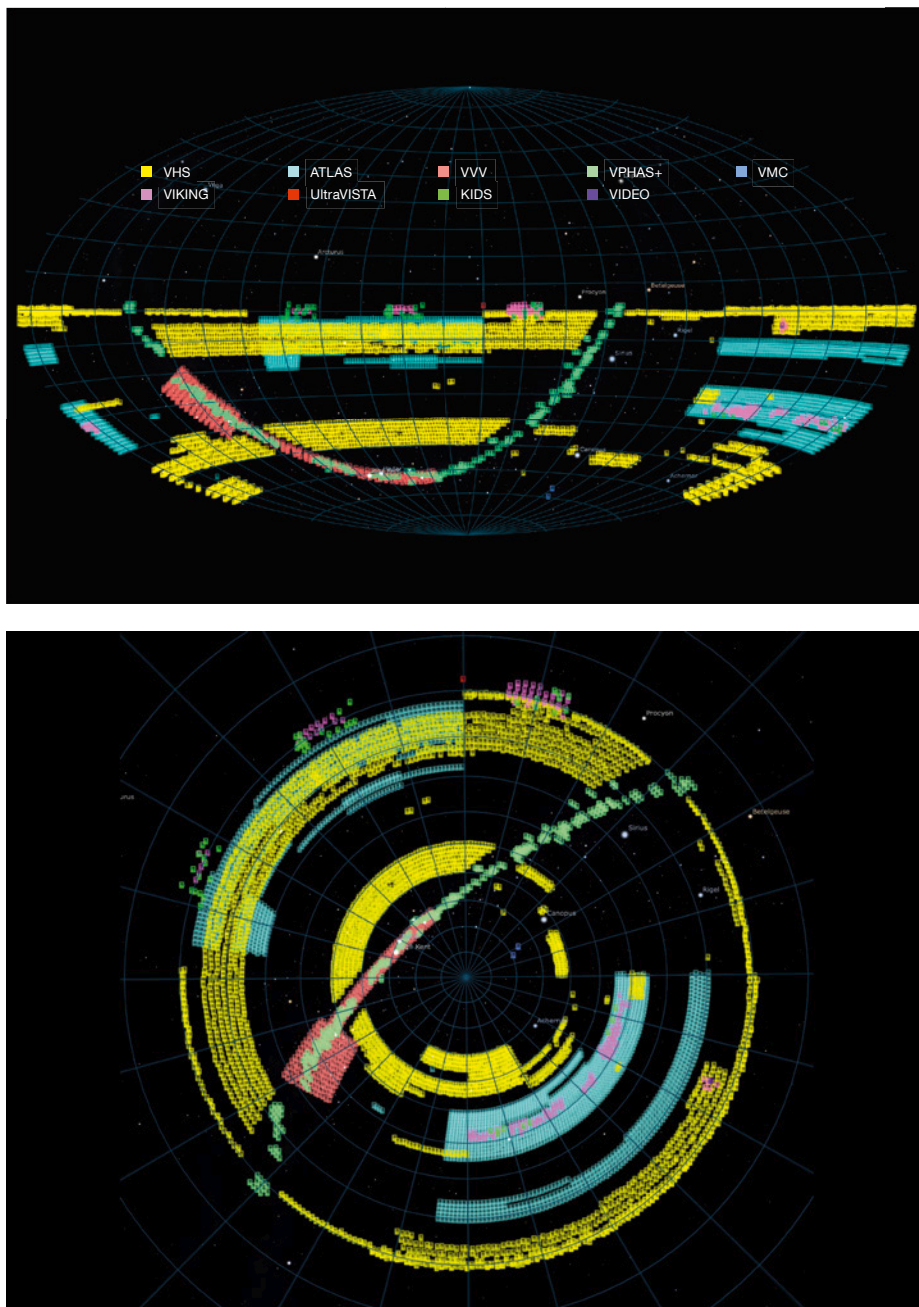


Figure 7. Sky coverage of ESO public survey products is shown in two projections. Upper: Full sky (Hammer–Aitoff projection); lower: Southern hemisphere (stereographic projection).

The year 2013 has been very important for Phase 3 activities, as all eleven ESO public surveys submitted and published their data products via the SAF. The milestones for Phase 3 were the second VISTA submission for images and source lists, and the first submission for cata-

logues. The first data release of the VST surveys was announced in September 2013. The spectroscopic public surveys are actively going through the process of content validation and it is planned that they will reach publication via the SAF by December 2013. Thus far, a total volume of 16 TB of data products — images, weight maps, source lists and catalogues — is now available and fully searchable via dedicated query interfaces. In Table 1 we provide an overview

of the data volume, wavelength and sky coverage of the data releases from the imaging surveys. Further information and detailed descriptions of the data releases from the ESO public surveys are available².

Public survey data are published through the ESO archive interfaces conjointly with other products such as the stream for the ultraviolet and visual echelle spectrograph (UVES) data that results from the in-house generation of science data products. All Phase 3 data products comply with the established standard for ESO science data products, thereby guaranteeing uniformity in terms of data format and characterisation across the ESO archive.

Figure 7 illustrates the current sky coverage of the ESO survey products in two projections. More than 4500 square degrees in the NIR bands and 2400 square degrees in the optical bands have been covered by data products, which are now accessible via the query interfaces of the SAF.

Merit parameters for ESO public surveys are the number of refereed publications by ESO survey teams and archive users, the number of press releases and the cumulative download of data products from the ESO archive. There are now 71 refereed publications from the survey teams with a significant increase in the number of refereed publications (+200%) since November 2012, including from four archive users, i.e., researchers who are not members of the survey teams. The contribution by Wegg & Gerhard (p. 54) is an example of exciting scientific results achieved using ESO archive data products (in this case from the VVV survey). There also are more than ten press releases based on VISTA data and more than four press releases for the VST.

The parameters on the data download by the community also demonstrate a strong interest. The cumulative download from the SAF since December 2011 amounts to more than 6.8 TB of data products and ~ 27 000 files. In Figures 8 and 9 these numbers are differentiated per survey project and data product type, respectively. The community is clearly eager to access the data, with the largest

volume download coming from VVV, UltraVISTA and KiDS; see Figure 8. The largest volume download for products is for the source lists, followed by the tile images. We believe that catalogues will represent very valuable assets, as they are the highest level products for the surveys. In this respect, we are working hard to reach a critical data volume soon, with the ingestion of the VIKING, VVV and VMC catalogues so that the community can benefit even more from the joint effort of ESO and the survey teams.

References

Arnaboldi, M. et al. 1998, *The Messenger*, 93, 30
 Arnaboldi, M. et al. 2007, *The Messenger*, 127, 28
 Arnaboldi, M. et al. 2011, *The Messenger*, 144, 17
 Emerson, J., McPherson, A. & Sutherland, W. 2006, *The Messenger*, 126, 41
 Kuijken, K. 2011, *The Messenger*, 146, 8

Links

¹ Quality control criteria: <http://www.eso.org/sci/observing/phase2/SMGGuidelines/ConstraintsSet.VIRCAM.html>
² Phase 3 data releases: http://www.eso.org/sci/observing/phase3/data_releases.html

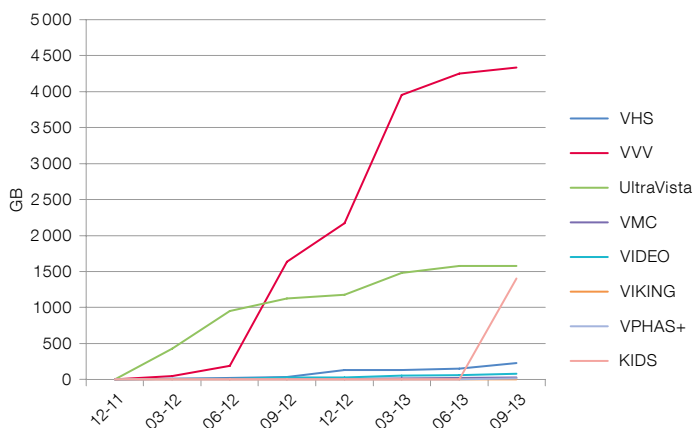


Figure 8. Data volume download for the imaging public surveys.

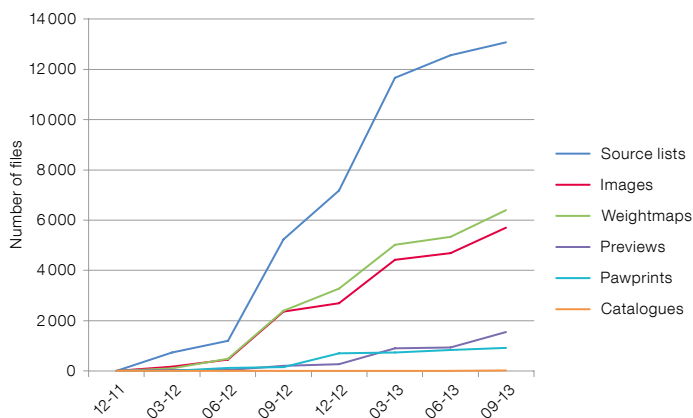


Figure 9. Number of files downloaded for the different data product types from the ESO SAF for the public imaging surveys.



The 2.6-metre VLT Survey Telescope (VST) is shown in its enclosure on Cerro Paranal. In the background are the nearby VLT Unit Telescopes 3 (Melipal, to the right) and 4 (Yepun, left).

The VMC ESO Public Survey

Maria-Rosa L. Cioni^{1,2}
 Peter Anders³
 Gemma Bagheri¹
 Kenji Bekki⁴
 Gisella Clementini⁵
 Jim Emerson⁶
 Chris J. Evans⁷
 Bi-Qing For⁴
 Richard de Grijs⁸
 Brad Gibson⁹
 Léo Girardi¹⁰
 Martin A. T. Groenewegen¹¹
 Roald Guandalini¹²
 Marco Gullieuszik¹⁰
 Valentin D. Ivanov¹³
 Devika Kamath¹²
 Marcella Marconi¹⁴
 Jean-Baptiste Marquette¹⁵
 Brent Miszalski¹⁶
 Ben Moore¹⁷
 Maria Ida Moretti¹⁴
 Tatiana Muraveva⁵
 Ralf Napiwotzki¹
 Joana M. Oliveira¹⁸
 Andrés E. Piatti¹⁹
 Vincenzo Ripepi¹⁴
 Krista Romita²⁰
 Stefano Rubele¹⁰
 Richard Sturm²¹
 Ben Tatton¹⁸
 Jacco Th. van Loon¹⁸
 Mark I. Wilkinson²²
 Peter R. Wood²³
 Simone Zaggia¹⁰

- ¹ University of Hertfordshire, United Kingdom
- ² Leibniz-Institut für Astrophysik Potsdam, Germany
- ³ National Astronomical Observatory of China, China
- ⁴ ICRAR, University of Western Australia, Australia
- ⁵ INAF, Osservatorio Astronomico di Bologna, Italy
- ⁶ Queen Mary University London, United Kingdom
- ⁷ Astronomy Technology Centre, Edinburgh, United Kingdom
- ⁸ Peking University, China
- ⁹ University of Central Lancashire, United Kingdom
- ¹⁰ INAF, Osservatorio Astronomico di Padova, Italy
- ¹¹ Royal Observatory of Belgium, Belgium
- ¹² Institute of Astronomy, KU Leuven, Belgium
- ¹³ ESO
- ¹⁴ INAF, Osservatorio Astronomico di Capodimonte, Italy
- ¹⁵ Institut d'Astrophysique de Paris, France
- ¹⁶ South African Astronomical Observatory, Cape Town, South Africa

- ¹⁷ University of Zurich, Switzerland
- ¹⁸ Lennard-Jones Laboratories, Keele University, United Kingdom
- ¹⁹ Observatorio Astronómico, Universidad Nacional de Córdoba, Argentina
- ²⁰ University of Florida, USA
- ²¹ Max-Planck-Institut für extraterrestrische Physik, Germany
- ²² University of Leicester, United Kingdom
- ²³ Australian National University, Australia

The VISTA near-infrared *YJKs* survey of the Magellanic Clouds system (VMC) has entered its core phase: about 50 % of the observations across the Large and Small Magellanic Clouds (LMC, SMC), the Magellanic Bridge and Stream have already been secured and the data are processed and analysed regularly. The initial analyses, concentrated on the first two completed tiles in the LMC (including 30 Doradus and the South Ecliptic Pole), show the superior quality of the data. The photometric depth of the VMC survey allows the derivation of the star formation history (SFH) with unprecedented quality compared to previous wide-area surveys, while reddening maps of high angular resolution are constructed using red clump stars. The multi-epoch *Ks*-band data reveal tight period–luminosity relations for variable stars and permit the measurement of accurate proper motions of the stellar populations. The VMC survey continues to acquire data that will address many issues in the field of star and galaxy evolution.

The VMC survey

The VMC survey observations are obtained with the infrared camera VIRCAM mounted on VISTA and reach stars down to a limiting magnitude of ~ 22 (5σ Vega) in the *YJKs* filters. The VMC strategy involves repeated observations of tiles across the Magellanic system, where one tile covers approximately uniformly an area of ~ 1.5 square degrees in a given band with three epochs at *Y* and *J*, and 12 epochs at *Ks* spread over a time range of one year or longer. Individual *Ks* epochs refer each to exposure times of 750 s and reach a limiting magnitude of ~ 19 for sources with photometric errors < 0.1 mag. The VMC data are acquired under homogeneous sky conditions, since observations take place in service mode, and their average quality corresponds to a full width at half maximum < 1 arcsecond. The VISTA astrometry, which is based on 2MASS, results in positional accuracies within 25 milliarcseconds (mas) across a tile. The VMC data are reduced with the VISTA Data Flow System (VDFS) pipeline and are archived

both at the VISTA Science Archive and at ESO. Further details about the VMC survey¹ are given in Cioni et al. (2011).

Stellar populations

One of the main goals of the VMC survey is the identification and characterisation of the mixture of stellar populations that have made up the Magellanic system over time. The star formation history of field stars, the physical parameters of stellar clusters, the links between these and the structure and dynamical processes are all embedded in the VMC data. Extracting a comprehensive picture of the system represents our major challenge, but fortunately we have access to sophisticated tools with which to do the job. In Rubele et al. (2012), we demonstrated that by using two colour–magnitude diagrams (CMDs) simultaneously, and a grid of models at various ages and metallicities, we could derive spatially resolved SFHs where systematic errors in the star formation rate and age–metallicity relations are reduced by a factor of two, relative to previous work, after accounting for the geometry of the galaxy. In our study we independently derive the mean extinction and distance modulus for twelve subsections of the original tiles.

In Figure 1 we show the CMD of a tile in the SMC including the Milky Way (MW) globular cluster 47 Tuc, highlighting the complexity of the SFH analysis in decomposing the different stellar populations. Using custom-derived point spread function photometry, we can push the sensitivity of the VMC data to highly crowded regions. Together with the wide area covered by VMC we will be able to investigate not only substructures in the LMC and SMC, but also streams attached to the 47 Tuc cluster, for example, as well as detecting the members of hundreds of stellar clusters in the Magellanic system waiting to be characterised.

The reddening map of the 30 Doradus field

Dust causes uncertainties in the measurements of the SFH and the structure of galaxies. Red clump stars ($0.8\text{--}2 M_{\odot}$ and $1\text{--}10$ Gyr old) are useful probes of interstellar reddening because of their large number and relatively fixed luminosity. Red clump stars belonging to the tile LMC 6_6 are selected from their location in the (*J*–*Ks*) vs. *Ks* CMD. Then, the amount of total reddening (along the line of sight and within the LMC) in terms of colour excess is obtained for each of $\sim 150\,000$ stars with respect to its intrinsic colour. The latter is derived accordingly from stellar evolution

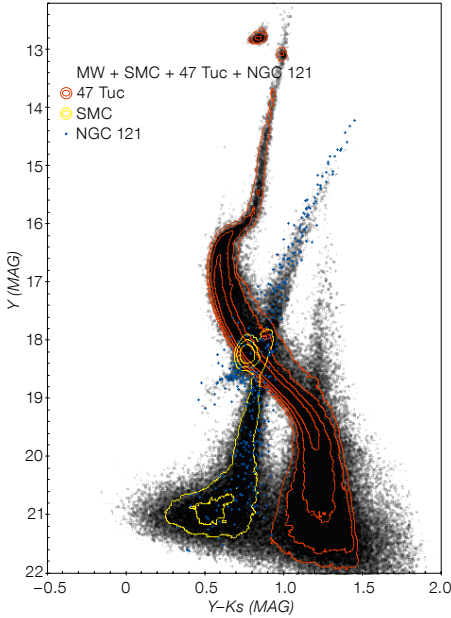


Figure 1. Colour–magnitude diagram of stellar sources in tile SMC 5_2. All sources are shown in grey; stars belonging to the SMC cluster NGC 121 are indicated in blue; the field population of the SMC is indicated with yellow contours; and the stars of the Milky Way cluster 47 Tuc are shown with red contours.

models, accounting for variations with age and metallicity. Extinction is subsequently converted into hydrogen gas column density. Compared to reddening maps produced using the same method at optical wavelengths, the near-infrared VMC data are more sensitive to higher extinction. Compared to $H\text{I}$ observations we derive that, on average, half of the stars lie in front of the $H\text{I}$ column and hydrogen becomes molecular in the dustiest clouds; the transition begins at $N_{H\text{I}} \approx 4 \times 10^{21} \text{ cm}^{-2}$. Figure 2 shows the location of molecular clouds superposed on the distribution of hydrogen column density inferred from the VMC data. There is overall agreement with maps of dust emission at $24 \mu\text{m}$ and $70 \mu\text{m}$ (see Tatton et al., 2013). Reddening maps will be created for other tiles in the VMC survey allowing red clump stars to be de-reddened; these results will be used in calculating the three-dimensional (3D) structure of the Magellanic system.

Variable stars

The other main goal of the VMC survey is the measurement of the 3D structure of the Magellanic system. Classical Cepheids are primary distance indicators and in the near-infrared obey period–luminosity (PL) relations

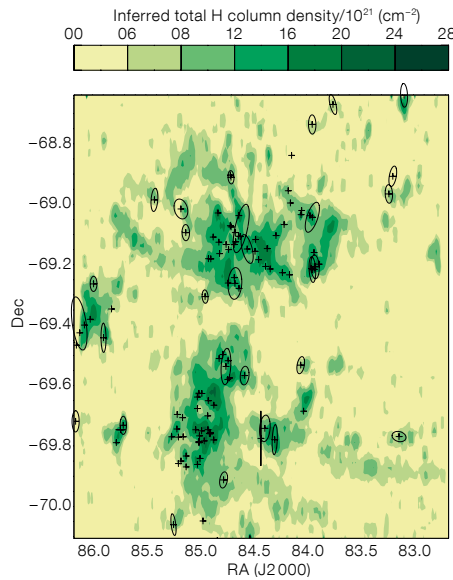


Figure 2. Hydrogen column density map inferred from VMC data in tile LMC 6_6 identifying regions where $N_{H\text{I}} > 8 \times 10^{21} \text{ cm}^{-2}$. Crosses represent molecular clouds catalogued in the literature and ellipses highlight those with measured properties.

that are less affected by reddening, chemical composition and nonlinearity than those at optical wavelengths, resulting in smaller intrinsic dispersion. First results for classical Cepheids in the tiles LMC 6_6 (Figure 3, left) and 8_8 have been presented in Ripepi et al. (2012). The identification of the variables is derived from the EROS-2 and OGLE-III catalogues and their VMC $K\text{s}$ light curves are very well sampled, with at least 12 epochs, and high precision, with typical errors of 0.01 mag, or better, for individual phase points. The $K\text{s}$ mag of the faintest Cepheids in the LMC, which are mostly first overtone pulsators, was measured for the first time thanks to the VMC observing strategy. Photometry for the brightest fundamental mode Cepheids (periods > 23 days), exceeding the linearity regime of VMC data, are taken from the literature. The dispersion of the PL relations is ~ 0.07 mag.

Anomalous Cepheids ($1.3\text{--}2.1 M_{\odot}$ and $[\text{Fe}/\text{H}] \approx -1.7$ dex) also play an important role both as distance indicators and stellar population tracers. The VMC survey has already observed many of the anomalous Cepheids discovered by the OGLE project in the LMC. These stars obey a tight PL relation in the $K\text{s}$ -band with a dispersion of 0.10 mag (Figure 3, right) that is shown for the first time in Ripepi et al. (2013).

Cepheids (< 200 Myr old) are mainly concentrated towards the bar and in a northwest

spiral arm of the LMC as well as in the central region of the SMC. Eclipsing binaries composed of main sequence stars trace a similar distribution, but with clustering mainly occurring in regions of recent star formation. On the other hand, RR Lyrae variable stars (> 10 Gyr old) are smoothly distributed and likely trace the haloes of the galaxies. These stars also follow a PL relation that is tight in the $K\text{s}$ -band. The VMC properties and the strategy to measure distances and infer the system 3D geometry of different age components from the variable stars is described in Moretti et al. (2013).

The magnitude of the brightest VMC objects ($10 < K\text{s} < 12$), which may be saturated in their central regions, is well recovered by the VDFS pipeline by integrating the flux in the outer parts. Most of these sources are asymptotic giant branch (AGB) stars. By fitting spectral energy distributions, created from the combination of VMC data and data at other wavelengths, with dust radiative transfer models, it is possible to derive mass-loss rates, luminosities and spectral classifications that offer strong constraints on AGB evolutionary models (Gullieuszik et al., 2012). These variable stars obey PL relations that may also be useful as distance and structure indicators.

The proper motion of the LMC

The astrometric accuracy and the photometric sensitivity of observations made with VISTA are of sufficient quality to select a large sample of targets and measure their proper motion. The proper motion of the LMC is measured from the combination of 2MASS and VMC data that span a time range of ~ 10 years and from VMC data alone across a time baseline of ~ 1 year (Cioni et al., 2013b). Different types of LMC stars (e.g., red giant branch, red clump and main sequence stars, as well as variable stars) are selected from their location in the $(J-K\text{s})$ vs. $K\text{s}$ CMD, and from lists of known objects, where MW foreground stars and background galaxies are also easily distinguished (Figure 4, left). The proper motion of $\sim 40\,000$ LMC stars in the tile, with respect to ~ 8000 background galaxies, is $\mu_{\alpha} \cos(\delta) = +2.20 \pm 0.06 \text{ mas yr}^{-1}$ and $\mu_{\delta} = 1.70 \pm 0.06 \text{ mas yr}^{-1}$. This value is in excellent agreement with previous ground-based measurements but our statistical uncertainties are a factor of three smaller and are directly comparable to uncertainties derived with the Hubble Space Telescope. The error budget is at present dominated by systematic uncertainties (a few mas yr^{-1}), but these will decrease due to the improved reduction of the VISTA data and the increase in the time baseline.

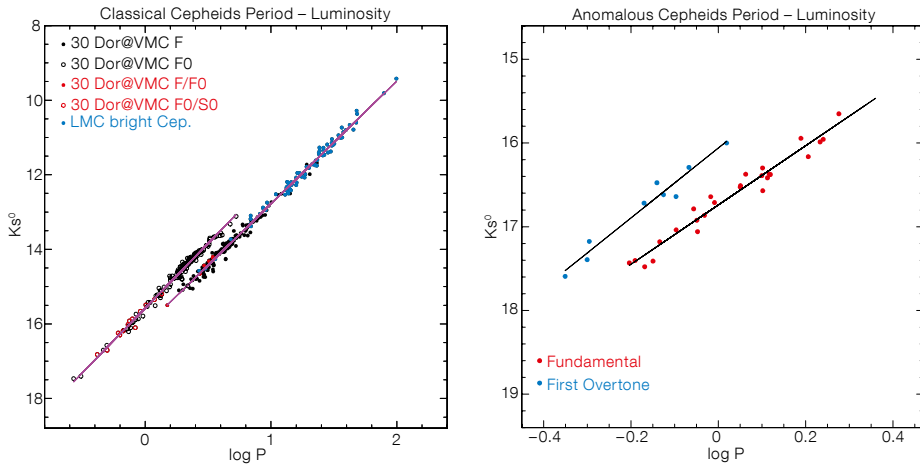


Figure 3. K_s -band period–luminosity relation for classical Cepheids in the 30 Dor field (left) and for LMC anomalous Cepheids (right). Fundamental and first overtone pulsators are indicated in blue and red respectively, and the solid lines are the result of least squares fits to the data.

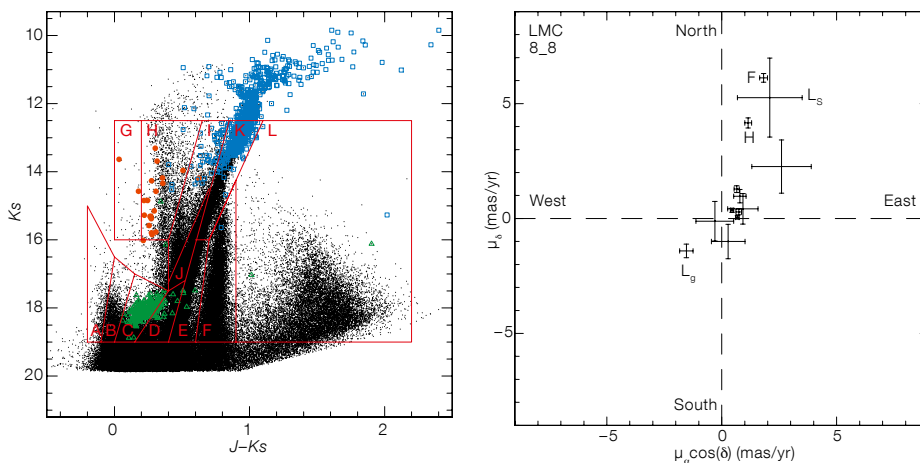


Figure 4. Left: Colour–magnitude diagram (CMD) of VMC sources in tile LMC 8_8. Region boundaries distinguish stars of different types. Colours highlight Cepheids (red), long period variables (blue) and RR Lyrae stars (green). Right: Proper motion derived from stars in each CMD region. Points corresponding to Milky Way stars (F, H and L_g) and to background galaxies (L_g) are indicated, while, for clarity, those corresponding to LMC stars are not labelled.

The mean proper motion of stars in each CMD region is shown in Figure 4 (right). The proper motions of LMC stars are clustered around zero except for region A, despite the large uncertainty. The proper motion of MW stars (regions F and H) is clearly distinct from those of LMC stars and background galaxies (region L_g). The latter refers to a sub-group of objects in region L with a galaxy-like morphology. Those with a stellar-like morphology are likely late-type MW dwarfs, since their proper motion value (L_g) is consistent with that of other MW stars. Using the best fitting model from Rubele et al. (2012) we can associate an age to each CMD region. We then measure a decrease of the proper motion with age where young stars stretch out to the northeast and old stars to the southwest. This difference is linked to both kinematic differences between young and old stars and to different hosting structures.

An alternative and established reference system is made of background quasars and hundreds of them have already been found behind the central regions of the Magellanic Clouds

as a result of spectroscopic observations of candidates identified from the OGLE light curves. The combination of VMC colours and K_s -band variability is also a valuable method to identify candidate quasars (Cioni et al., 2013a). The contamination by background galaxies, foreground late-type dwarf stars, young stellar objects and planetary nebulae, for which some nebular morphologies are revealed for the first time with VMC data (Miszalski et al., 2011), is reduced to $\sim 20\%$.

Perspective

The first years of observations have shown that the VMC data meet expectations and our understanding of the SFH across the Magellanic system will no longer be limited to small area observations. With the approaching completion of the SMC and Bridge areas it will be possible to start comparing theoretical predictions with observations on the age and metallicity distributions and their relations with the interaction between the LMC and SMC, the

formation of the Bridge and the existence of stripped stars. The VMC survey has a high legacy value and represents the sole counterpart in the K_s -band to current and future ground-based (STEP at the VST, SkyMapper, SMASH at the Blanco 4-metre, Large Synoptic Survey Telescope [LSST]) and space-based imaging missions (e.g., Gaia and Euclid) targeting or including the Magellanic system. It also provides a wealth of targets for wide-field spectroscopic follow-up investigations, e.g., with the Apache Point Observatory Galactic Evolution Experiment (APOGEE)-South, High Efficiency and Resolution Multi-Element Spectrograph (HERMES) at the Anglo-Australian Observatory, 4-metre Multi-Object Spectroscopic Telescope (4MOST) and Multi-Object Optical and Near-infrared Spectrograph (MOONS) at ESO.

References

Cioni, M.-R. L. et al. 2011, *A&A*, 527, A116, Paper I
 Cioni, M.-R. L. et al. 2013a, *A&A*, 549, A29, Paper VI
 Cioni, M.-R. L. et al. 2013b, *A&A*, accepted, Paper IX
 Gullieuszik, M. et al. 2012, *A&A*, 537, A105, Paper III
 Miszalski, B. et al. 2011, *A&A*, 531, A157, Paper II
 Moretti, M. I. et al. 2013, *A&A*, accepted, Paper X
 Ripepi, V. et al. 2012, *MNRAS*, 424, 1807, Paper V
 Ripepi, V. et al. 2013, *MNRAS*, accepted, Paper VIII
 Rubele, S. et al. 2012, *A&A*, 537, A106, Paper IV
 Tatton, B. et al. 2013, *A&A*, 554, A33, Paper VII

Links

¹ VMC survey: <http://star.herts.ac.uk/~mcioni/vmc/>

The VISTA Deep Extragalactic Observations (VIDEO) Survey

Matt J. Jarvis^{1,2}
 Boris Häußler^{1,3}
 Kim McAlpine²

¹ Astrophysics, Department of Physics, Oxford, United Kingdom

² Physics Department, University of the Western Cape, Bellville, South Africa

³ Centre for Astrophysics, Science & Technology Research Institute, University of Hertfordshire, Hatfield, United Kingdom

The VIDEO survey is designed to answer key questions regarding the formation and evolution of galaxies, in particular the role of accretion onto black holes and how galaxy evolution may vary depending on environment. VIDEO undertakes deep near-infrared imaging over three well-observed extragalactic fields allowing in-depth study of galaxy evolution over $1 < z < 4$, linking the shallower VST and VISTA surveys with the UltraVISTA survey. The area and depth of the VIDEO survey enables the detection of the bulk of the luminosity density arising from galaxies over 90% of the history of the Universe, as well as the most massive galaxies at all epochs and any associated accretion activity. A few scientific highlights from the early VIDEO data are provided.

How and when were massive galaxies formed?

When did they assemble the bulk of their stellar mass and how?

Where does this mass assembly occur?

These are the crucial questions that VIDEO is designed to answer.

VIDEO enables us to perform an in-depth study of the Universe over the redshift range $1 < z < 4$, linking the shallower surveys such as the VISTA Hemisphere Survey (VHS) and the VISTA Kilo-Degree Survey (VIKING; see de Jong et al. p. 44) with the deeper UltraVISTA survey (McCracken et al. p. 29). The depths of the VIDEO survey have been chosen to detect all “typical” elliptical galaxies out to redshifts of $z \sim 4$, and much fainter galaxies at around a tenth of the luminosity of a typical elliptical galaxy at $z \sim 1$, thereby enabling us to detect the bulk of the luminosity density arising from galaxies over 90% of the history of the Universe, and the most massive galaxies at the highest redshifts.

Thus we are able to investigate in exquisite detail which galaxies are in place first, and address the issue of downsizing in the mass function of forming galaxies, where the

massive early-type galaxies appear to be in place before the less massive galaxies.

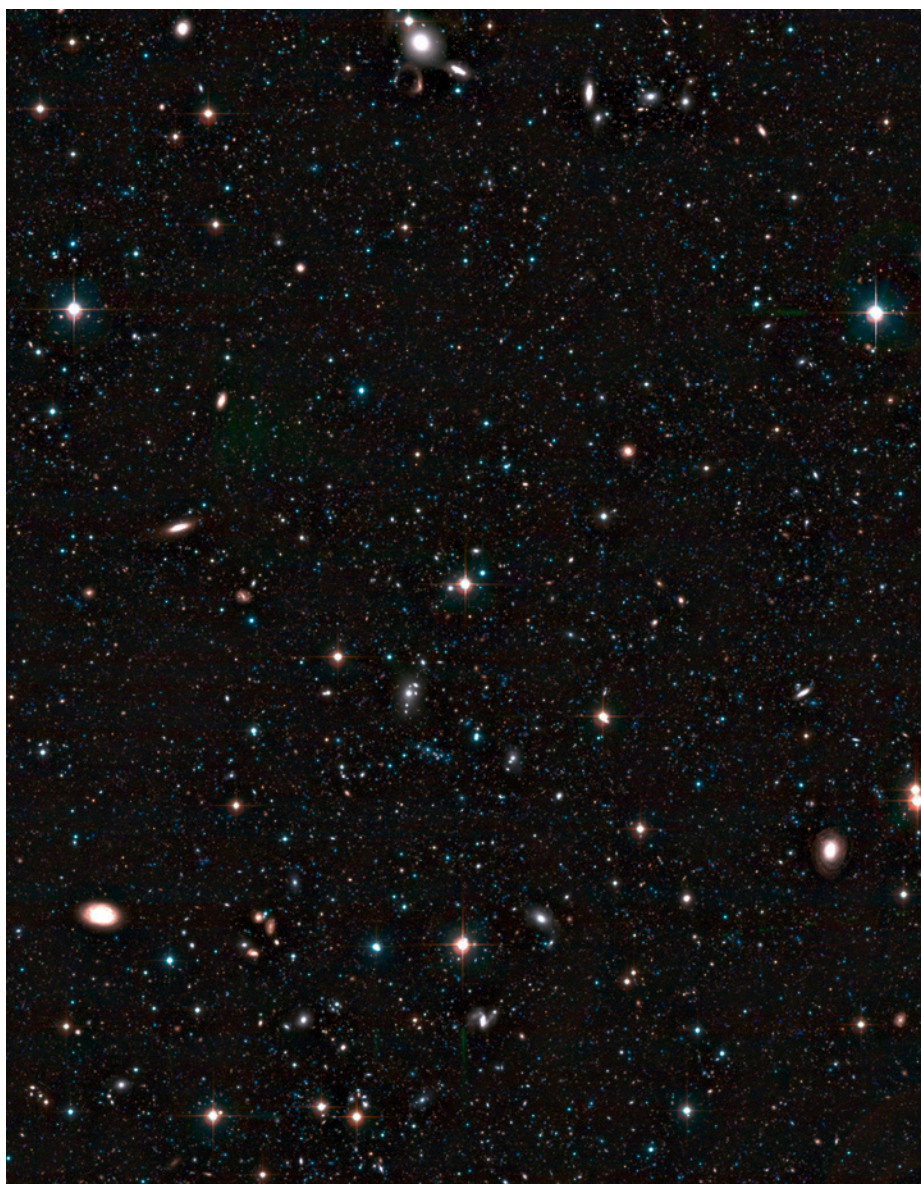
The epoch for which VIDEO is aimed is also a crucial one in the history of the Universe, as this is when the bulk of the star formation and accretion activity took place. VIDEO is therefore the ideal survey with which to investigate the effects that star formation and accretion activity have on galaxy evolution in general.

Moreover, the intrinsic rarity of the most luminous active, starburst and elliptical galaxies means that it is important to survey a large enough area, from which the luminosity function and clustering of particular galaxy populations can be measured. VIDEO covers

12 square degrees, improving on previous area-limited surveys that have measured the clustering of various galaxy populations to scales of < 0.5 degrees. Crucially, VIDEO will have sufficient area to carry out these investigations as a function of both redshift and environment.

VIDEO not only can detect the galaxies which contribute the bulk of the luminosity density at these redshifts, but the five near-infrared (NIR) filters, along with ancillary data from visible-wavelength surveys and the Spitzer Space

Figure 1. Colour image containing around 1/100 of the total 12 square degree area of the VIDEO field, centred on a region within the XMM-LSS field.



Telescope, will provide photometric redshifts for galaxies all the way out to $z \sim 6$ for the most massive galaxies.

Survey fields

The VIDEO survey is being carried out over three of the most widely observed high Galactic latitude fields: these are two VISTA tiles (3 square degrees) in the ELAIS-S1 field; three VISTA tiles (4.5 square degrees) in the XMM-Newton Large Scale Structure (XMM-LSS) field; and another three tiles in the extended Chandra Deep Field South. The total area covered is ~ 12 square degrees. A small fraction of the VIDEO survey data is shown in Figure 1. The three fields have a wealth of data from the X-ray through to the radio waveband, and are, along with COSMOS/Ultra-VISTA, the primary fields for observation with future facilities in the southern hemisphere.

Figure 1 in Jarvis et al. (2013) shows the footprint of the VIDEO observations in each of these three fields. The design of these positions was driven by the need to cover the wealth of ancillary data available in these fields, including Spitzer (e.g., Mauduit et al., 2012) and Herschel (Oliver et al., 2012), in addition to future ground-based optical data from both the VST and the Dark Energy Survey. Further in the future these areas will also be targeted with the deepest radio observations by the Square Kilometre Array precursor telescope MeerKAT (Jarvis, 2012) and also form part of the Large Synoptic Survey Telescope (LSST) deep drilling fields.

Photometric redshift accuracy

One of the key elements of the VIDEO survey is to provide the NIR data needed to obtain accurate photometric redshifts over all cosmic epochs, but particularly at $z > 1$, where the spectral break at 4000 \AA is redshifted beyond the visible wavelength window. These photometric redshifts underpin much of the science that is and will continue to be carried out with the VIDEO survey data. To show the accuracy to which we can measure photometric redshifts with VIDEO, we cross-match the publicly released deep-imaging data in the VIDEO-XMM3 field with the latest release of the VIMOS-VLT Deep Survey (VVDS) spectroscopic survey (Le Fevre et al., 2013) over the same region of sky. We select all of those spectroscopic sources with very secure spectroscopic redshifts and compare them with their photometric redshifts derived from the VIDEO photometry, combined with optical data from the Canada France Hawaii

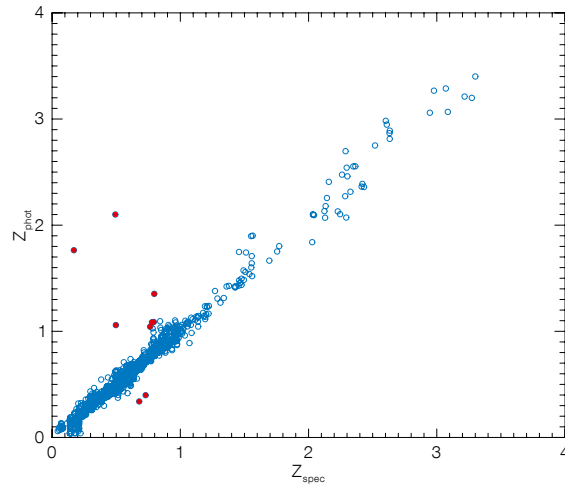
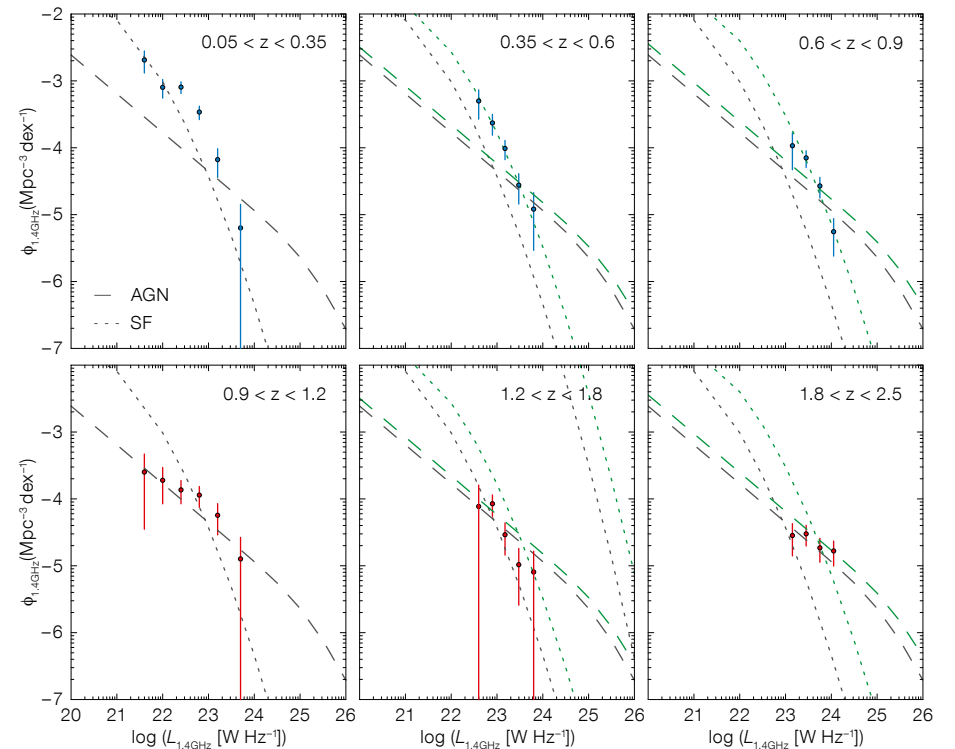


Figure 2. Photometric redshifts from VIDEO+CFHT data (z_{phot}) are plotted versus high-reliability spectroscopic redshifts (z_{spec}) from the VVDS spectroscopic survey. Filled red circles denote the nine sources classified as catastrophic outliers.



Telescope (CFHT), resulting in 1403 galaxies at $0 < z < 3.5$. By only using those sources that were classified as galaxies by the Le Phare photometric redshift code (Ilbert et al., 2006) we find that the normalised median absolute deviation of $(z_{\text{spec}} - z_{\text{phot}})/(1 + z_{\text{spec}})$ is 0.014 and the catastrophic outlier fraction, defined as $|z_{\text{spec}} - z_{\text{phot}}|/(1 + z_{\text{spec}}) > 0.15$, is just 0.65%. In Figure 2 we show the spectroscopic redshifts from the VVDS against the photometric redshifts from the VIDEO.

Figure 3. The star-forming (top panel — blue points) and active galactic nuclei (AGN; bottom panel — red points) radio luminosity function (RLF) in three redshift bins. Star-forming galaxies are identified as objects fitted by blue templates in the photometric redshift fitting procedure. The local luminosity function for star-forming galaxies and AGN from Mauch & Sadler (2007) are plotted as black dotted and dashed lines respectively. The green dotted line is the evolved RLF of star-forming galaxies and the green dashed line is the evolved RLF of AGN assuming the evolution parameters from McAlpine et al. (2013).

Disentangling low luminosity radio AGN from star-forming galaxies to $z \sim 2$

Over the past decade it has become clear that active galactic nuclei (AGN) may provide a critical feedback process that truncates star formation in massive galaxies. In particular, radio-loud AGN may provide an additional form of feedback via the mechanical deposition of energy resulting from jets. The predominantly low luminosity AGN, which are thought to be responsible for the bulk of mechanical feedback at $z < 1$, and are believed to be powered by inefficient accretion of hot gas, appear to inhabit gas-poor, quiescent massive galaxies. On the other hand the higher luminosity sources that are efficiently accreting cold gas tend to reside in similarly massive galaxies, but with indications of recent star formation activity. However, decoupling the low luminosity AGN activity from star formation activity at radio wavelengths can be challenging, due to the large overlap in radio luminosity between the lowest luminosity AGN and moderately star-forming galaxies. However, with deep optical imaging coupled with the NIR imaging provided by VIDEO, we may have an efficient method of tracing the evolution of these different populations.

McAlpine, Jarvis & Bonfield (2013) used a combination of visible imaging, NIR imaging from VIDEO and deep radio data from the Jansky Very Large Array to decouple the evolution of star-forming galaxies and AGN traced by radio emission. In Figure 3 we show the radio luminosity function in three redshift bins for galaxies classified as a) star-forming, and b) quiescent, based on their optical-NIR

spectral energy distributions. We can see that this split is consistent with the differential evolution of both populations with redshift, showing that it is possible to use multi-colour imaging data to categorise AGN and star-forming galaxies. Given the rarity of AGN and the most luminous star-forming galaxies, with the full VIDEO survey area we will have a unique dataset with which to answer the key questions on AGN evolution and its impact on galaxy evolution.

Additionally the area coverage of VIDEO allows us to study the environments of such AGN. In Karouzos, Jarvis & Bonfield (2013) we find that such radio sources tend to reside in environments of increased density with respect to a stellar-mass matched sample of elliptical galaxies. This in turn implies that the fuelling source for low luminosity radio sources may indeed come from the hot intracluster medium.

The high-redshift Universe

VIDEO is uniquely placed to quantify the density and spatial clustering of the most massive galaxies at the earliest epochs. Initial work on this topic by Willott et al. (2013) used VIDEO data to show that the bright end of the galaxy luminosity function at $z \sim 6$ follows an exponential decline and that these massive galaxies appear to be both larger and dustier than their fainter counterparts discovered in deep Hubble Space Telescope (HST) imaging. VIDEO data will be crucial in helping to pin down the luminosity function of high-redshift ($z > 6$) galaxies. Although much shallower than

the very deep NIR surveys conducted with the HST Wide Field Camera 3 (WFC3), the area is such that we can measure the shape of the bright end of the galaxy luminosity function within the epoch of reionisation and gain a full picture of the galaxy population at these high redshifts.

With the full VIDEO survey area we will be able carry out the first statistically significant clustering analysis of massive galaxies towards the epoch of reionisation, providing a direct link between the underlying dark matter distribution and galaxy populations and how this evolves up to the highest redshifts. The VIDEO survey will detect a factor of ~ 10 more $M > 10^{11} M_{\odot}$ galaxies than UltraVISTA at $z \sim 6$, as the limiting factor is area rather than depth.

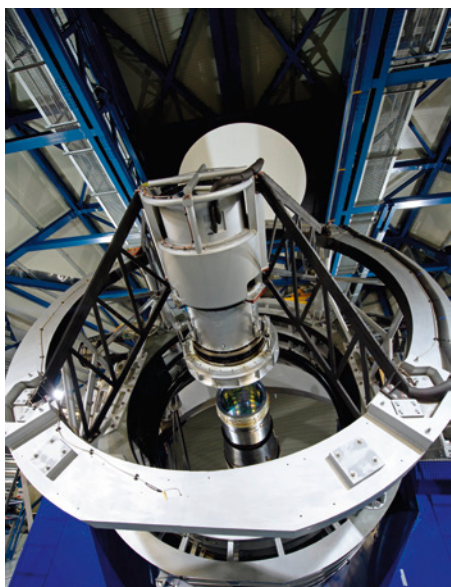
Acknowledgements

We would like to thank David Bonfield for the tremendous amount of work that he put in for the first few years of the VIDEO survey.

References

- Ilbert, O. et al. 2006, A&A, 457, 841
- Jarvis, M. J. 2012, African Skies, 16, 44
- Jarvis, M. J. et al. 2013, MNRAS, 428, 1281
- Karouzos, M., Jarvis, M. J. & Bonfield, D. G. 2013, MNRAS, submitted
- Le Fèvre, O. et al. 2013, A&A, 55, 14
- Mauch, T. & Sadler, E. M. 2007, MNRAS, 375, 931
- Mauduit, J.-C. et al. 2012, PASP, 124, 714
- McAlpine, K., Jarvis, M. J. & Bonfield, D. G. 2013, MNRAS, 436, 1084
- Oliver, S. et al. 2012, MNRAS, 424, 1614
- Willott, C. J. et al. 2013, AJ, 145, 4

ESO/C. Wehr



A view from the top of the VISTA telescope showing the secondary mirror assembly and the primary mirror. The dome screen for flat field illumination is seen at the rear.

UltraVISTA: A VISTA Public Survey of the Distant Universe

Henry J. McCracken¹
 Bo Milvang-Jensen²
 James Dunlop^{3*}
 Marijn Franx^{4*}
 Johan P. U. Fynbo^{2*}
 Olivier Le Fèvre^{5*}
 Joanna Holt⁴
 Karina I. Caputi^{3,6}
 Yuliana Goranova¹
 Fernando Buitrago³
 Jim Emerson⁷
 Wolfram Freudling³
 Olivier Herent¹
 Patrick Hudelot¹
 Carlos López-Sanjuan⁵
 Frédéric Magnard¹
 Adam Muzzin⁴
 Yannick Mellier¹
 Palle Møller⁸
 Kim K. Nilsson²
 Will Sutherland⁷
 Lidia Tasca⁵
 Johannes Zabl²

* co-PI

¹ Institut d'Astrophysique de Paris, UMR7095 CNRS, Université Pierre et Marie Curie, Paris, France

² Dark Cosmology Centre, Niels Bohr Institute, University of Copenhagen, Denmark

³ SUPA, Institute for Astronomy, University of Edinburgh, Royal Observatory, Edinburgh, United Kingdom

⁴ Leiden Observatory, Leiden University, the Netherlands

⁵ Laboratoire d'Astrophysique de Marseille, Aix-Marseille Université, France

⁶ Kapteyn Astronomical Institute, University of Groningen, the Netherlands

⁷ Astronomy Unit, School of Physics and Astronomy, Queen Mary University of London, United Kingdom

⁸ ESO

Large samples of distant galaxies covering degree-scale areas are an unparalleled source of information concerning the first sources that ionised the Universe and the origin of cosmic structures. The UltraVISTA public survey, using the unique capabilities of the VISTA telescope, aims to assemble a unique sample of remote, very high-redshift galaxies. The characteristics of the first UltraVISTA data release (DR1) and the upcoming DR2 data products are described. The DR1 data, comprising just a few months of observing time, already equals or exceeds in depth all previous wide-field near-infrared images taken on the COSMOS field in the last decade. The first scientific results from

UltraVISTA are presented, including new measurements of the high redshift ($z \sim 7$) galaxy luminosity function and an accurate determination of the type-dependent galaxy stellar mass function from $z \sim 0$ to $z \sim 4$. DR2 will reach one to two magnitudes deeper in all bands and provide our clearest picture of the structure and composition of the Universe at high redshifts.

Introducing UltraVISTA

In the last two decades, the utility of deep-field observations for extragalactic astrophysics has been conclusively demonstrated. These surveys, typically comprising effective exposure times totalling tens or hundreds of hours per pixel, have revolutionised our knowledge of the high-redshift Universe, leading to the detection and subsequent spectroscopic confirmation of significant numbers of high-redshift ($z \sim 3$) and very high-redshift ($z > 4$) objects. However, the largest ultra-deep fields probed by space-based observatories, whilst reaching very faint magnitude limits (typically $AB \sim 27$) using the Wide-Field Camera 3 on the Hubble Space Telescope typically have contiguous areas of only a few tens of arcminutes, leaving the region of parameter space comprising square degree angular coverage and moderate depth in near-infrared (NIR) wavelengths unexplored.

This combination of depth, wavelength and areal coverage is crucial for a number of reasons. Firstly, as the first structures in the Universe form at the peaks of the underlying dark matter density field, the numbers of objects at megaparsec scales will fluctuate significantly. Secondly, because the number densities of galaxies fall off exponentially at the bright end of the galaxy luminosity function, a wide-area survey is essential to yield a useful sample of high-redshift galaxies of sufficient brightness for spectroscopic follow-up with the current generation of large telescopes. Finally, this combination of depth and areal coverage will find large numbers of objects suitable for spectroscopic follow-up with the James Webb Space Telescope and the next generation of ground-based extremely large telescopes. The characterisation of these high-redshift, moderately bright objects is essential to understand the nature of the sources that re-ionised the Universe and which are the origin of the seeds of present-day large-scale structures.

The arrival of the VISTA telescope, and the prospect of a substantial time allocation for public surveys, prompted four independent responses to the initial call for VISTA surveys

of the very distant Universe, each capitalising on the strengths of VISTA and the excellent observing conditions at Paranal. Given the factor of three or four speed improvement with VIRCAM, compared to existing cameras such as WIRCAM (Canada France Hawaii Telescope [CFHT]) or WFCAM (United Kingdom Infra-Red Telescope), it became possible, for the first time, to think of a ground-based survey reaching to AB limiting magnitudes of 25–26 over ~ 0.9 square degrees in the time envelope allocated to VISTA surveys. These independent proposals were merged to form the UltraVISTA survey¹, which was subsequently allocated 1800 hours of telescope time. Survey operations started in December 2009. UltraVISTA lies in the COSMOS field (Scoville et al., 2007), where a rich data heritage means that a wealth of secondary science has been enabled by UltraVISTA observations.

The UltraVISTA project comprises two components: a deep survey covering the central 1.6 square degrees of COSMOS, and an ultra-deep part covering 0.9 square degrees in four parallel stripes, each of which is separated by one VIRCAM detector width. Observations are made in four broadband filters, Y , J , H , and K_s , as well as a narrowband filter. By blocking bright OH sky-lines, this narrowband (NB) filter enables the most extensive search to date for Lyman- α emitters at $z \sim 8.8$ (Milvang-Jensen et al. [2013] describe this filter in detail). In addition to Lyman- α emitters at very high redshift, the NB survey will detect hundreds of [O II]-emitters at $z = 2.2$ and thousands of H α emitters at $z \sim 0.8$. A dedicated survey using this filter only on the ultra-deep stripes has been incorporated into the UltraVISTA survey plan.

The projected AB depths at survey completion are ~ 25 (5σ for 2 arcseconds) for the deep part and ~ 26 for the ultra-deep part. As of the time of writing (October 2013), the deep survey has been largely completed, and around 40% of the ultra-deep survey has been finished. At this rate of progress, we expect the survey to be completed by around 2017.

UltraVISTA DR1: The first VISTA survey of the high-redshift Universe

The first UltraVISTA data release, DR1², which took place in February 2012, contains stacks created from data taken during approximately the first five months of survey operations (around 8000 images) and contains only deep survey data. As the survey's primary scientific objective relies on detecting objects several orders of magnitude fainter than the bright NIR sky, the principal processing challenge

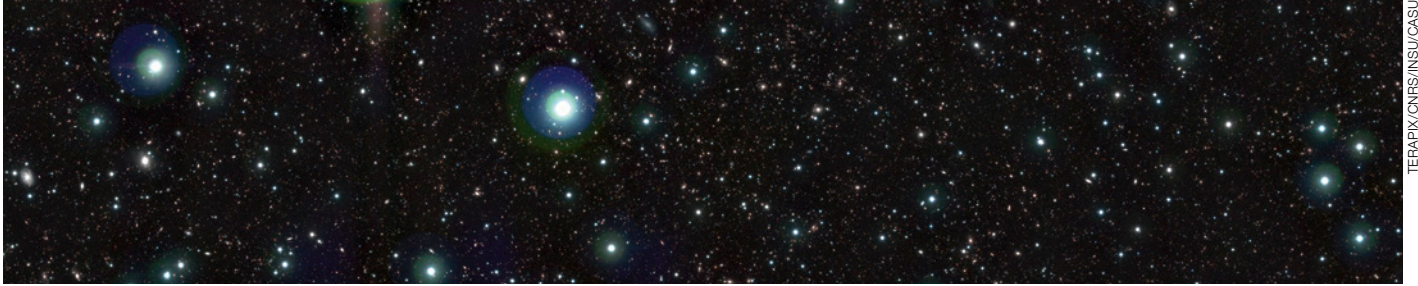


Figure 1. UltraVISTA DR2 ultra-deep image. This colour image comprises K_s , J , Y (RGB) stacks with an effective exposure time per pixel in each band of 82, 35 and 53 hours respectively.

involves an accurate and uniform sky-subtraction. To do this, we used the normal two-pass sky background subtraction method, starting from individual images pre-processed by the Cambridge Astronomy Survey Unit (CASU), adding back the already-subtracted sky, and using an object mask computed from the stacked image in each band to compute and subtract an individual sky frame for each of the 8000 images.

The same techniques have been applied to the upcoming DR2 release, containing almost 20 000 images. Such a computationally intensive technique was possible thanks to the use of the TERAPIX facility at the Institut Astrophysique de Paris. The advantage of this method is that the stacked images are extremely flat and uniform. They also bear testament to the excellent optical design of the VIRCAM camera and the high quality of the detector and amplifier chain (almost all remaining instrumental effects can be removed in software either at TERAPIX or CASU). Figure 1 shows a tiny area of one of the “deep stripes” observations from the upcoming DR2 release, where objects as faint as $K_s \sim 23$ AB mag are easily visible. This image is a colour composite of separate Y , J and K_s stacks.

DR1 images have appeared in an ESO press release³ and also featured prominently on Phil Plait’s well-known *Bad astronomy* blog⁴, attracting hundreds of comments. Catalogues extracted from these images were released by ESO as part of the DR1 Phase 3 catalogue release in September 2012². The processing steps used to create and validate these images and catalogues are described fully in McCracken et al. (2012).

The UltraVISTA DR1 represents a significant advance over previous NIR data in the COSMOS field. In only five months of operations, the depths in each of the broadband images meets or exceeds all previous

near-infrared images taken in COSMOS over the past ten years. In bluer wavebands (Y and J) it is more than two magnitudes deeper. This enhanced sensitivity in bluer wavelengths (and overall better NIR wavelength coverage) is one of the defining features of UltraVISTA compared to previous NIR surveys at this depth and areal coverage. It ensures that lower-redshift ($z \sim 2$) interlopers for high-redshift galaxies can be reliably rejected and that secure photometric redshifts at $z \sim 1-1.5$, free from systematic errors, can be computed. At the time of writing, it remains the deepest NIR survey of the sky on square-degree areas, and is likely to remain so for the foreseeable future. Thanks to queue-scheduled observations and stringent seeing control, all final stacked images have seeing better than 1 arcsecond full width at half maximum, with variation in seeing between the bands less than 20%, further limiting the impact of systematic photometric errors.

Mass assembly and the high-redshift galaxy luminosity function

Scientific exploitation of this first release has proceeded rapidly. Bowler et al. (2012), by

combining DR1 UltraVISTA images with multi-band data from the Subaru Observatory, the CFHT and the Spitzer Space Telescope, searched for UltraVISTA objects undetected in optical wavelengths and derived a new list of ten candidate high-redshift ($z > 6.5$) galaxies. Stacking the four most robust of these candidates, they derived a photometric redshift of $z \sim 7$ and (thanks to UltraVISTA Y and J data) show that low-redshift galaxy contaminants and T-dwarf star solutions are convincingly rejected. These are the first robust, bright very high-redshift galaxies discovered in COSMOS. This demonstrates also how future UltraVISTA data releases will place stringent limits on the bright-end slope of the high-redshift luminosity function (Figure 2).

The overall depths of the initial DR1 release precluded the discovery of significant numbers of high-redshift objects (although nevertheless demonstrating that our filter selection could reliably find such objects). However, for the redshift $z \sim 2$ population it represents a considerable advance over the existing COSMOS datasets, making possible the most precise assessment to date of the build-up in stellar mass in the Universe from $0 < z < 4$, and providing new constraints on the evolution

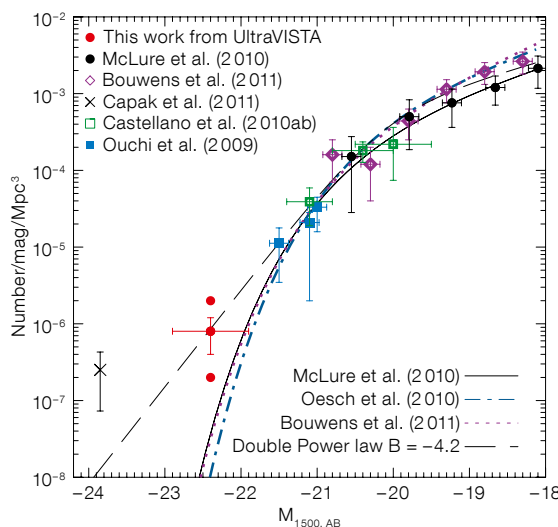


Figure 2. Ultraviolet $z \sim 7$ galaxy luminosity function (from Bowler et al., 2012). The red point shows UltraVISTA measurements if ten, four or one of the candidate objects are at $z \sim 7$. A literature compilation of similar measurements and Schechter function fits to fainter data is also shown.

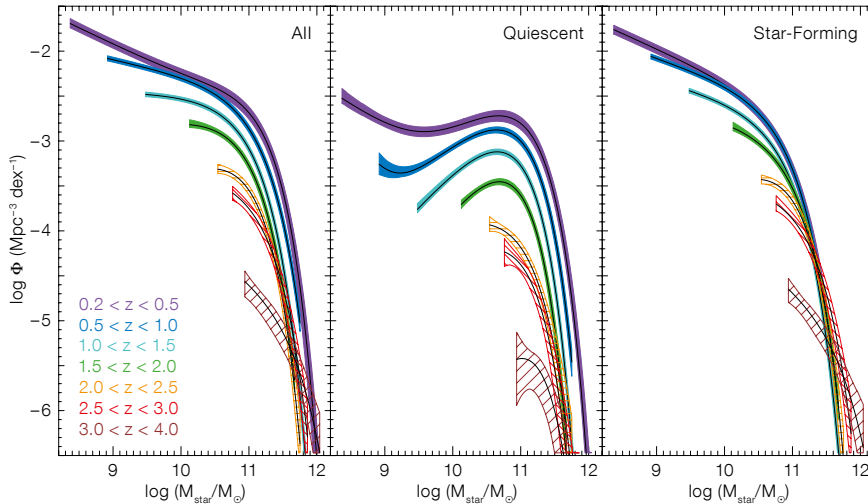


Figure 3. UltraVISTA galaxy stellar mass functions separated by star formation activity and redshift (colour-coded) are shown (from Muzzin et al., 2013).

of the faint-end slope of the mass function several magnitudes below M^* . In addition, the galaxy population can be separated into star-forming and non-star-forming (quiescent) objects, the first time that this has been possible over such a large redshift range. The uniquely rich spectral coverage of the COSMOS field (more than 25 bands) and large numbers of extremely difficult-to-acquire spectroscopic redshifts in the $1 < z < 2$ redshift range, means that we can compute the most accurate photometric redshifts to date over a wide redshift baseline with low numbers of catastrophic failures.

Two independent papers (Ilbert et al., 2013; Muzzin et al., 2013) derived UltraVISTA–COSMOS photometric redshifts and used them to compute how the amount of mass in stars per cubic megaparsec (the stellar mass function) evolves as a function of cosmic time and star formation activity (Figure 3). Both confirm that most of the evolution in the stellar mass function is driven by a rapidly changing population of quiescent galaxies and that this evolution is mass-dependent. Massive galaxies are already in place at early times and the amount of stellar mass in these systems evolves only slowly. In contrast, the rapid build-up of mass in quiescent galaxies in the lower redshift Universe seems to be the result of different physical processes, which stop star formation in more massive galaxies at higher redshifts and less massive galaxies at

lower redshifts. Furthermore, the cosmic evolution of the stellar mass density inferred from these measurements has now been shown to be consistent with the latest measurements of the evolution of the star formation rate (green shaded area in Figure 4). These photometric redshift catalogues and stellar mass measurements have been made publicly available⁵.

Further and deeper: UltraVISTA DR2

Today, DR2 data processing has been completed, and the forthcoming release will contain all data taken during the first three years of operations. The deep survey component remains approximately the same depth as DR1. The ultra-deep stripes, however, have much longer integration times (30–50 hrs per pixel) and now reach $K_s \sim 25$ AB mag (5σ , 2 arcsecond).

The UltraVISTA–COSMOS field remains unparalleled in wavelength coverage and in the next four years several supplementary datasets will enhance the unique legacy value of the UltraVISTA dataset. Ultra-deep Spitzer observations will extend current CH1 and CH2 observations by the Infrared Array Camera (IRAC) to AB ~ 25.5 mag (the SPLASH programme), enabling reliable stellar mass measurements at $z \sim 4$. In addition, in 2014 the COSMOS-UltraVISTA field will be observed by the Hyper-Suprime-Cam on Subaru, increasing depths in optical bands by one to two magnitudes. Coupled with the complete UltraVISTA dataset, this will provide an unparalleled picture of representative volumes of the high-redshift Universe until the advent of Euclid in 2020.

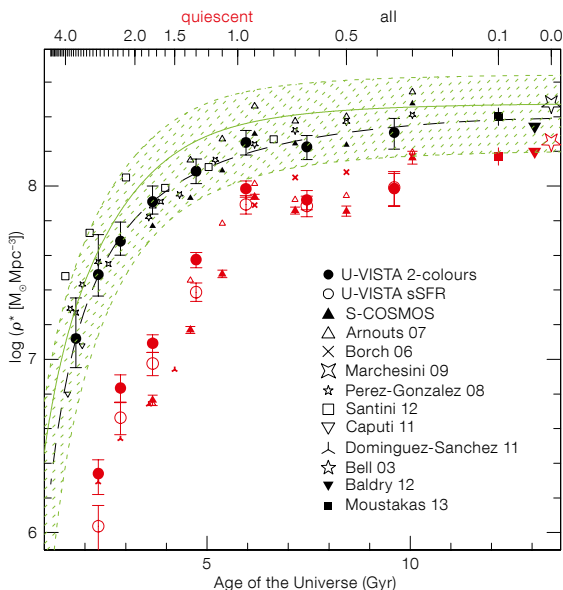


Figure 4. The total stellar mass density as a function of cosmic time as measured in UltraVISTA is shown (filled circles; from Ilbert et al., 2013) for all galaxies (in black) and for quiescent galaxies (in red). Other measurements from the literature are also shown.

References

- Bowler, R. A. A. et al. 2012, MNRAS, 426, 2772
- Ilbert, O. et al. 2013, A&A, 556, A55
- McCracken, H. J. et al. 2012, A&A, 544, A156
- Milvang-Jensen, B. et al. 2013, arXiv:1305.0262
- Muzzin, A. et al. 2013, ApJ, in press, arXiv:1303.4409
- Scoville, N. et al. 2007, ApJS, 172, 1

Links

- 1 UltraVISTA web page: <http://home.strw.leidenuniv.nl/~ultravista/>
- 2 UltraVISTA DR1 public release: http://www.eso.org/sci/observing/phase3/data_releases/ultravista_dr1.html
- 3 ESO Release 1213: <http://www.eso.org/public/news/eso1213/>
- 4 Phil Plait's Bad astronomy blog: http://www.slate.com/blogs/bad_astronomy.html
- 5 UltraVISTA catalogue availability: http://terapix.iap.fr/article.php?id_article=844

The VISTA Kilo-degree Infrared Galaxy (VIKING) Survey: Bridging the Gap between Low and High Redshift

Alastair Edge¹
 William Sutherland²
 Konrad Kuijken³
 Simon Driver^{4,5}
 Richard McMahon⁶
 Steve Eales⁷
 Jim P. Emerson²

¹ Department of Physics, University of Durham, United Kingdom

² Astronomy Unit, School of Physics and Astronomy, Queen Mary University of London, United Kingdom

³ Leiden Observatory, Leiden University, the Netherlands

⁴ ICRAR, University of Western Australia, Crawley, Australia

⁵ SUPA — School of Physics and Astronomy, University of St. Andrews, United Kingdom

⁶ Institute of Astronomy, University of Cambridge, United Kingdom

⁷ School of Physics and Astronomy, Cardiff University, United Kingdom

VIKING is a medium-deep survey of 1500 square degrees over two areas of the extra-galactic sky with VISTA in *zYJHKs* bands to sample the restframe optical for galaxies at $z \geq 1$. VIKING complements the two other surveys — VHS with its large area but shallower depth and VIDEO with its greater photometric depth and smaller spatial coverage. In addition to a $0.7 < z < 2$ galaxy survey, the area and depth of VIKING enables other studies, such as detection of distant quasars and low-mass stars and many galaxy clusters and superclusters. The early results are summarised and future prospects presented.

The remarkable improvement in the near-infrared survey speed that VISTA delivers offers the opportunity to study a volume of the distant ($z > 1$) Universe in the restframe optical bands that is many times larger than the Sloan Digital Sky Survey (SDSS). A survey of the full southern sky to reach a depth to detect an L^* galaxy requires more time than is available, but even a few percent of the available area is sufficient for the vast majority of projects.

It was with the goal of creating a legacy dataset with a wide range of science goals that we proposed the VISTA Kilo-degree Infrared Galaxy (VIKING) survey. In conjunction with its sister survey KiDS (Kilo-Degree Survey; Principal Investigator [PI]: K. Kuijken) on the VST, VIKING will cover 1500 square degrees in five bands (*z*, *Y*, *J*, *H* and *Ks*) to an AB depth of

23.1, 22.3, 22.1, 21.5 and 21.2 respectively. This combination of depth and area reaches our science goals for the $z > 1$ Universe and sits neatly between the VISTA Hemisphere Survey (VHS) and VIDEO surveys.

The VIKING survey area is split into two areas: an equatorial strip between right ascension 9 and 15.8 hours and 8 degrees wide; and a strip over the South Galactic Pole between right ascension 22 and 3.5 hours and 10 degrees wide. Our choice of survey area was made to maximise the overlap with existing multi-wavelength datasets that cover > 100 square degrees. The most prominent of these are the Galaxy And Mass Assembly (GAMA) survey (PIs: S. Driver and A. Hopkins) and the Herschel Astrophysical Terahertz Large Area Survey (H-ATLAS) (PIs: L. Dunne and S. Eales) covering over 148 and 360 square degrees of the VIKING area respectively.

Synergy with other surveys — GAMA, H-ATLAS and KiDS

The primary focus of GAMA science is on the combination of imaging and spectroscopy for $z < 0.2$ galaxies to determine the structure and evolution of galaxies over a wide range of mass and environment. The quality of the imaging data is particularly important in this context as the balance of bulge to disc in galaxies is key to our understanding of galaxy structure, but the stellar populations in the two components can differ significantly. Therefore, performing bulge–disc decomposition analysis at many different wavelengths can be used to constrain the evolution of the stellar population in the two components of the galaxy independently. To do this requires relatively deep photometry to constrain the lower surface brightness outer regions of the galaxy. Figure 1 illustrates the improvement in image quality going from the Two Micron All Sky Survey (2MASS), UKIRT InfraRed Deep Sky Surveys: Large Area Survey (UKIDSS LAS) to VIKING for a single galaxy (Andrews et al., 2013). The importance of depth to enhance the science potential in the lower-redshift Universe is just as significant as it is at higher redshift.

H-ATLAS represents the largest investment of time into any Herschel project and it has returned results from the lowest redshift (Burton et al., 2013) to lensed high-redshift galaxies (González-Nuevo et al., 2012). The dusty nature of far-infrared (FIR) selected galaxies means that it is particularly important to use near-infrared (NIR) imaging to identify these sources. Fleuren et al. (2012) find

counterparts in VIKING for at least 51% of all 250 μm sources and a substantially higher fraction of sources with FIR fluxes consistent with lower redshift. This fraction is 40% higher than equivalent matches in the optical *r*-band. The VIKING depth is sufficient to make a matched detection with at least the deepest band in the KiDS survey for any $z < 1$ galaxy. However, for more distant galaxies, particularly systems with a low specific star formation rate, then many will be too faint to be detected at the KiDS depth of 24 mag AB. Fortunately, for the equatorial strip, the Subaru Hyper SuprimeCam (HSC) Survey (PI: A. Miyazaki) will cover the same area to at least 1–1.5 mag deeper. This will allow for the selection of an unprecedentedly large sample of Extremely Red Objects (EROs; $[i-Ks]_{\text{AB}} > 2.45$) that are known to cluster very strongly (Kim et al., 2011) and also trace the most distant clusters of galaxies at $z > 1.6$ (Stanford et al., 2012).

QSO and low-mass star discrimination

The combination of deep optical data and moderately deep NIR data are particularly important when considering the selection of the most distant quasars and the lowest-mass stars. The discovery of the first $z > 7$ quasar (QSO) from the UKIDSS LAS by Mortlock et al. (2011) demonstrated the potential of NIR selection to push back the detection of the most distant active galactic nuclei (AGN), with all the associated insights they provide on the reionisation of the Universe. The combination of depth and area makes VIKING very well suited to the selection of $z > 6.4$ QSOs that fall beyond the grasp of silicon detectors in the optical. Venemans et al. (2013) have amply demonstrated this by the selection of the second, third and fourth most distant QSOs at $z = 6.89$, 6.75 and 6.61 respectively (see Figure 2). The selection of these three QSOs from the first 300 square degrees of the VIKING area required a significant investment of ESO New Technology Telescope (NTT) follow-up time to remove the contamination of low-mass stars and dusty, lower-redshift galaxies, as the KiDS survey had not started in 2011. Now that KiDS has covered the same area as VIKING, this additional screening is not required, so future target selection will be significantly faster. Venemans et al. (2013) predict the discovery of ~ 20 QSOs at $6.44 < z < 7.44$, so the prospects for future constraints on the evolution of QSOs into the epoch of reionisation are very promising.

At the opposite extreme, VIKING offers an excellent combination of bands to select low-mass stars. The differentiation between

low-mass stars and distant QSO candidates in (Z-Y) vs. (Y-J) colour space means that VIKING data can make a clean selection of L- and T-dwarfs. Adding in Wide-Field Infrared Survey Explorer (WISE) photometry and KiDS/HSC *i*-band data, means that VIKING will recover a significant number of these stars, allowing constraints on their scale height given the range of Galactic latitude and longitude covered by VIKING.

Galaxy and cluster surveys

The bulk of the galaxies detected in VIKING will be at redshifts of 0.7 to 2.0. The volume sampled between these two limits is $\sim 20 \text{ Gpc}^3$ which is nearly an order of magnitude larger than that of the SDSS DR10 within $z < 0.3$. Therefore rare objects such as clusters and superclusters will be recovered in large numbers. Given the overlap with Sunyaev-

Zel'dovich surveys such as the Atacama Cosmology Telescope (ACT; Marriage et al., 2011) and the substantial increase in X-ray survey depth provided by eROSITA (Predehl et al., 2009), VIKING will provide an important resource for the confirmation of cluster candidates from other techniques, as well as providing clusters selected from their member galaxies alone. The selection of more distant clusters is of particular importance when

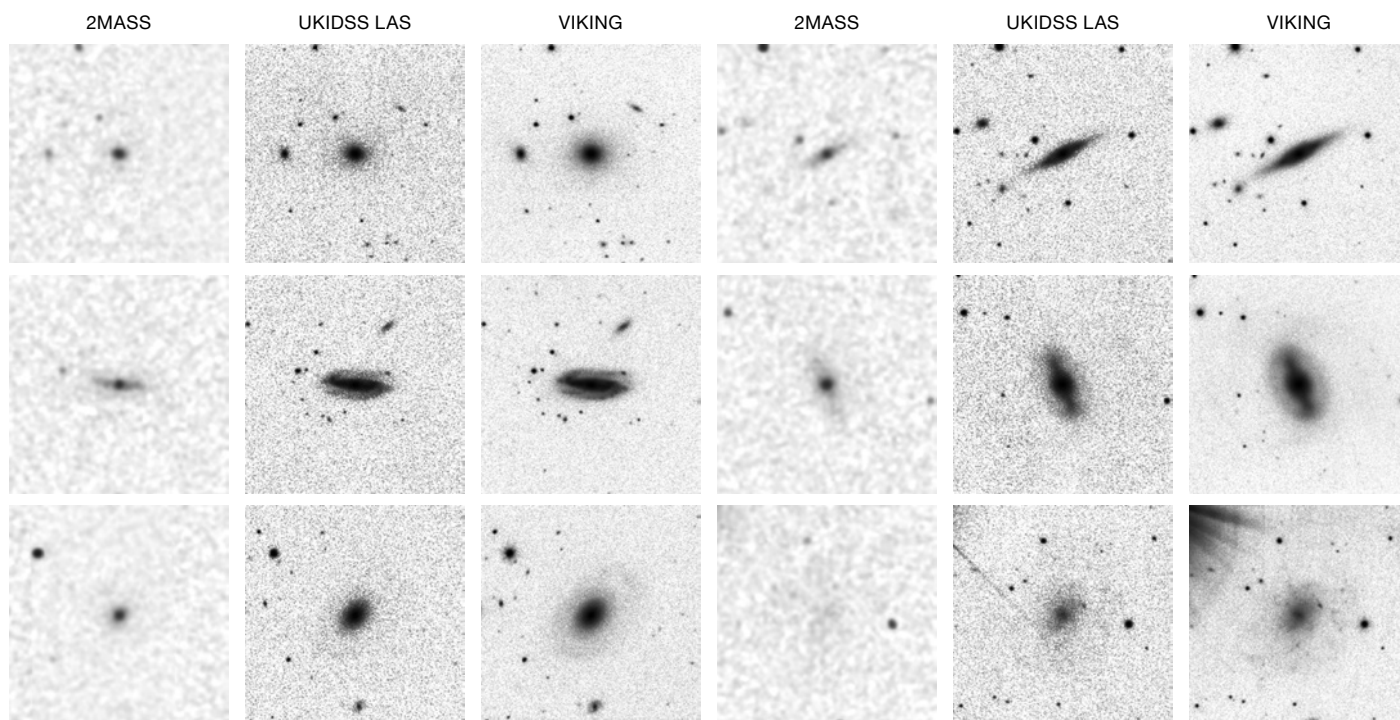


Figure 1. The 2MASS, UKIDSS LAS and VIKING images of six GAMA galaxies in the K_s -band. Note the extended, low surface brightness emission that only becomes clear in the deepest data. A full description of these comparisons can be found in Andrews et al. (2013).

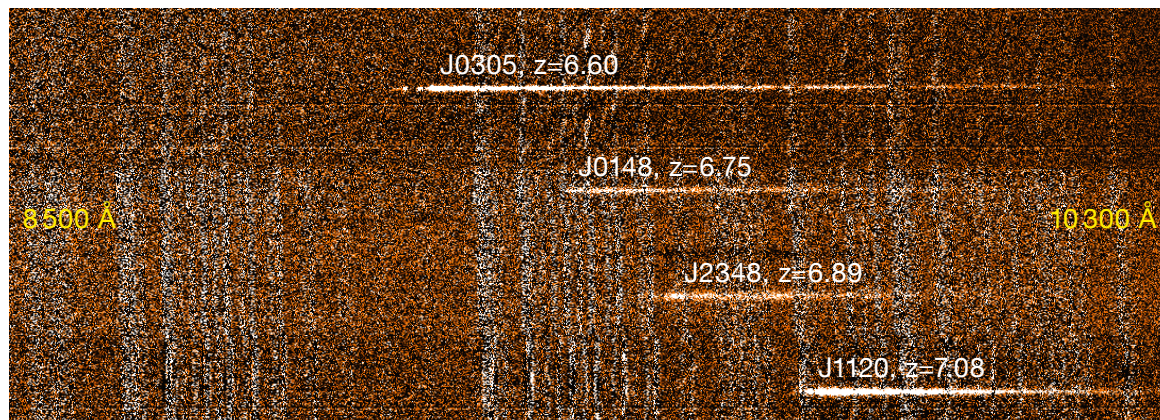


Figure 2. A montage of the 2D FORS2 spectra of the three VIKING $z > 6.5$ quasars with the $z = 7.1$ UKIDSS quasar for comparison. Note the excellent red sensitivity of FORS2 and the very abrupt cut-off blueward of the Lyman- α line in these systems.

considering the cosmological constraints that can be determined from the evolution of the cluster mass function (Eke, Cole & Frenk, 1996). VIKING will recover a significant number of the most massive clusters at $z > 1$ that are only found in small numbers in serendipitous X-ray cluster surveys, such as the XMM Cluster Survey (XCS; Mehrtens et al., 2012), or Spitzer mid-infrared surveys, such as the Spitzer Adaptation of the Red-sequence Cluster Survey (SpARCS; Wilson et al., 2009), which cover much smaller areas of sky.

In addition to clusters, VIKING will select the most massive galaxies within the survey volume and these are known to cluster particularly strongly (Kim et al., 2011). The combination of excellent photometry and the large area coverage of VIKING/KiDS will allow us to trace the angular clustering of massive galaxies at $z > 1$ (where the angular clustering scales are least affected by redshift) in a number of independent redshift slices.

Serendipity and legacy aspects

VIKING will also provide a wide margin for serendipitous discoveries of rare or extreme sources, given the overlap with many other multi-wavelength surveys. For instance, extremely obscured AGN can be selected

from WISE photometry relatively easily (Eisenhardt et al., 2012), but are very faint in the optical, so NIR data are essential. VIKING photometry will fill an important niche for a number of projects that need deeper photometry than that provided by UKIDSS LAS or VISTA VHS, but wider area coverage than UKIDSS Deep Extragalactic Survey (DXS) or VISTA VIDEO.

The legacy value of the VIKING/KiDS survey will be extended with the extensive spectroscopic surveys planned in this area using the spectrographs 4MOST, MOONS and Subaru Prime Focus Spectrograph (PFS). The complementary nature of these optical and NIR surveys means that the spectral coverage will be very dense, allowing many new observational strategies related to the lensing and intervening absorption of background objects by a fully constrained foreground to be explored. The vital foundation of these surveys will be the reliable photometric catalogue that VIKING/KiDS provides.

The VIKING data will be made available through the VISTA Science Archive (VSA¹) and the ESO Phase 3 facility², but the VIKING consortium will be creating an additional set of images that are optimised to match the seeing of other optical surveys (SDSS, KiDS and/or HSC) to ensure the best possible aperture

photometry is extracted. These additional images will be made available to the community through the VSA. The first 226 square degrees of the VIKING data have been released through the VSA and ESO Phase 3 databases and we encourage the community to contact us if they have any questions.

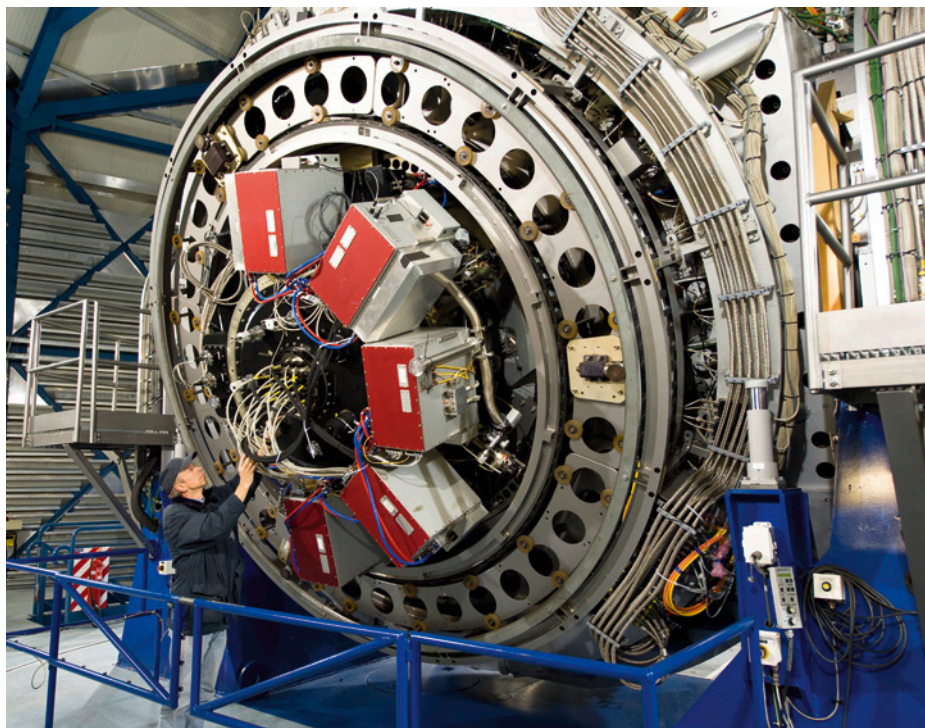
References

- Andrews, S. K. et al. 2013, PASA, submitted
 Burton, C. S. et al. 2013, MNRAS, 433, 771
 Eisenhardt, P. R. M. et al. 2012, ApJ, 755, 173
 Eke, V. R., Cole, S. & Frenk, C. S. 1996, MNRAS, 282, 263
 Fleuren, S. et al. 2012, MNRAS, 423, 2470
 González-Nuevo, J. et al. 2012, ApJ, 749, 65
 Kim, J.-W. et al. 2011, MNRAS, 410, 241
 Marriage, T. A. et al. 2011, ApJ, 737, 61
 Mehrtens, N. et al. 2012, MNRAS, 423, 1024
 Mortlock, D. J. et al. 2011, Nature, 474, 616
 Predehl, P. et al. 2009, AIPC, 1248, 543
 Stanford, S. A. et al. 2012, ApJ, 753, 164
 Venemans, B. et al. 2013, ApJ, 779, 24
 Wilson, G. et al. 2009, ApJ, 698, 1943

Links

¹ VISTA Science Archive (VSA): <http://horus.roe.ac.uk/vsa/>

² ESO Phase 3 VIKING data release 1: http://www.eso.org/sci/observing/phase3/data_releases/viking_dr1.pdf



View of the Cassegrain focus of VISTA housing the VIRCAM camera. VIRCAM consists of 16 2048 square Raytheon VIRGO HgCdTe 0.84–2.5 μm detectors covering a field of 45×45 arc-minutes (with inter-detector gaps). This image shows Paranal engineer Gerhard Hüdepohl checking VIRCAM.

First Scientific Results from the VISTA Hemisphere Survey (VHS)

Richard G. McMahon^{1,2}
 Manda Banerji^{1,3}
 Eduardo Gonzalez¹
 Sergey E. Koposov¹
 Victor J. Bejar^{4,5}
 Nicolas Lodieu^{4,5}
 Rafael Rebolo^{4,5}
 and the VHS collaboration

¹ Institute of Astronomy, University of Cambridge, United Kingdom

² Kavli Institute for Cosmology, University of Cambridge, United Kingdom

³ Department of Physics and Astronomy, University College London, United Kingdom

⁴ Instituto de Astrofísica de Canarias, La Laguna, Tenerife, Spain

⁵ Departamento de Astrofísica, Universidad de La Laguna, Tenerife, Spain

The first Galactic and extragalactic results from the VISTA Hemisphere Survey (VHS) are presented. The aim of the VHS is to carry out a near-infrared survey which, when combined with other VISTA public surveys, will result in coverage of the whole southern celestial hemisphere (~20 000 square degrees) to a depth 30 times fainter than the Two Micron All Sky Survey in at least two wavebands (*J* and *Ks*). The VHS vision includes a deep optical survey over the same area and this is now being realised

with the VST surveys and the Dark Energy Survey, which has recently started. A summary of the survey progress is presented, with some follow-up results on low-mass stars and high-redshift quasars.

Introduction

The goal of the Vista Hemisphere Survey (VHS¹) is to carry out a near-infrared (NIR) survey of all of the southern hemisphere (an area of ~ 20 000 square degrees) in at least two wavebands (*J* and *Ks*), with an exposure time of 60 seconds per waveband to produce median 5σ point source (Vega) limits of $J = 20.2$ and $Ks = 18.1$. This is ~ 30 times deeper than the Two Micron All Sky Survey (2MASS; Skrutskie et al., 2006) in the same bands. This total area coverage is achieved by combining with data from other VISTA public surveys, such as VIKING.

In the South Galactic Cap, ~ 5000 square degrees will be imaged more deeply with an exposure time of 120 seconds, and also including the *H*-band to produce median 5σ point source limiting magnitudes of: $J = 20.6$, $H = 19.8$ and $Ks = 18.5$. In this region of the sky, deep multi-band optical (*grizY*) imaging data will be provided by the Dark Energy Survey (DES). The remainder of the high Galactic latitude ($|b| > 30^\circ$) sky will be imaged in *YJHKs* for 60 s per band, to be combined with *ugriz*

waveband observations from the VST ATLAS survey.

The medium-term scientific goals of the VHS include:

- the discovery of the lowest-mass and nearest stars;
- deciphering the merger history of the Galaxy via stellar galactic structure;
- measurement of large-scale structure of the Universe out to $z \sim 1$ and measuring the properties of dark energy;
- discovery of quasars with $z > 7$ for studies of the baryons in the intergalactic medium during the epoch of reionisation;
- discovery of the most luminous quasars at all redshifts in the southern hemisphere as probes of the intergalactic medium and the formation of the most massive supermassive black holes in the Universe.

In addition the VHS survey will provide essential multi-wavelength support for the European Space Agency (ESA) Cornerstone missions; XMM-Newton, Planck, Herschel and Gaia.

Survey status

Figure 1 shows the sky coverage of VHS observations completed up to 1 October 2013. A total of 5511 observation blocks (OBs) have been completed. Each OB is equivalent to a single VISTA tile and covers 1.5 square

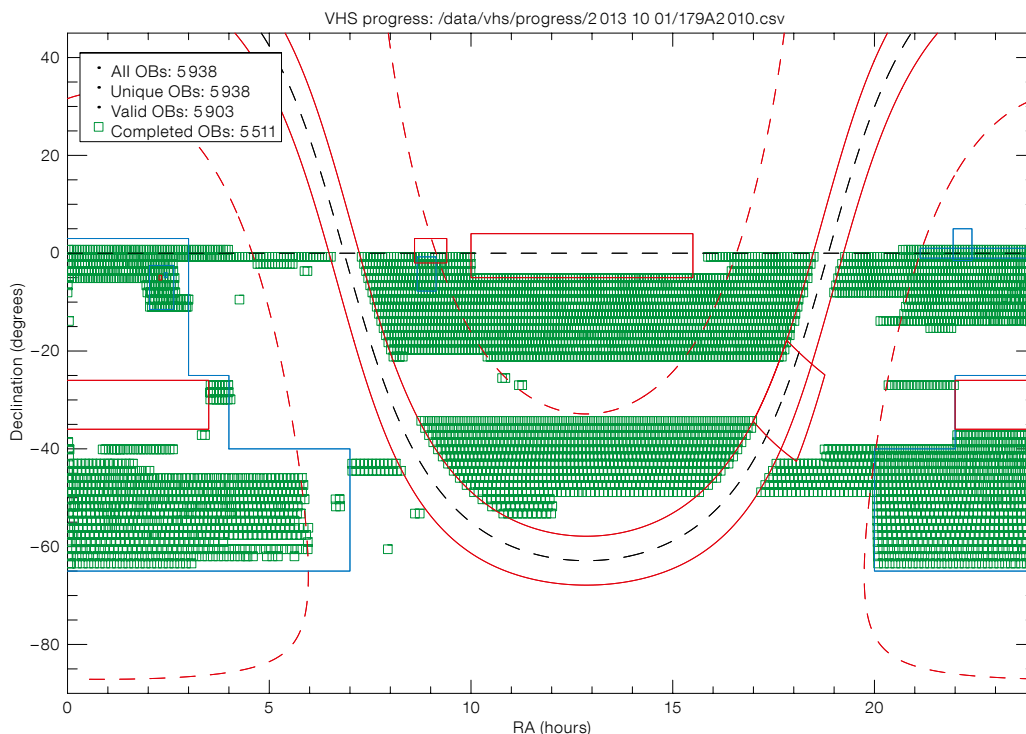


Figure 1. Sky coverage of the VHS survey completed up to 1 October 2013 based on ESO portal report tables. The green rectangles show completed tiles. The red solid lines show nominal regions outside the VHS observing footprint. The dashed red line is Galactic latitude $+30$, -30 degrees. The blue lines show the provisional DES footprint, circa April 2012.

degrees. The total observed area is around 8300 square degrees. All data is pipeline processed with the VISTA Data Flow System (Irwin et al., 2004; Lewis, Irwin & Bunclark, 2010; Cross et al. 2012) and the science products are available from the ESO Science Archive Facility and the VISTA Science Archive².

Scientific results

Many of the proposed scientific programmes for VHS require optical survey data from the VST surveys and DES. These surveys have only recently started and hence scientific exploitation has focused on science that can be carried out without optical data.

Figure 2 shows a comparison between VHS positions and the very long baseline interferometry (VLBI) radio reference frame³. The results are summarised in Table 1 and compared with the Sloan Digital Sky Survey (SDSS) and the UKIRT Infrared Deep Sky Survey (UKIDSS): there is a statistically significant systematic error of 0.05 arcseconds in declination. This is consistent with expected proper motions of 2MASS stars (Roeser et al., 2010) due to the ten year difference in epoch between 2MASS and VHS. Note that this systematic error varies depending on the direction in the sky of the Solar System motion with respect to an average 2MASS reference star. Proper motions will be included in future Cambridge Astronomical Survey Unit (CASU) processing based on the Fourth U.S. Naval Observatory CCD Astroglyph Catalogue (UCAC4) or PPMXL catalogues (Roeser et al., 2010).

Survey (number of sources)	σ (statistical) (arcseconds)		Systematic uncertainty (arcseconds)	
	RA	Dec	RA	Dec
VHS (563)	0.11	0.09	0.011 ± 0.005	0.051 ± 0.004
SDSS (2308)	0.05	0.05	0.006 ± 0.001	0.003 ± 0.001
UKIDSS (599)	0.10	0.09	-0.031 ± 0.004	-0.068 ± 0.004

Table 1. VHS astrometry comparison with VLBI radio reference frame, contrasted with SDSS and UKIDSS.

Low-mass stars

Gauza et al. (2012) are conducting a search for very low-mass common proper motion companions of nearby (< 25 pc) stars using VHS data and the shallower but earlier epoch (baseline around ten years) 2MASS catalogue. A search around the star HD 221356, which lies at a distance of 26.1 pc, has resulted in the discovery of a new common proper motion companion star located at an angular separation of 12.1 ± 0.2 arcseconds, corresponding to a projected distance of ~ 317 astronomical units (au). Figure 3 shows the VISTA discovery image. Near-infrared spectroscopy indicates a L0–L2 spectral type. Evolutionary models combined with an effective temperature of 2100–2300 K indicate a mass of $0.079 \pm 0.006 M_{\odot}$. Since the distance and metallicity of the HD 221356 system are well known, the detailed study of this new ultra-cool companion, which is located close to the frontier between stars and brown dwarfs, can provide valuable constraints on evolutionary models and, in particular, shed light on the properties of objects at the transition from stellar to substellar regime.

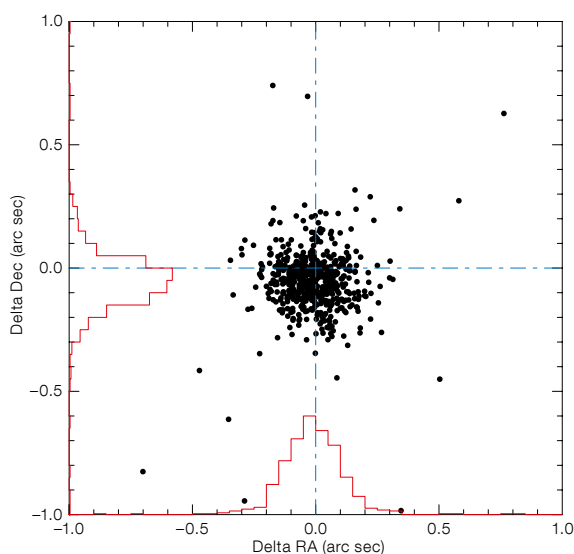
Lodieu et al. (2012) are using VHS in a project to improve our current knowledge of the density of T dwarfs and the shape of the substellar initial mass function by identifying a magnitude-limited sample of T-dwarfs in the

full southern sky. Lodieu et al. (2012) have used VHS data combined with longer wavelength photometric data from the Wide Infrared Survey Explorer (WISE) satellite mission (Wright et al., 2010) to select candidates with red mid-infrared colours and NIR to mid-infrared colours characteristic of cool brown dwarfs.

In this first stage of the survey, which only covers a few hundred square degrees, five new T-dwarf stars have been confirmed spectroscopically with the VLT with spectral types between T4.5 and T8 (see Figure 4). Two are estimated to be T6 dwarfs and lie within 16 pc, while a T4.5 dwarf is situated within 25 pc.

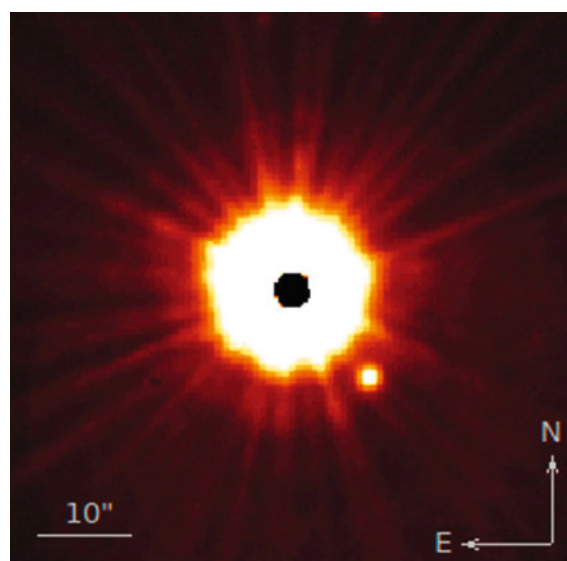
Quasars

Banerji et al. (2013) present the first results of a project that uses VHS data combined with WISE data to identify heavily reddened broad-line type 1 quasars in the redshift range 1.5 to 3. This redshift extent represents the cosmological epoch at the peak of star formation activity and accretion onto supermassive black holes as manifested by luminous quasars. Up until now it has been impossible to detect these luminous dust-enshrouded quasars, since existing NIR surveys like 2MASS are too shallow and deeper surveys have not covered enough area. Such luminous quasars



Left: Figure 2. Astrometric comparison between VHS positions and the VLBI radio reference frame³.

Right: Figure 3. False colour VISTA J-band image of HD 221356AD. The angular separation of the newly identified companion is 12.13 ± 0.18 arcseconds and the position angle 222 ± 2 degrees. Saturation in the image centre of the primary star is visible. Scale and orientation are shown.



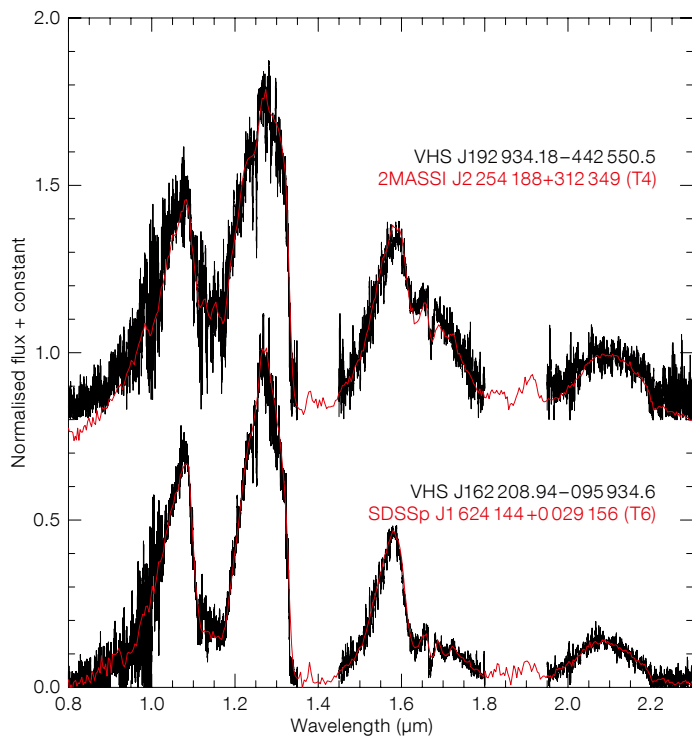


Figure 4. Near-infrared spectra obtained with VLT X-shooter and normalised at $1.265 \mu\text{m}$. Overplotted in red are the known T-dwarf T4 and T6 templates that best fit the observed spectra.

are expected to be in a short-lived transition phase from a heavily reddened dusty starburst to ultraviolet (UV)-luminous quasar. Optical surveys like SDSS and those with the VST are unable to detect quasars in this dusty formation phase due to the restframe UV extinction, which can be larger than 10 magnitudes at observed optical wavelengths.

With the new generation of wide NIR surveys, like UKIDSS and VHS, this field will be transformed. Luminous, heavily reddened, quasars detected by VHS will be ideally suited to follow up with the Atacama Large Millimeter/submillimeter Array (ALMA). Figure 5 shows how VHS and WISE colours are used to select the heavily obscured quasars with extremely red ($J-K_s > 2.5 \text{ mag}$) colours. At high Galactic latitudes, obscured high-redshift quasars dominate this colour locus at $15 < K_s < 17$. SINFONI spectra have been used to detect broad $H\alpha$ with line widths that imply supermassive black holes with masses of more than $10^9 M_\odot$.

References

- Banerji, M. et al. 2013, MNRAS, 429, L55
 Cross, N. J. et al. 2012, A&A, 548, A119
 Gauza, B. et al. 2012, MNRAS, 427, 2457
 Irwin, M. J. et al. 2004, SPIE, 5493, 411
 Lewis, J. R., Irwin, M. J. & Bunclark, P. S. 2010, ASP Conf. Ser., 434, 91
 Lodieu, N. et al. 2012, A&A, 548, A53
 Roeser, S. et al. 2010, AJ, 139, 2440
 Skrutskie, M. F. et al. 2006, AJ, 131, 1163
 Wright, E. L. et al. 2010, AJ, 140, 1868

Links

- ¹ VHS web page: <http://www.vista-vhs.org>
² VISTA Science Archive: <http://horus.roe.ac.uk/vsa/>
³ VLBI radio reference frame: http://astrogeo.org/vlbi/solutions/rfc_2012b

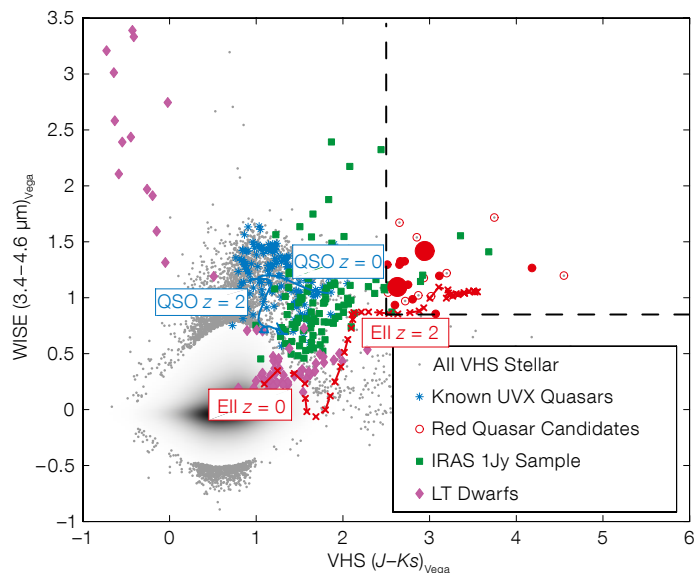


Figure 5. VHS ($J-K$) versus WISE ($W1-W2$) colour selection of our red quasar candidates are shown. All stellar objects detected over 180 square degrees are shown with greyscale representing the density, while the 1% of outliers in the distribution are shown as the individual grey points. Known UV-luminous quasars, local Ultraluminous Infrared Galaxies (ULIRGs) from the IRAS 1Jy sample and known LT dwarf stars have also been plotted. Also shown are the tracks of a typical unreddened quasar and an elliptical galaxy template with a formation redshift of $z = 5$. Heavily reddened quasars are marked as red circles. The small filled circles represent the spectroscopically confirmed sample from UKIDSS, the large filled circles are two newly confirmed quasars from VHS and the open circles are all candidates detected in the Banerji et al. (2013) study down to $K_s < 17$.

VST ATLAS First Science Results

Tom Shanks¹
 Vasily Belokurov²
 Ben Chehade¹
 Scott M. Croom³
 Joe R. Findlay¹
 Eduardo Gonzalez-Solares²
 Mike J. Irwin²
 Sergey Kposov²
 Robert G. Mann⁴
 Nigel Metcalfe¹
 David N. A. Murphy⁵
 Peder R. Norberg⁶
 Mike A. Read⁴
 Eckhard Sutorius⁴
 Gabor Worseck⁷

¹ Department of Physics, Durham University, United Kingdom

² Cambridge Astronomical Surveys Unit, Cambridge, United Kingdom

³ School of Physics, University of Sydney, Australia

⁴ Wide Field Astronomy Unit, Institute for Astronomy, University of Edinburgh, Royal Observatory, Edinburgh, United Kingdom

⁵ Instituto de Astrofísica, Universidad Católica de Chile, Chile

⁶ ICC, Department of Physics, Durham University, United Kingdom

⁷ Max-Planck-Institut für Astronomie, Heidelberg, Germany

The VST ATLAS is a *ugriz*-imaging survey targeting ~ 4500 square degrees of the southern sky. It reaches similar magnitude limits to the Sloan Digital Sky Survey in the north, i.e., $r \sim 22.5$, but ATLAS has better median seeing of 1 arcsecond full width half maximum. ATLAS is a companion survey to the VISTA Hemisphere Survey, which supplies *YJHK* imaging over much of its area. In addition, the Wide-field Infrared Survey Explorer (WISE) satellite supplies a further four mid-infrared bands. Together these

surveys complement each other and provide excellent multi-wavelength data for both Galactic and extragalactic science projects.

Survey description

The VLT Survey Telescope (VST) ATLAS imaging exposures are 2×60 s in *u*-band, 2×50 s in *g*-band and 2×45 s in *riz*-bands. The *iz* images are observed in grey time and the *ugr* in dark. The median seeing of 1 arcsecond is well sampled by the 0.21-arcsecond pixels of VST OmegaCAM. The current status of the VST ATLAS in the *ugriz* band can be queried¹. Ultimately we are targeting most of the available high latitude sky in the northern and southern Galactic Caps. So far we have covered approximately 2200 square degrees in each band with a little less coverage in *ugr* and somewhat more in *iz*. Thus the survey which started in September 2011 is roughly at its half-way point. The survey is unique in terms of southern surveys in having *u*-band sensitivity and the ATLAS Chilean *u*-band extension (Principal Investigator [PI]: L. Infante) doubles the *u*-band exposure to four minutes. As well as VHS supplying *YJHK* imaging, ATLAS is well complemented by the WISE satellite near-infrared (NIR) survey covering 3.4–22 μm . The WISE survey depth is particularly well matched to ATLAS in the W1 (3.4 μm) and W2 (4.6 μm) bands and several of the science aims, outlined in the following sections, exploit this complementarity. The OmegaCAM Science Archive² will publish ATLAS data, and federate it with GALEX, WISE and the VISTA surveys, to facilitate these multi-wavelength analyses.

$z < 2.5$ quasar redshift surveys

ATLAS has two routes to quasar surveys at lower redshifts: via ultraviolet excess (UVX) selection by virtue of its *u*-band sensitivity; via “KX” selection using the W1 (3.4 μm) band.

Both these methods distinguish the power-law spectra of quasars from the thermal spectra of stars at their respective wavelength extremes. Chehade et al. (in prep.) have made the first spectroscopic follow-up of quasars selected using ATLAS+WISE, using the Two-degree-Field Galaxy Redshift Survey (2dF) and AAOmega at the Australian Astronomical Telescope (AAT). They found that while UV selection wins at the faintest magnitudes ($g < 22.5$), NIR selection using $(g-i):(i-W1)$ significantly increases the quasar number counts by around $\sim 15\%$ in the fields where it has been applied to $g < 22$, mostly comprising a population of dust-reddened quasars (see Figure 1a), leading to quasar sky densities of up to 95 per square degree. We now have a sample of $\sim 10\,000$ quasars with which to analyse the luminosity functions and clustering in a more complete and fainter redshift survey than the best previous surveys, such as 2SLAQ. The ATLAS quasar surveys will provide future targets for the ESO 4MOST fibre spectrograph and will also gain X-ray coverage with the eROSITA satellite, soon to be launched.

$5 < z < 6$ quasar redshift surveys

The combination of WISE and ATLAS shows further potential. Findlay et al (in prep.) have shown that the $(r-z):(i-W1)$ colour–colour plane (see Figure 1b) can easily distinguish $5 < z < 6$ quasars from red stars and galaxies, since previously discovered SDSS quasars in this redshift range lie in a valley between the loci of stars and galaxies. This immediately reduces background contamination for such quasar searches by about two orders of magnitude to $i = 21.5$ even before a *g*-band dropout technique is applied. Using the combination of these techniques, it should be possible to add significantly to the relative dearth of known quasars in this redshift range and so bridge the gap between the $z \sim 5$ and $z \sim 6$ quasar luminosity functions. Increasing the numbers of

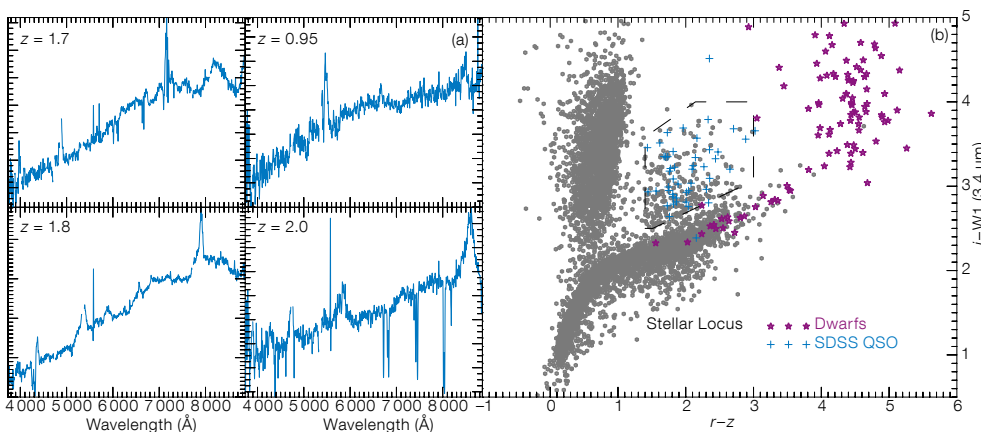


Figure 1. (a) Four examples of a new population of dust-absorbed red quasars at $z < 2.5$ selected from $(g-i):(i-W1)$ colour–colour plot by a combination of WISE and ATLAS. Spectra are from AAT 2dF AAOmega. (b) WISE and ATLAS $(r-z):(i-W1)$ colour–colour plot shows high efficiency in isolating previously discovered SDSS $5 < z < 6$ quasars.

$5 < z < 6$ quasars will also provide the sight-lines required to characterise better the properties of the intergalactic medium (IGM) at redshifts approaching the end of reionisation.

New UV-bright quasars for helium reionisation studies

VST ATLAS provides a unique opportunity to select rare UV-transmitting high-redshift quasars to study the reionisation epoch of He. Far-UV spectra of background quasars obtained with the Hubble Space Telescope (HST) probe the redshifted Lyman- α transition of singly ionised helium, with strong absorption signalling that He is not yet fully ionised (e.g., Worseck et al., 2011). To date, very few quasars allow for such analysis due to the near-ubiquitous occurrence of strong Lyman continuum absorption by neutral hydrogen at longer wavelengths. Current quasar catalogues have been almost fully exploited, yielding high-quality helium absorption spectra of only 19 quasars. The very low predicted surface density of quasars for He absorption spectroscopy with HST (~ 6 per 1000 square degrees; Worseck & Prochaska, 2011) requires large-area surveys. Moreover, the optical colours of most of these quasars are degenerate with stellar colours (see Figure 2, upper), and only the combination with multi-wavelength photometry from the Galaxy Evolution Explorer (GALEX; UV) and WISE (mid-IR) allows their selection at high efficiency. With VST ATLAS it is now possible to extend these multi-wavelength studies to the southern hemisphere, complementing similar

efforts with Sloan Digital Sky Survey (SDSS) and the Panoramic Survey Telescope and Rapid Response System (Pan-STARRS). Confirmation of quasar candidates is under way (see Figure 2, lower) to maximise the number of potential targets for He reionisation studies before the end of HST's lifetime.

Luminous red galaxy surveys out to $z \sim 1$

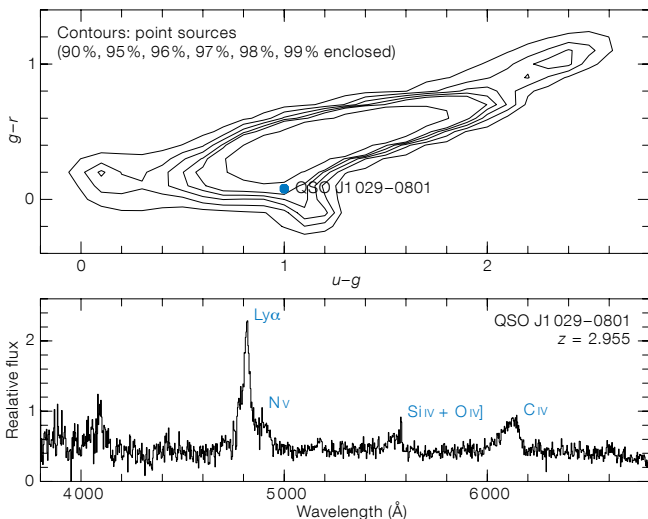
Using ATLAS *gri* colour cuts at $z \sim 0.35$ and $z \sim 0.55$ and *riz* cuts at $z \sim 0.68$, new catalogues containing up to one million luminous red galaxies (LRGs) can be made. One aim is to use the angular clustering of the LRGs to test the evidence for non-Gaussianity found in similar SDSS LRG samples. Again there may be a possibility to extend the LRG redshift range to $z \sim 1$ by incorporating WISE data in (*i-z*):(*z-W1*) galaxy colour cuts. But the prime aim is to use the ATLAS LRGs to measure the strength of the Integrated Sachs-Wolfe (ISW) effect in the southern hemisphere by cross-correlating with Planck cosmic microwave background data. Such a cross-correlation is only predicted in cosmological models with an accelerating expansion. Previously Sawangwit et al. (2010) found only a weak ISW effect at $z = 0.35$ and $z = 0.55$ and a null result at $z = 0.68$. It is therefore important to repeat this test of the accelerating expansion in the south. Since the test cannot be made at high redshift, the southern hemisphere ATLAS data will provide the only decisive independent new evidence for universal acceleration.

imaging data from the far-UV to the radio, via optical, NIR, mid-IR and far-IR (Driver et al., 2011). GAMA is the first multi-wavelength spectroscopic survey covering hundreds of square degrees over a 5 Gyr lookback time.

Since 2008, GAMA has executed a comprehensive and complete spectroscopic survey down to $r_{AB} = 19.8$ (i.e., two magnitudes deeper than the main SDSS survey) in five roughly equal-sized areas covering a large range in right ascension: three equatorial 60 square degree regions (G09, G12 and G15), a 50 square degree patch overlapping with the Canada France Hawaii Telescope Legacy Survey (CFHTLS) W1 (G02) and another of similar size centred within the VST ATLAS survey (G23). The latter, defined as $339 < RA < 351$ degrees and $-35 < Dec < -30$ degrees, is currently only 37% complete spectroscopically, but is due to be completed by autumn 2014.

GAMA represents the highest priority target areas for the Herschel-ATLAS, VST ATLAS/KiDS, VISTA VIKING and Hyper SuprimeCam surveys. The G23 region was specifically motivated for future Australian SKA Pathfinder (ASKAP) DINGO observations free from any known bright continuum sources. Crucially, G23 enables unique science that is not possible in the other GAMA regions, as interferometric radio facilities, such as ASKAP, produce a dramatically larger, noisier beam-width at the equator due to the lack of rotation of the sky. To provide complementary UV star formation rates (SFRs), the entire G23 region has been covered in the final six months of GALEX operations to 3000 s depth (double that of the GAMA equatorial fields). G23 combined with

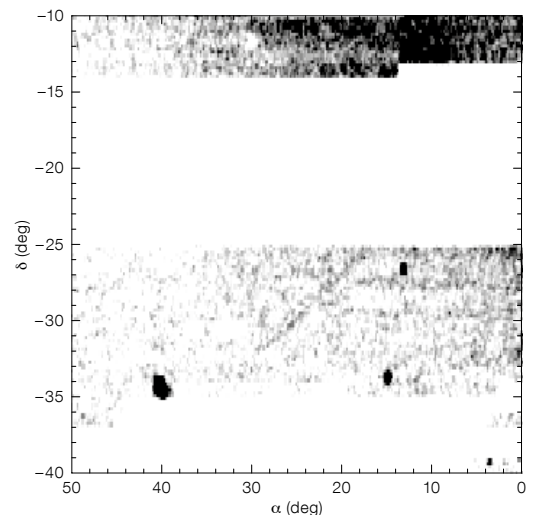
Figure 2. Upper: VST ATLAS *ugr* selection of candidate quasars with UV flux at lower wavelengths than the H α Lyman limit where He II 304 Å Lyman alpha absorption may be detected. Lower: The spectrum of the above candidate for helium reionisation studies.



GAMA and VST ATLAS

The Galaxy And Mass Assembly (GAMA) project originated as a large optical spectroscopic survey on the AAT with complementary

Figure 3. The spatial density variation of stellar sources in the combined *g*- and *r*-bands over part of the ATLAS survey of the southern Galactic Cap.



ASKAP will be capable of measuring whether the cosmic H I has remained static or declined to within a factor of two over a 4 Gyr baseline.

G23 will thereby provide a unique multi-wavelength database from the far-UV to the radio, that is not possible with the equatorial regions, for the investigation of the conversion of gas into stars as a function of redshift, stellar mass, age and metallicity. Additionally, by using a state-of-the-art group catalogue (like the one already created for the GAMA equatorial fields by Robotham et al. [2011]), a new door in extragalactic astronomy is opened on how galaxy formation processes (e.g., mass–metallicity relation, SFRs, morphologies, etc) correlate with halo mass.

Galactic archaeology with ATLAS

A simple diagnostic for the overall quality of the ATLAS photometric calibration is to examine the uniformity of stellar density maps selected from a relatively narrow colour and magnitude range. With a sensible choice of colour–magnitude loci these maps can, in addition, be used as a first pass probe of nearby Milky Way and satellite foreground populations. An example of this, cut from more extensive coverage of the south Galactic Cap available in autumn 2012, is shown in Figure 3.

In addition to the obvious density enhancements due to previously known satellites such as the Fornax and Sculptor dwarfs, toward the bottom of the map, and the globular cluster NGC 288 right of centre, are two stellar streams. The broad enhancement in stellar density from the Sagittarius dwarf southern stream is visible towards the top and a newly discovered stellar stream near the centre, pointing just south of the Fornax dwarf. This new stream can be traced quite clearly over about 10 degrees before petering out to the south and being lost to the north in a gap in coverage.

The likely nature of the stream can be inferred from its angular width and comparing on-stream vs. off-stream colour–magnitude diagrams; it is found to be consistent with the stream being at a distance of around 20 kpc and originating from an old metal-poor low velocity dispersion satellite. This suggests that the stream most likely comes from a disrupted globular cluster, and in the current coverage there is no sign of any obvious progenitor. When further observations for this region have been fully processed, many of the gaps in coverage should be filled and further exploration of the stream, and of other nearby stellar populations, can be made.

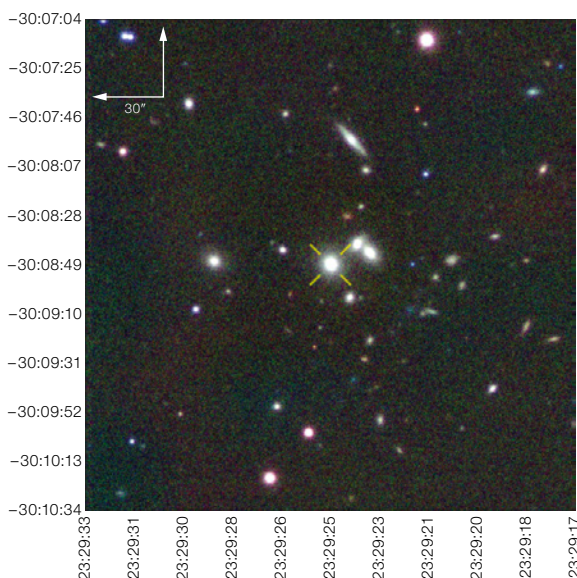


Figure 4. A *gri* composite image of a $z \sim 0.1$ galaxy group identified by ORCA in the VST ATLAS survey. The brightest group member is denoted by the yellow cross at the centre of the image.

The SAMI galaxy survey

VST ATLAS imaging has formed part of the target selection for the new survey being carried out using SAMI (the Sydney-AAO Multi-object Integral field spectrograph) on the AAT. SAMI can target 13 galaxies at once over a 1 degree diameter field of view. The target is to build a sample of 3400 galaxies, spanning a large range in both mass and environment to address key questions in galaxy formation, including: the primary physical mechanisms causing environmental suppression of star formation and morphological changes in galaxies; the frequency of inflows and outflows of gas and how they influence galaxy properties; the distribution of angular momentum in the galaxy population and how mass is built up.

SAMI is targeting galaxies in field and group environments, using the GAMA survey as input, together with clusters selected over the southern sky. VST photometry is particularly crucial for target selection in the SAMI clusters, as no other optical multi-band imaging exists over the cluster regions. The photometry, together with 2dFGRS redshifts, forms the basis for SAMI target selection, with further AAOmega redshifts being measured to give complete sampling across each cluster. The SAMI team has already observed over 100 galaxies using VST photometry for selection, and these, together with further observations, will shed light on numerous issues in galaxy formation.

Galaxy groups and clusters

Based on a pilot band-merged *gri* galaxy catalogue, a 50 square degree region of VST ATLAS

has been searched for galaxy clusters. In the absence of photometric redshifts, we identify clusters via the red sequence using the overdense red-sequence cluster algorithm (ORCA; Murphy et al. 2012). This algorithm is robust to systematic magnitude errors and does not require redshift data. The initial search yielded 93 clusters, an example of which is shown in Figure 4, but analysis suggests that some are spurious detections arising from the fragmentation of stellar haloes. Future work will reduce the level of stellar contamination in the source catalogue. Comparison against calibrated measurement of sequence normalisations in *g-r* and *r-i* from the Geach et al. (2011) ORCA cluster catalogue suggest this group has a redshift of $z \sim 0.1$. Five-band photometric redshifts will be used in the future to better determine the redshifts of VST clusters identified with ORCA.

References

- Driver, S. P. et al. 2011, MNRAS, 413, 971
- Geach, J. E., Murphy, D. N. A. & Bower, R. G. 2011, MNRAS, 413, 3059
- Murphy, D. N. A., Geach, J. E. & Bower, R. G. 2012, MNRAS, 420, 1861
- Robotham, A. S. G. et al. 2011, MNRAS, 416, 2640
- Sawangwit, U. et al. 2010, MNRAS, 402, 2228
- Worseck, G. & Prochaska, J. X. 2011, ApJ, 728, 23
- Worseck, G. et al. 2011, ApJ, 733, L24

Links

- ¹ VST ATLAS status:
<http://astro.dur.ac.uk/Cosmology/vstatlas/>
- ² OmegaCam Science Archive:
<http://surveys.roe.ac.uk/osa/>

VST Photometric H α Survey of the Southern Galactic Plane and Bulge (VPHAS+)

Janet E. Drew¹
 Geert Barentsen¹
 Juan Fabregat²
 Hywel Farnhill¹
 Michael Mohr-Smith¹
 Nicholas J. Wright¹
 Eduardo Gonzalez-Solares³
 Michael J. Irwin³
 Jim Lewis³
 Aykub K. Yoldas³
 Robert Greimel⁴
 Jochen Eisloffel⁵
 Paul Groot⁵
 Michael J. Barlow⁷
 Romano Corradi⁸
 Boris T. Gänsicke⁹
 Christian Knigge¹⁰
 Antonio Mampaso⁵
 Rhys Morris¹¹
 Tim Naylor¹²
 Quentin A. Parker¹³
 Roberto Raddi⁹
 Stuart E. Sale¹⁴
 Danny Steeghs⁹
 Yvonne C. Unruh¹⁵
 Jorick S. Vink¹⁶
 Jeremy R. Walsh¹⁷
 Nicholas A. Walton³
 Roger Wesson¹⁷
 Albert Zijlstra¹⁸

- ¹ School of Physics, Astronomy & Mathematics, University of Hertfordshire, Hatfield, United Kingdom
- ² Observatorio Astronómico, Universidad de Valencia, Paterna, Spain
- ³ Institute of Astronomy, Cambridge University, United Kingdom
- ⁴ IGAM, Institute of Physics, University of Graz, Austria
- ⁵ Thüringer Landessternwarte, Tautenburg, Germany
- ⁶ Afdeling Sterrenkunde, Radboud Universiteit Nijmegen, the Netherlands
- ⁷ Department of Physics & Astronomy, University College London, United Kingdom
- ⁸ Instituto de Astrofísica de Canarias, La Laguna, Tenerife, Spain
- ⁹ Department of Physics, University of Warwick, Coventry, United Kingdom
- ¹⁰ School of Physics & Astronomy, University of Southampton, United Kingdom
- ¹¹ School of Physics, Bristol University, United Kingdom
- ¹² Department of Physics, University of Exeter, United Kingdom
- ¹³ Department of Physics, Macquarie University, NSW 2109, Australia
- ¹⁴ Rudolf Peierls Centre for Theoretical Physics, Oxford University, United Kingdom
- ¹⁵ Department of Physics, Blackett Laboratory, Imperial College London, United Kingdom

- ¹⁶ Armagh Observatory, College Hill, Northern Ireland, United Kingdom
- ¹⁷ ESO
- ¹⁸ Jodrell Bank Centre for Astrophysics, School of Physics & Astronomy, University of Manchester, United Kingdom

The VST Photometric H α survey of the Southern Galactic Plane and Bulge (VPHAS+) is collecting single-epoch Sloan u , g , r , i and H α narrowband photometry, at arcsecond resolution, down to point-source (Vega) magnitudes of ~ 21 . The survey footprint encloses the entire southern Galactic Plane within the Galactic latitude range $-5^\circ < b < +5^\circ$, expanding to $b = \pm 10^\circ$ in the Galactic Bulge. This brief description of VPHAS+ includes sample data and examples of early science validation.

Overview

VPHAS+ is the southern counterpart to two existing northern hemisphere surveys: the Isaac Newton Telescope Photometric H α Survey of the Northern Galactic Plane (IPHAS), which covers the Northern Plane from La Palma in r , i and H α (Drew et al., 2005; Barentsen et al. in preparation) and the UV-excess survey of the Northern Galactic Plane (UVEX), which does the same in u , g , and r (Groot et al., 2009). The combination of these three surveys will ultimately provide a $360^\circ \times 10^\circ$ square-degree view of the entire Galactic Plane at roughly one arcsecond spatial resolution. This will result in a photometric catalogue containing approximately half a billion stars — two thirds of which will be captured by VPHAS+, surveying the denser southern Plane and Bulge.

The original motivation for IPHAS was to provide the digital update to photographic H α surveys of the mid-twentieth century. In the south, VPHAS+ is the digital successor to the UK Schmidt H α survey (Parker et al., 2005). However, the legacy of VPHAS+ will extend beyond the traditional H α applications of identifying emission line stars and nebulae. For example, the survey's unique (r -H α) colour, when combined with broadband colours, offers a rough extinction-free proxy for intrinsic stellar colour. This opens the door to a wide range of Galactic science applications, including the mapping of extinction across the Plane in three dimensions (e.g., Sale et al., 2009). VPHAS+ is also efficient in identifying OBA stars on the basis of their blue colours, and it enables comparative studies of clusters using homogeneous data. The final photometric catalogue is likely to achieve an externally validated accuracy of 0.02 to 0.03 magnitudes. The first data release is already available from the ESO archive¹ as images and single-band catalogues, calibrated against nightly standard-star data.

The original survey plan drawn up in 2006 envisaged contemporaneous five-band photometry per survey field, providing optical snapshots of stellar spectral energy distributions. During the commissioning of VST and the camera, OmegaCAM, it became evident that working to this ideal would not permit VPHAS+ to proceed in a timely manner. Hence it was agreed to adopt a more flexible strategy of splitting the data-taking into blue (u, g, r) and red (H α, r, i) filter sets that can be combined, post-observation, using the repeated r -band exposures as aids to calibration and checks on variability. As a result, VPHAS+ follows an observing strategy that echoes the northern

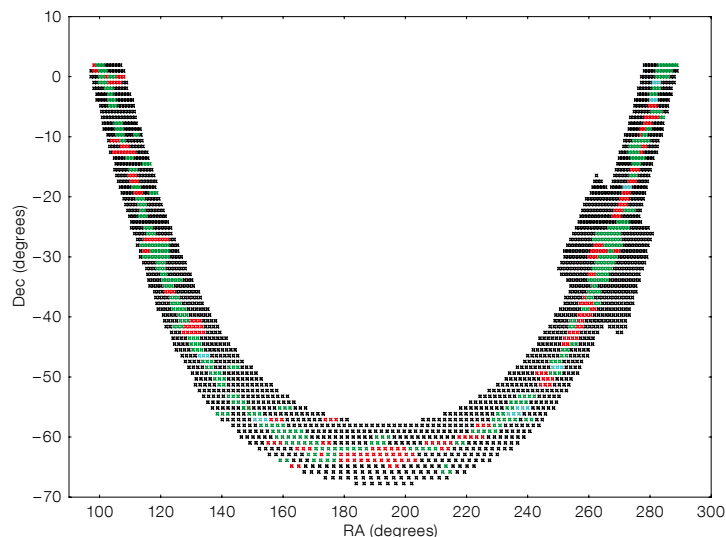


Figure 1. A map of the VPHAS+ survey footprint showing status on 30 September 2013. 2269 fields make up the survey: those shown in black had not yet been observed, while those in green have already been completed. Red is used for fields observed only in the H α , r - and i -bands, while blue is used for those only observed in the u -, g - and r -bands.

Filter	Total exposure time: No. of exposures \times exposure (s)	5 σ (Vega) magnitude limit per exposure
<i>u</i>	2 \times 150	21.5
<i>g</i>	3 \times 30 or 40	22.5
<i>r</i>	2 \times 25	21.6
H α	3 \times 120	20.8
<i>i</i>	2 \times 25	20.8

Table 1. VPHAS+ exposures per field and sensitivity. (The shorter *g* exposure time applies to data first obtained prior to 19 February 2013.)

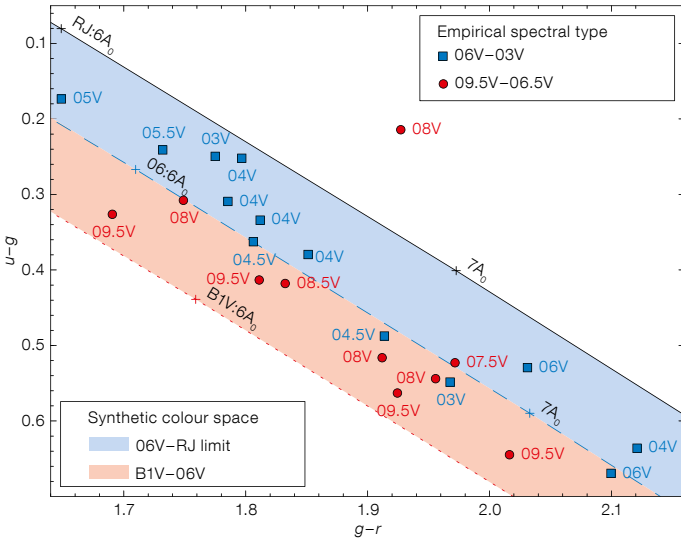


Figure 2. The VPHAS+ (*u-g*) vs. (*g-r*) colour-colour diagram is shown for known O stars in and close to Westerlund 2.

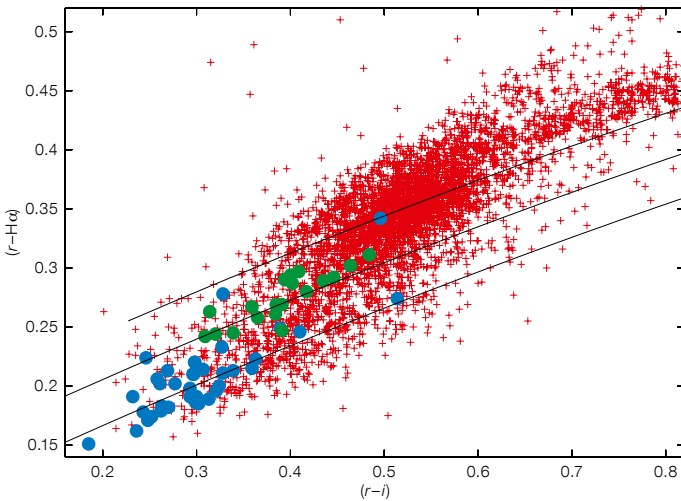


Figure 3. The (*r-H α*) vs. (*r-i*) photometric diagram from VPHAS+ field 33 (centred on RA 06 44 16.7, Dec $-00\ 58\ 04$, J2000). Red points represent all stars in the field with magnitude *r* < 16.5. Blue and green points represent stars with spectroscopically determined spectral types in the range A0–3V and F0–1V respectively. The solid lines are, from bottom to top, the model reddening lines corresponding to A2V, F0V and F5V respectively.

hemisphere IPHAS and UVEX survey pair. It remains the case that each filter set delivers a robust contemporaneous colour-colour diagram, straight from the pipeline. At the beginning of October 2013, complete data had been obtained for 404 fields, out of 2269. The blue filters are progressing more slowly than the red because they require darker observing conditions. A map of the survey pointings, picking out those already executed to survey standard, is presented in Figure 1.

The quality of data delivered by OmegaCAM is, in most respects, excellent. We have set

the target maximum seeing at 1.2 arcseconds for all except the densest fields, where it is 0.9 or 1.0 arcseconds. The outcome is that the median seeing in all filters, except *u*, is around 0.8 arcseconds. In *u*, the most challenging filter, the median is 0.95 arcseconds. At the same time, image quality across the full square degree of field has also been very good. Bright Moon is avoided for VPHAS+ data-taking because experience with IPHAS has taught us that the mix of diffuse H α background and bright moonlight can become impossible to separate. Given that the southern Galactic Plane is threaded by even more

H α nebulosity than the north, this is an important precaution. There is room for improvement with respect to scattered light: presently this is significant and variable — to the extent that it has posed a challenge to the photometric calibration. We look forward to the installation of the planned baffles on the VST that should cut this scattered light down substantially.

The H α filter procured for the VST by the VPHAS+ consortium is named NB-659 and is segmented: four 13.6 \times 13.6 square-centimetre pieces of coated glass are held in place in the mount by a pair of blackened T-bars. This creates some extra vignetting — a factor that has been taken to account in our offsetting strategy. The filter’s full width at half maximum (FWHM) transmission is close to 10 nm and the transmission at peak is \sim 95 percent, making the filter 20% more sensitive than its IPHAS/La Palma counterpart. Median magnitude limits achieved in all five bands are set out in Table 1. All VPHAS+ data are processed by the Cambridge Astronomical Survey Unit (CASU), via a pipeline similar to the VISTA Data Flow System that presently delivers flux-calibrated images and aperture photometry. The main features of VPHAS+ will be presented in a forthcoming paper (Drew et al., in preparation).

VPHAS+ science validation

A well-established technique for identifying O- and early B-type stars is to pick them out above the main stellar locus in the Johnson (*U-B*) vs. (*B-V*) diagram. The same is possible using Sloan (*u-g*) vs. (*g-r*) and we provide an example that shows that VPHAS+ is ready for the same kind of exploitation — one of the survey aims: Figure 2 shows how known and typed O stars lying within and close to the massive cluster Westerlund 2 fall in this colour-colour plane. The plotted stars range in *g* magnitude from 14 down to 18. It can be seen clearly that there is good, if not perfect, separation between the later- and earlier-type O stars, with one prominent failure — an O8V star that has escaped to above the theoretical Rayleigh–Jeans limit (only because it is in a close blend right at the heart of this very dense bright cluster — others have deblended more successfully). A more profound validation has come from comparing our data on these stars with the results of Vargas Alvarez et al. (2013) from Hubble Space Telescope (HST) data. We conclude, as they do, that the reddening law must be characterised by $R = 3.8$, and find that the mean difference in visual extinction is only 0.13 mag (Mohr-Smith et al., in preparation).

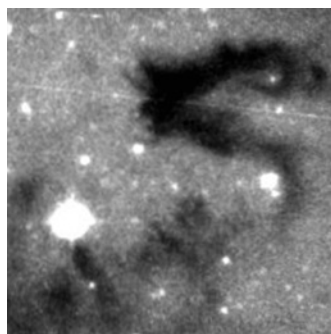
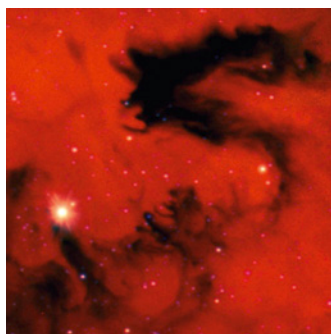
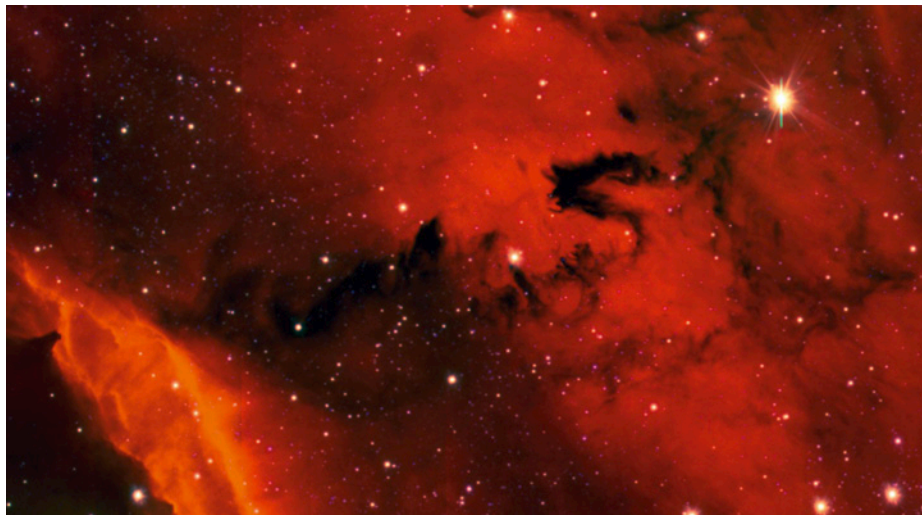


Figure 4. A 12.3×7.1 arcminute cut-out image from M8, the Lagoon Nebula, centred on RA 18 09 36, Dec -24 01 51 (J2000), in which r , i and $H\alpha$ data are combined. Below left, a 2.5×2.5 arcminute zoom into some of the detail. Below right, the same detail as imaged in the R -band by the UKIRT Schmidt survey.

Synergies with other surveys now and in the future

The VPHAS+ footprint encloses the entire Variables in the *Via Lactea* (VVV) footprint and hence will provide complementary optical coverage to this near-infrared (NIR) survey of the Galactic Bulge and inner disc. The same synergy exists with respect to the other NIR photometric surveys — the Two Micron All Sky Survey (2MASS) and the UKIRT InfraRed Deep Sky Surveys: Galactic Plane Survey (UKIDSS/GPS). On combining VST optical magnitudes with 2MASS magnitudes, particularly for early-type stars, we are already finding that we can obtain good constraints on sight-line reddening laws — such data can play a critical role in three-dimensional extinction mapping of the Milky Way (c.f., the work of Sale, 2012 and Berry et al., 2012). VPHAS+, along with IPHAS and UVEX in the north, already have achieved full optical coverage of the Spitzer and Herschel legacy surveys of the Galactic mid-plane.

The beginning of VPHAS+ data collection closely coincided with the beginning of the Gaia–ESO spectroscopic survey (GES), described by Randich et al. (p. 47). GES needs high-quality photometry of the type VPHAS+ can supply, as input to its target selections programme. There have already been transfers of photometric catalogues, particularly to support open-cluster observations. A major design effort is currently underway in connection with plans to build the next generation of massively-multiplexed spectrographs for Europe’s astronomy community — notably 4MOST and MOONS. Homogeneous, astrophysically informative optical photometry will continue to be needed to feed targets to these advanced instruments. VPHAS+, as it transforms into a complete five-band survey catalogue, will be there to meet this need for Galactic Plane and Bulge science.

References

- Berry, M. et al. 2012, ApJ, 757, 166
- Drew, J. E. et al. 2005, MNRAS, 362, 753
- Groot, P. J. et al. 2009, MNRAS, 400, 1413
- Guenther, E. W. et al. 2012, A&A, 543, A125
- Parker, Q. A. et al. 2005, MNRAS, 362, 689
- Sale, S. E. et al. 2009, MNRAS, 392, 497
- Sale, S. E. 2012, MNRAS, 427, 2119
- Sebastian, D. et al. 2012, A&A, 541, A34
- Vargas Alvarez, C. A. et al. 2013, AJ, 145, 125

Links

- ¹ VPHAS+ first data release: <http://archive.eso.org/cms/eso-archive-news/first-data-release-of-vst-public-survey-vphas--imaging-data.html>

The VPHAS+ (r – $H\alpha$) vs. (r – i) photometric diagram can be used in a more general way to select samples of stars of different spectral types, capitalising on the sensitivity of (r – $H\alpha$) to intrinsic stellar colour. Figure 3 illustrates how this can be done: the colour–colour diagram for brighter stars in VPHAS+ field No. 33, centred on RA 06 44 16.7, Dec –00 58 04 (J2000) is plotted. This is a part of the sky that the CoRoT satellite has observed twice and that has also been followed up spectroscopically (Guenther et al., 2012; Sebastian et al., 2012). The blue and green points plotted in the diagram correspond to stars with MK spectral types and luminosities obtained from the spectroscopy, in the A0–3V and F0–1V ranges respectively. Their positions are compared with model reddening lines, including the A2V line which lies along the bottom of the main stellar locus (A2V stars have the strongest $H\alpha$ absorption of all non-degenerate stars). From this figure it is apparent that most of the early A main sequence stars are confined to a strip ~ 0.05 mag wide, with observational error taking them across the A2V reddening line, while the F0–1V stars are mostly well-separated and cluster around the F0V line.

Nebulae and diffuse interstellar medium emission

In terms of the integrated light received, the imaging capability of VPHAS+ is not greatly different to that of the UK Schmidt $H\alpha$ Survey (SHS; Parker et al., 2005). Because of the effort that was made using the SHS to search for well-resolved planetary nebulae, it is unlikely that VPHAS+ will find many more. But there is discovery space in the domain of compact nebulae — which are either very young or very far away — that other ground-based surveys have failed to resolve.

The outstanding advantage of VPHAS+ relative to SHS is the sub-arcsecond seeing commonly encountered at Paranal. Figure 4, showing a portion of M8 (the Lagoon Nebula), provides an example of the refinement of detail relative to the SHS that is apparent even in imagery combining exposures in three different filters. Ionisation fronts, dust lanes and other dynamically revealing structures at the arcsecond scale are now much more readily accessed from the ground.

The Kilo-Degree Survey

Jelte T. A. de Jong¹
 Konrad Kuijken¹
 Douglas Applegate²
 Kor Begeman³
 Andrey Belikov³
 Chris Blake⁴
 Jeffrey Bout³
 Danny Boxhoorn³
 Hugo Buddelmeijer³
 Axel Buddendiek²
 Marcello Cacciato¹
 Massimo Capaccioli⁵
 Ami Choi⁶
 Oliver-Mark Cordes²
 Giovanni Covone⁵
 Massimo Dall'Ora⁷
 Alastair Edge⁸
 Thomas Erben²
 Jeroen Franse¹
 Fedor Getman⁷
 Aniello Grado⁷
 Joachim Harnois-Deraps⁹
 Ewout Helmich¹
 Ricardo Herbonnet¹
 Catherine Heymans⁶
 Hendrik Hildebrandt²
 Henk Hoekstra¹
 Zhuoyi Huang⁷
 Nancy Irisarri¹
 Benjamin Joachimi¹⁰
 Fabian Köhlinger¹
 Thomas Kitching¹¹
 Francesco La Barbera⁷
 Pedro Lacerda¹²
 John McFarland³
 Lance Miller¹³
 Reiko Nakajima²
 Nicola R. Napolitano⁷
 Maurizio Paolillo⁵
 John Peacock⁶
 Berenice Pila-Diez¹
 Emanuella Puddu⁷
 Mario Radovich¹⁴
 Agatino Rifatto⁷
 Peter Schneider²
 Tim Schrabback²
 Cristobal Sifon¹
 Gert Sikkema³
 Patrick Simon²
 William Sutherland¹⁵
 Alexandru Tudorica²
 Edwin Valentijn³
 Remco van der Burg¹
 Edo van Uitert²
 Ludovic van Waerbeke⁹
 Malin Velander¹³
 Gijs Verdoes Kleijn³
 Massimo Viola¹
 Willem-Jan Vriend³

¹ Leiden Observatory, Leiden University, the Netherlands

- ² Argelander Institute for Astronomy, University of Bonn, Germany
³ OmegaCEN – University of Groningen, the Netherlands
⁴ Centre for Astrophysics & Supercomputing, Swinburne University, Hawthorn, Australia
⁵ Dept. of Physical Sciences, University Federico II, Naples, Italy
⁶ SUPA, Institute for Astronomy, University of Edinburgh, United Kingdom
⁷ INAF – Osservatorio Astronomico Capodimonte Napoli, Italy
⁸ Department of Physics, Durham University, United Kingdom
⁹ Department of Physics and Astronomy, University of British Columbia, Vancouver, Canada
¹⁰ Department of Physics and Astronomy, University College London, United Kingdom
¹¹ Mullard Space Science Laboratory, Holm-bury St Mary, Dorking, United Kingdom
¹² Queen's University Belfast, United Kingdom
¹³ Department of Physics, University of Oxford, United Kingdom
¹⁴ INAF – Osservatorio Astronomico di Padova, Italy
¹⁵ Astronomy Unit, School of Physics and Astronomy, Queen Mary University of London, United Kingdom

The Kilo-Degree Survey (KiDS), a 1500-square-degree optical imaging survey with the recently commissioned OmegaCAM wide-field imager on the VLT Survey Telescope (VST), is described. KiDS will image two fields in u -, g -, r - and i -bands and, together with the VIKING survey, produce nine-band (u - to K -band) coverage over two fields. For the foreseeable future the KiDS/VIKING combination of superb image quality with wide wavelength coverage will be unique for surveys of its size and depth. The survey has been designed to tackle some of the most fundamental questions of cosmology and galaxy formation of today. The main science driver is mapping the dark matter distribution in the Universe and putting constraints on the expansion of the Universe and the equation of state of dark energy, all through weak gravitational lensing. However, the deep and wide imaging data will facilitate a wide variety of science cases.

Survey design

KiDS is part of a long heritage of ever improving wide-field optical sky surveys, starting with the historical photographic plate surveys. The KiDS survey targets two areas of extragalactic sky, some 750 square degrees each, to

ensure that observations can be done all year. While KiDS observes in four filters (u, g, r, i), the companion VIKING project on the neighbouring Visible and Infrared Survey Telescope for Astronomy (VISTA) is already covering the same area in five near-infrared bands: z, Y, J, H and K_s . The two fields (Figure 1) are chosen to overlap with previous and ongoing galaxy redshift surveys, which means that the foreground galaxy distribution is already mapped out, and that spectral diagnostics for several 100 000 galaxies are already available. One of the central aims of KiDS is to “weigh” these galaxies systematically as function of their type and environment.

The exposure times of KiDS (see Table 1) are chosen such that the survey will reach a median galaxy redshift of 0.7. They are also well-matched to the natural exposure times for efficient VST operations, and balanced over the astro-climate conditions on Paranal (seeing and Moon phase, see Table 1) so that all bands can be observed at the same average rate. This strategy takes advantage of the Paranal queue-scheduling system, which makes it possible to use the best seeing time for deep r -band exposures, for example, and the worst seeing for u -band. After completion of the survey, repeat observations of the full area in the g filter with a minimum time difference of two years are planned, allowing proper motion measurements.

Half of the KiDS area overlaps with the Sloan Digital Sky Survey (SDSS; Abazajian et al., 2009), and, since very similar filter bands are used, the KiDS photometric calibration can be checked thoroughly. All VST observations are observed in the context of a nightly calibration plan that relies on a number of large standard star fields established as part of the OmegaCAM instrument development (Verdoes Kleijn et al., 2013). As the survey grows and information from overlapping pointings is incorporated, the overall photometric accuracy will continue to improve.

Filter	Exposure time	FWHM	Moon phase
u	900 s	< 1.1"	< 0.4
g	900 s	< 0.9"	< 0.4
r	1800 s	< 0.8"	< 0.4
i	1080 s	< 1.1"	any

Table 1. KiDS exposure times, maximum point spread function size (full width at half maximum [FWHM]) and Moon phase per filter.

Science drivers

The central science case for KiDS is mapping the matter distribution in the Universe through weak gravitational lensing and photometric

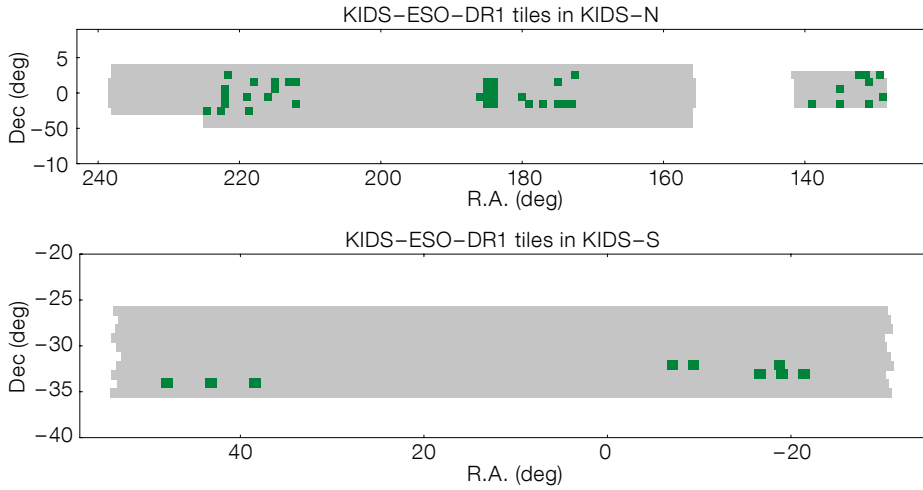


Figure 1. Layout of the two KiDS fields. The KiDS-North (upper) and KiDS-South (lower) fields are indicated in grey. Green rectangles show the pointings that are included in the first KiDS data release (KiDS-ESO-DR1).

matter haloes at large scales. At smaller scales complex baryonic physics starts to play an important role, and this is not represented realistically in current models (e.g., van Daalen et al., 2011). The relation between dark matter and baryons is crucial to our understanding of galaxy formation and evolution. Galaxy-galaxy lensing (GGL) can provide observational constraints on the relation between mass and light at scales ranging from 10 kpc to several Mpc. Since the gravitational lensing effect from single galaxies is very weak, it can only be detected statistically, by averaging over large numbers of galaxies. The size of KiDS will afford an enormous sample of galaxies, allowing the GGL effect to be studied as function of galaxy type and redshift.

Several ramifications of the current cosmological paradigm for the formation and evolution of galaxies have, until now, eluded rigorous observational testing. For example, the influence of galaxy mergers is poorly determined, and the number of known galaxy clusters at $z > 1$ is too small to constrain the models. Also here, KiDS can make an important contribution. The survey is expected to yield 10^8 galaxies with a median redshift of 0.7, and $1-2 \times 10^4$ galaxy clusters, 5% of which are at redshifts greater than 1. Since KiDS also overlaps with two nearby superclusters (Pisces-Cetus and Fornax-Eridanus), the relation between galaxy properties and environment can be studied from cluster cores to the cosmic web.

To study the stellar halo of the Milky Way, photometry of faint stars over large areas of sky is required. The SDSS proved to be a milestone in Milky Way science, unveiling many previously unknown stellar streams and faint dwarf spheroidal galaxies (e.g., Belokurov et al., 2006). Although it has a smaller footprint than SDSS, KiDS is more sensitive and will provide a view of more distant parts of the halo. Because the KiDS-S area is still uncharted at the KiDS depth, new substructures may still be uncovered.

Figure 2. Histograms showing the data quality of KiDS-ESO-DR1. Left: PSF FWHM distribution. Middle: average ellipticity distribution. Right: limiting magnitude (5σ in a 2-arcsecond aperture) distribution. In all columns the panels show from top to bottom u (blue), g (green), r (red), and i (magenta) bands respectively.

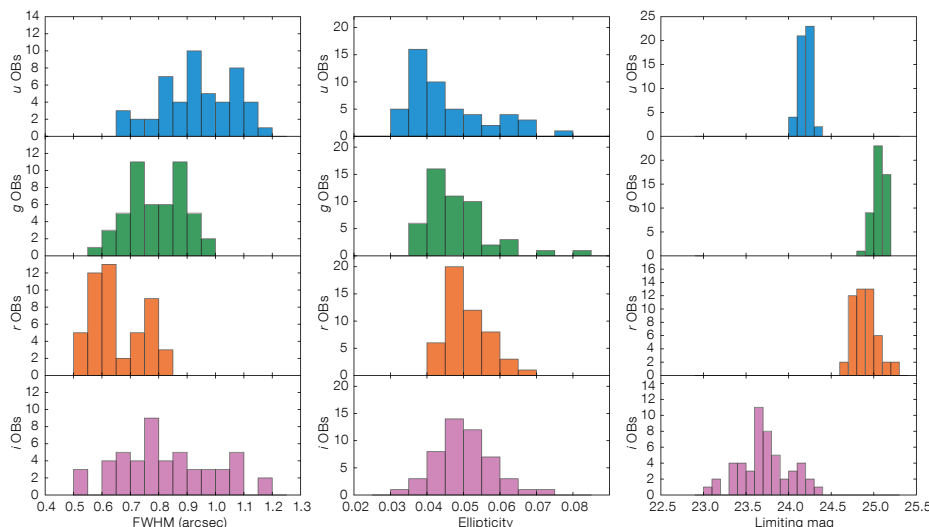
redshift measurements. The power of using weak gravitational lensing as a cosmological probe relies on two facts: it is a very geometric phenomenon; and, it is sensitive to mass inhomogeneities along the line of sight (see e.g., Peacock et al., 2006). This makes gravitational lensing both a good probe of the growth of structure with time (redshift), as well as a purely geometrical distance measure. Both the distance-redshift relation and the rate of growth of overdensities with cosmic time depend directly on the expansion history of the Universe, and thus form the most fundamental measures of the energy content of the Universe. Weak lensing is an excellent method for making such a measurement, although the requirements on the systematics of shape measurements and photometric redshifts are challenging.

With the combination of KiDS and VIKING we have put ourselves in the optimal position

to attempt this, by ensuring the best image quality in our instrument, and having a wide wavelength coverage that maximises the accuracy of the photometric redshifts. An independent measurement of the expansion history of the Universe can be made using baryon acoustic oscillations (BAO), utilising the high-precision photometric redshift measurements that will be provided by KiDS and VIKING.

However, the KiDS dataset will have many more possible applications, and the main science interests pursued by the KiDS team are briefly discussed below. Note that the primary gravitational lensing science case sets tight requirements on the astrometric and photometric calibration of the data, which is of direct benefit to other analyses as well.

Numerical simulations provide a detailed picture of the assembly and structure of dark



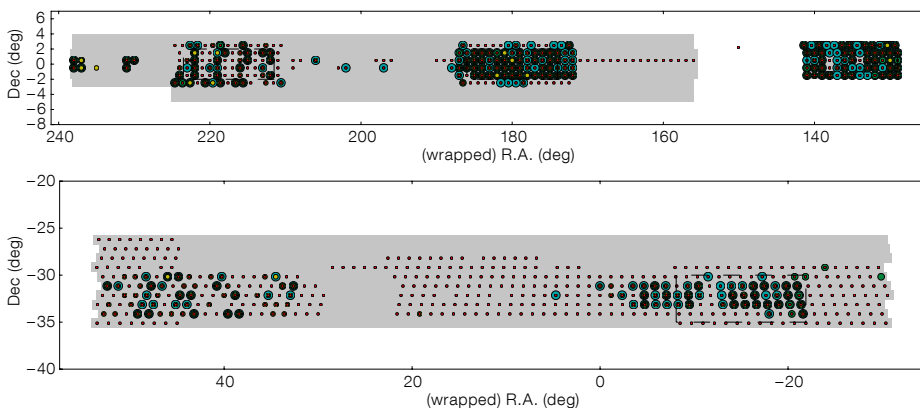
Finally, the deep, multicolour object catalogues that KiDS will produce are also ideal hunting grounds for rare objects. In particular, the combination with VIKING data is ideal for detecting high-redshift quasars (see Mieske et al. p.12 and Venemans et al., 2013), while the good optical image quality benefits the search for strongly lensed systems. When the planned repeat-pass in g -band is completed, the proper motion information will allow the identification of nearby objects, for example brown dwarfs or ultra-cool white dwarfs.

KiDS-ESO-DR1

The first public data release (DR) of the KiDS survey, dubbed KiDS-ESO-DR1, was made available through the ESO Science Archive in July 2013¹. Since colour information is important for verifying the photometric accuracy of the data, each DR will only contain pointings that have been observed in all four filters. KiDS-ESO-DR1 comprises the 50 pointings that were completed during the first year of VST operations (15 October 2011 to 1 October 2012) and the preceding Early Science Time period. For these 50 square degrees, DR1 includes the following data products: i) photometrically and astrometrically calibrated stacked images; ii) their associated weight frames; iii) masking flag maps; and iv) single-band source lists. Data products can also be accessed via the KiDS consortium's Astro-WISE information system, which allows the full data lineage to be traced. Note that since the first year of observations, the data rate has increased substantially!

Figure 2 illustrates the data quality of KiDS-ESO-DR1. The image quality (IQ) distribution, expressed as the full width at half maximum of the point spread function, reflects the seeing constraints in Table 1. In i -band this distribution is very broad, because most of the bright time with seeing < 1.1 arcseconds is used for KiDS. Designed specifically to deliver good, constant image quality over the full one square degree field of view, the VST/OmegaCAM system generally performs very well, producing images with very low point spread function (PSF) ellipticity. The limiting magnitudes (5σ measured in a 2-arcsecond aperture) obtained are around 25th mag for g and r , while u -band is 0.8 mag shallower. In i -band the limiting magnitudes span a wide range due to the larger range in sky brightness.

All data products in KiDS-ESO-DR1 have been produced by the KiDS production team, using a pipeline based on the Astro-WISE astronomical data processing system (de Jong et al., 2013; McFarland et al., 2013). The pipeline



version used for this release includes electronic crosstalk correction, satellite track removal, and illumination correction. By tying stellar photometry between the dithers and overlapping CCDs together, pointings are photometrically homogenised, resulting in photometry that is flat within typically 2% over the full field of view. Absolute photometry is based on nightly calibration field observations. Due to the scattered on-sky distribution of the observations (see Figure 1), the photometry is not homogenised over the whole survey; this will be possible for future DRs encompassing more homogeneous sky coverage.

Automated masking software, dubbed Pulecenella (Huang et al., in prep), was developed for KiDS. This software produces “flag maps” that distinguish between different types of masked areas, such as saturated pixels, readout spikes, diffraction spikes, and reflection haloes. Certain other defects, for example reflections introduced by the open structure of the telescope, have been masked as well. Another stand-alone procedure was developed to produce single-band source lists, relying on SExtractor for source detection and extraction. The source lists provided in this release include star/galaxy separation and a large set of source parameters².

Current status

Apart from continuing to prepare and process the ongoing observations in preparation for DR2 next year, the KiDS team is also engaged in scientific analysis of the data. Much of this analysis is focussed on the opportunities that the synergy of KiDS with the Galaxy and Mass Assembly (GAMA; Driver et al., 2011) project offers. The fields of the GAMA survey, a dense spectroscopic survey on the Australian Astronomical Telescope (AAT), lie inside the KiDS areas, and they have been prioritised in the KiDS observations (see Figure 3, which shows the distribution of all data in hand at the time

Figure 3. Status of KiDS observations at 1 October 2013. The grey areas correspond to the survey fields KiDS-North (upper panel) and KiDS-South (lower panel). Coloured circles indicate which data has been obtained successfully at each position in a specific filter: u = cyan, g = green, r = yellow, i = red. The GAMA spectroscopic survey fields are outlined with black dashed lines.

of writing). Combining the large-scale structure (as mapped by GAMA) with the detailed KiDS imaging of the galaxies is enabling an unprecedented study of the relation between galaxy structure, environment and, via lensing, the dark matter distribution.

To extract the cleanest possible lensing signal from the data, the team is also performing a dedicated, lensing-optimised, reduction of the data using the Bonn THELI pipeline (Erben et al., 2013) that was also used for the weak lensing analysis of the Canada France Hawaii Telescope (CFHT) Legacy Survey (e.g., Heymans et al., 2012). Initial indications are that the KiDS data are very well suited to this type of analysis.

References

- Abazajian, K. et al. 2009, ApJS, 182, 543
- Belokurov, V. et al. 2006, ApJ, 642, L137
- de Jong, J. T. A. et al. 2013, ExA, 35, 25
- Driver, S. P. et al. 2011, MNRAS, 413, 971
- Erben, T. et al. 2013, MNRAS, 433, 2545
- Heymans, C. et al. 2012, MNRAS, 427, 146
- McFarland, J. P. et al. 2013, ExA, 35, 45
- Peacock, J. A. et al. 2006, ESO/ESA Working Group Report No. 3 Fundamental Cosmology
- van Daalen, M. P. et al. 2011, MNRAS, 415, 3649
- Venemans, B. et al. 2013, ApJ, 779, 24
- Verdoes Kleijn, G. et al. 2013, ExA, 35, 103

Links

¹ Access to KiDS ESO DR1: http://archive.eso.org/wdb/wdb/adp/phase3_main/form?phase3_collection=KiDS&release_tag=1

² For more details on the KiDS-ESO-DR1 pipeline see: <http://kids.strw.leidenuniv.nl/DR1>

The Gaia–ESO Large Public Spectroscopic Survey

Sofia Randich¹
Gerry Gilmore²
on behalf of the Gaia–ESO Consortium

¹ INAF–Osservatorio Astrofisico di Arcetri, Italy

² Institute of Astronomy, University of
Cambridge, United Kingdom

The Gaia–ESO Public Spectroscopic Survey has completed about one third of the data taking and continues to acquire high-quality spectroscopy, with both Giraffe and UVES, of representative samples of all Galactic stellar populations, including open clusters — young and old, nearby and distant, interior and exterior to the Sun — and field stars in the Galactic Halo, the thick Disc, the thin Disc and the Galactic Bulge. A large sample of stars in the Solar Neighbourhood, selected to include all possible ages and metallicities, is also being observed with UVES. This will be the first such large internally homogeneous study of the Milky Way stellar populations. Besides the intrinsic range of exciting scientific results, the Gaia–ESO Survey is also a pathfinder for future massive Gaia follow-up. Equally importantly, we are building an ESO-wide community of stellar spectroscopists, sharing, optimising, refining and cross-calibrating complementary approaches, strengths and experience. Internal Science Verification has started with several results demonstrating the huge potential of the survey and the first release of spectra to ESO has occurred.

An introductory overview of the Gaia–ESO survey was presented in *Messenger* 147 (Gilmore et al., 2012). Briefly, the survey is obtaining high-quality spectra with Giraffe at several wavelength settings, depending on the stellar type, high-resolution (HR) spectra ($R \sim 20\,000$) of some 100 000 cluster and field stars down to $V = 19$, with parallel Ultraviolet and Visual Echelle Spectrograph spectra (UVES; $R \sim 47\,000$) obtained in each field for brighter stars. Data-taking began at the end of 2011, and will continue for four years until the ESO progress review. A wealth of kinematic and abundance information, along with astrophysical parameters will be obtained for the bulk of our targets, facilitating the impressive range of science foreshadowed in our earlier article.

One of the special features of the Gaia–ESO survey is that a wider range of stellar types (from O- to M-type, from pre-main sequence to evolved stars, from very low to solar and super solar metallicity) is being observed than

was attempted in previous large surveys, and that we are working at very much higher spectral resolution. These aspects make it necessary and desirable that a large consortium of groups is involved, implementing many spectrum analysis methods and approaches. The consortium has grown to nearly 400 members, from nearly 100 institutes. The survey project is structured in 19 working groups, each dedicated to the different aspects. Five of these groups focus on spectrum analysis and benefit from the contribution of several analysis teams. We communicate through our web page¹, newsletters, regular meetings and telecons, and with an actively used internal wiki.

Target selection and preparation of the observations are now in a routine phase. So far our efforts have been dominated by optimising the data reduction and radial velocity pipelines, as well as by the challenge of ensuring that all the many analysis approaches are internally consistent and that we are able to combine astrophysical parameters and abundances from many groups appropriately. None of these turn out to be trivial. For the Giraffe spectra, Jim Lewis at the Cambridge Astronomy Survey Unit (CASU) has developed a new special-purpose reduction pipeline, taking the data from “as acquired” to “ready for analysis” (Gilmore et al., 2013, in preparation). For UVES spectra we have been working closely with ESO, in particular with Andrea Modigliani, to remedy the difficulties with the reduction pipeline, which has now been successfully achieved (Sacco et al., 2013, in preparation). These substantial pipeline developments will of course benefit the entire ESO community. Considerable effort has also been invested in radial velocity pipelines and quality assessment, since precise radial velocities are critical for several of the top-level science goals.

An early lesson from working with many analysis teams was the critical need to have a well-understood, common, suitable line-list for the analyses, a common set of model atmospheres and a common grid of synthetic spectra. All of these have been made available to the analysis groups and are regularly updated thanks to the efforts of dedicated teams. Another (expected) challenge was that of combining, intelligently, astrophysical parameters and elemental abundances from many pipelines and for different types of stars. This remains work in progress, but one significant (planned) advance has been a focus on observations — largely in twilight — of the Gaia benchmark stars. This list of well-studied stars, with good coverage across parameter space, has been under development as part of the Gaia mission preparation. By combining

our efforts, much progress has been made both with optimising the Gaia benchmark star parameters, but also ensuring that Gaia and Gaia–ESO will be calibrated onto a consistent scale (c.f., Jofre et al., 2013).

Internal as well external calibration also depends heavily on observations of many stars in many clusters, both open and globular, where we also complement our observations with re-analysis of ESO archive spectra. We are also planning synergies with other large spectroscopic surveys globally (RADial Velocity Experiment [RAVE]; GALactic Archaeology with HERMES [HERMES/GALAH]; Baryon Oscillation Spectroscopic Survey/ Sloan Extension for Galactic Understanding and Exploration [BOSS/SEGUE]; Apache Point Observatory Galactic Evolution Experiment [APOGEE]) to share our calibrations and lead towards a new era of consistent stellar spectroscopic parameters. A further dataset, which is ideal for calibration, and of high scientific interest in meeting some of the original Gaia–ESO scientific goals, is the use of giant stars observed by CoRoT, for which asteroseismic gravities are available.

Making all this progress has taken some time, but Gaia–ESO is now in its first internal SV phase. A few scientific early highlights are noted below. However, our progress so far in so short a time makes us confident that this combination of European space and ground data for enhanced science is a small foretaste of what is to come when Gaia is combined with the current ESO imaging and planned spectroscopic surveys, and other complementary surveys. Each of these Gaia–ESO developments noted above is a major advance. All are currently being prepared for publication.

Early Science: Clusters

The top-level scientific goals for the cluster component of Gaia–ESO include the understanding of how clusters form, evolve and dissolve into the Milky Way field, to be obtained through the investigation of: internal cluster kinematics and dynamics; the calibration of the complex physics that affect stellar evolution; and the detailed study of the properties and evolution of the Milky Way thin Disc. With this aim, a very large sample of clusters and cluster stars will be observed, covering the age–distance–metallicity–position–density parameter space. Early focus has been put both on young, nearby regions and on intermediate–old more distant clusters, in order to start addressing all the main science topics in the Science Verification phase.

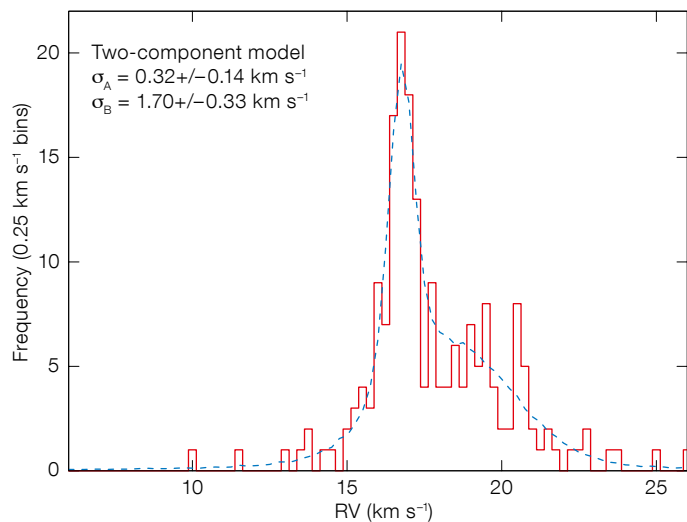


Figure 1. The radial velocity distribution of young, lithium-selected members of the γ Velorum association (red histogram), along with the best-fitting model (blue curve), consisting of two Gaussian distributions convolved with a model of the RV uncertainties and a contribution from binaries. The width of the distributions is reported in the figure.

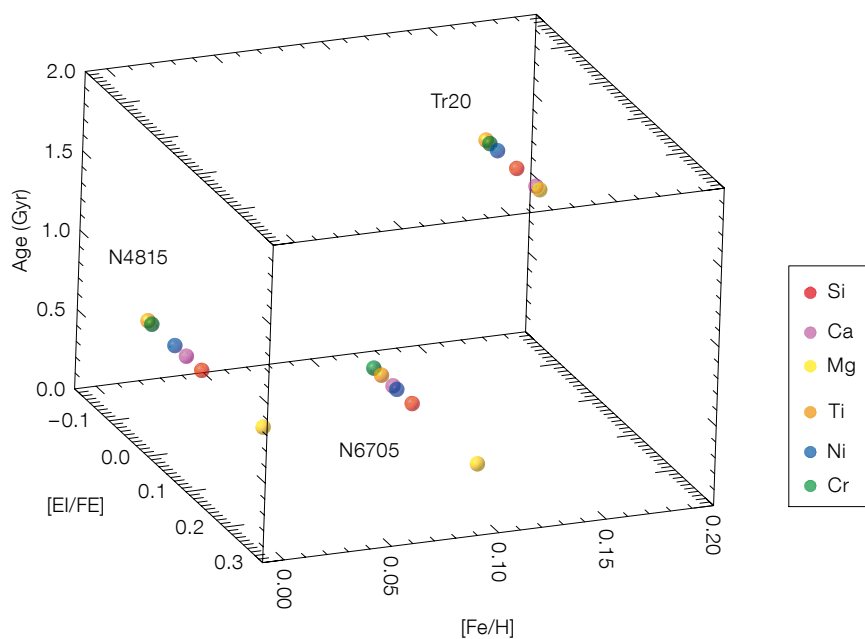


Figure 2. The three-dimensional plot shows the abundance ratios of different elements for the three open clusters NGC 6705, NGC 4815 and Trumpler 20 as a function of $[Fe/H]$ and age. The three clusters have Galactocentric distances of 6.3, 6.9 and 6.88 kpc, respectively.

One of the currently debated issues is whether young clusters are characterised by kinematic substructures and/or radial velocity gradients. In turn this question is related to the initial conditions and the mechanism of cluster formation. Gaia–ESO observations of γ Velorum, a 5–10 Myr old, nearby association, located in the very composite Vela complex, have indeed confirmed that our radial velocity (RV) measurements have high enough precision to

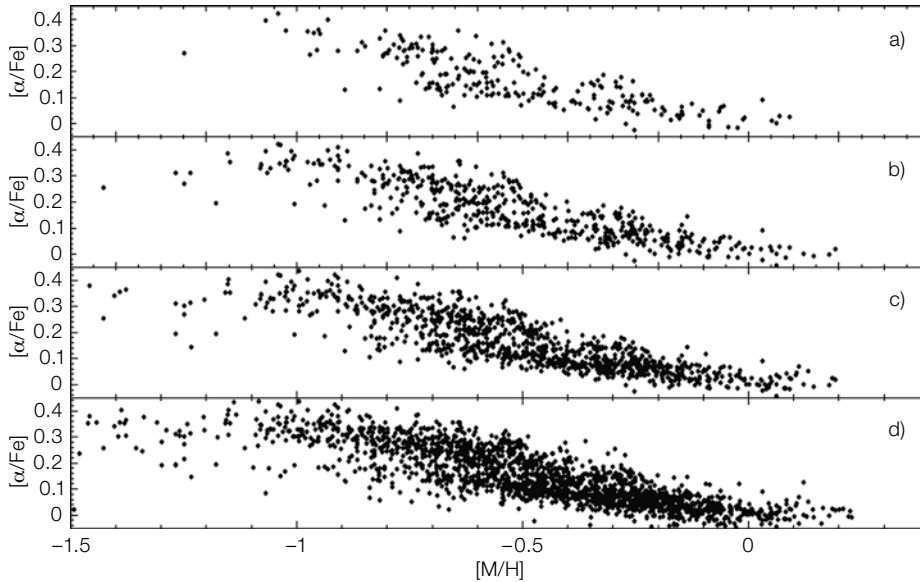
resolve velocity substructures (Jeffries et al., 2013, in preparation). Specifically, the RV distribution of members of the association plotted in Figure 1 shows that the excellent radial velocity precision ($\sim 0.3 \text{ km s}^{-1}$) of Gaia–ESO resolves the distribution into (at least) two sub-components, a very narrow one, probably in virial equilibrium, and a significantly broader and super-virial one. The narrower component appears to be more centrally concentrated around the massive binary star at the centre of the association. Interestingly, different tracers suggest that the low-mass stars are older than 10 Myr, while the massive binary cannot be as old as this. Whereas this result needs further investigation in the framework of different model predictions, on the one hand it implies

a complex star formation history in the association and, on the other hand, it proves the potential of Gaia–ESO for this type of study.

The determination of precise abundances in open clusters represents a valuable tool for the study of the formation and evolution of the thin Disc, as clusters are rare fossils of its past star formation history. Naively, one would expect that abundances of open clusters with similar ages and positions in the Galaxy are similar, and also match those of the field stars at similar distances from the Galactic Centre. However, observations are revealing differences (see, e.g., Yong et al., 2005, 2012; De Silva et al., 2007) and these differences, if confirmed, may contain important information about, e.g., the place where the clusters were born, the homogeneity of the Disc at any Galactocentric distance at the epoch when the cluster formed, etc. In this context Gaia–ESO will allow, for the first time, a comparison of different populations based on homogeneous analysis. The first three intermediate-age/old clusters observed in the survey (NGC 6705, NGC 4815, Trumpler 20) have already enabled an initial step in this direction. Figure 2 shows that each cluster is characterised by unique features with respect to the others. These differences must be signatures of the intrinsic characteristics of the chemical composition of the interstellar medium from which each cluster was born, even if at present the three clusters are located at similar distance from the Galactic Centre. Comparison with the field population, in particular with the inner Disc stars, and with models of Galactic evolution seems to support the hypothesis that at least one of these clusters has migrated from its original birthplace (Magrini et al., 2013).

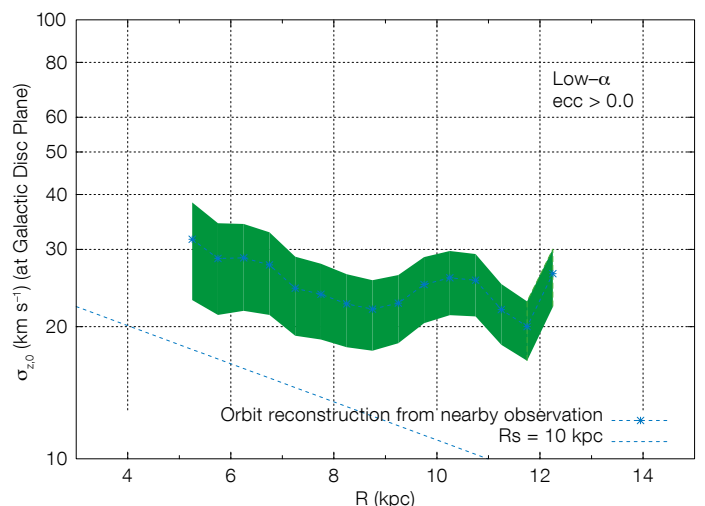
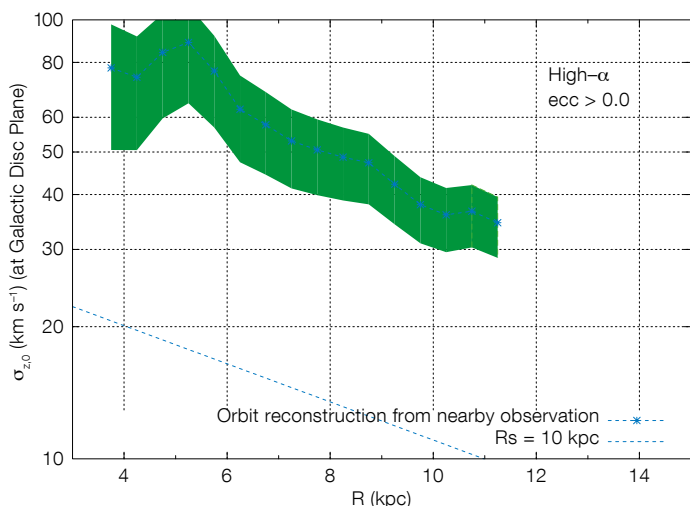
Early Science: Milky Way

The Milky Way aspects of the Gaia–ESO survey include the field star populations, and special calibration efforts. Much early focus in the Milky Way fields, driven by the available sky, was on the properties of the thick Disc. Topical issues here include the issue of discreteness between the thick and thin Disc in element ratio data at a given abundance of $[Fe/H]$. This has implications for the history of the Milky Way, strongly supporting the formation of the thick Disc as a discrete event early in the history of the Galaxy. All recent high-quality spectroscopic studies have shown such discreteness, though this result has been challenged by some analyses of very large low-precision surveys, especially SEGUE, where the claim is that the earlier surveys were highly biased. There is also much



ongoing confusion over the radial scale length of the thick Disc, with the answer being sensitively dependent on one's definition. Gaia-ESO has a well-defined selection function, and carefully avoids all the usual sample biases, so is ideally suited to provide a definitive result. The first Gaia-ESO results are shown in Figure 3, which shows $[\alpha/\text{Fe}]$ vs. $[\text{Fe}/\text{H}]$ from Giraffe spectra, with the different panels selected only by measurement error. Bimodality is indeed apparent (Recio Blanco et al., 2013). A supplementary study, led by student Kohei Hattori, uses a new dynamical analysis technique to deduce the local in-plane kinematics of stars

Figure 4. Reconstructed radial profile of $\sigma_{z,0}$ (the velocity dispersion in the z-direction at the Galactic Plane) from the Gaia-ESO survey is shown (in green) for high- α (left) and low- α (right). As a reference, the curve $\sigma_{z,0}(R) = \text{const.} \times e^{-R/(10 \text{ kpc})}$, is also shown.



far from the Sun (Figure 4). These kinematic dispersions are directly, although non-trivially, related to population scale length. This study suggests that the high- α (thick Disc) stars do merge into a thin-Disc-like vertical scale height a few kiloparsecs exterior to the Sun.

Prospects

The Gaia-ESO Large Public Spectroscopic Survey has become the first large European collaboration of stellar spectroscopists, working together to identify opportunities, strengths and limitations in the way we have approached the science challenges in stellar populations, and understanding the evolution of the Galaxy and its constituents. We are learning to work as the galaxy survey community does. This opportunity to learn and

Figure 3. α -elements over iron abundance as a function of metallicity for four different sub-samples of stars with increasing errors in the abundance determination. Panel a) shows the results for stars with errors in $[\text{M}/\text{H}]$ and $[\alpha/\text{Fe}]$ smaller than 0.07 dex and 0.03 dex respectively (209 stars); panel b) for errors smaller than 0.09 dex and 0.04 dex in $[\text{M}/\text{H}]$ and $[\alpha/\text{Fe}]$ (505 stars); panel c) illustrates the values for 1008 stars with errors smaller than 0.15 dex and 0.05 dex respectively; panel d) shows all stars with errors in T_{eff} lower than 400 K, errors in $\log g$ lower than 0.5 dex and a spectral signal-to-noise ratio higher than 15 for the HR10 configuration (1952 stars).

respect each other, building a stronger, more expert, more efficient ESO community in a key science area, is arguably one of the most important achievements of Gaia-ESO. There are immediate community-wide quantitative benefits, in data reduction pipelines, standard stars, atomic and molecular line-lists, calibrations, and so on, which are already being realised. The impressive range of scientific papers being prepared from the available SV data will soon be public, and demonstrate the substantial scientific advances being facilitated by this ESO survey.

References

De Silva, G. M. et al. 2007, AJ, 133, 1161
 Gilmore, G. et al. 2012, The Messenger, 147, 25
 Jofre, P. et al. 2013, arXiv:1309.1099
 Magrini, L. et al. 2013, A&A, submitted
 Recio-Blanco, A. et al. 2013, A&A, submitted
 Yong, D., Carney, B. W. & Teixeira de Almeida, M. L. 2005, AJ, 130, 597
 Yong, D., Carney, B. W. & Friel, E. D. 2012, AJ, 144, 95

Links

¹ Gaia-ESO Survey web page: www.gaia-eso.eu

PESSTO: The Public ESO Spectroscopic Survey of Transient Objects

Stephen J. Smartt¹
 Stefano Valentini^{2,3,4}
 Morgan Fraser^{1,5}
 Cosimo Inserra¹
 David R. Young¹
 Mark Sullivan⁶
 Stefano Benetti²
 Avishay Gal-Yam⁷
 Cristina Knapic⁸
 Marco Molinaro⁸
 Andrea Pastorello²
 Riccardo Smareglia⁸
 Ken W. Smith¹
 Stefan Taubenberger⁹
 Ofer Yaron⁷

¹ Astrophysics Research Centre, School of Mathematics and Physics, Queen's University Belfast, United Kingdom

² Osservatorio Astronomico di Padova, INAF, Italy

³ Las Cumbres Observatory Global Telescope Network, Goleta, USA

⁴ Department of Physics, University of California Santa Barbara, USA

⁵ Institute of Astronomy, University of Cambridge, United Kingdom

⁶ School of Physics and Astronomy, University of Southampton, United Kingdom

⁷ Benoziyo Center for Astrophysics, Weizmann Institute of Science, Rehovot, Israel

⁸ INAF–Osservatorio Astronomico di Trieste, Italy

⁹ Max-Planck-Institut für Astrophysik, Garching, Germany

Team members:

Joe P. Anderson¹, Christophe Balland², Charles Baltay³, Cristina Barbarino⁴, Franz E. Bauer^{5,6,7}, Sylvain Baumont², David Bersier⁸, Sebastian Bongard², Maria Teresa Botticella⁹, Filomena Bufano¹⁰, Mattia Bulla¹¹, Enrico Cappellaro¹², Flora Cellier-Holzem², Ting-Wan Chen¹¹, Michael J. Childress¹³, Alejandro Clocchiatti^{5,6}, Massimo Dall'Ora⁹, John Danziger¹⁴, Massimo DellaValle⁹, Michel Dennefeld¹⁵, Patrick El Hage², Nancy Elias-Rosa^{12,16}, Nancy Elman³, Mathilde Fleury², Elisabeth Gall¹, Santiago Gonzalez-Gaitan¹⁷, Laura Greggio¹², Ellie Hadjijyska³, Wolfgang Hillebrandt¹⁸, Simon Hodgkin¹⁹, Isobel M. Hook^{20,21}, Phil A. James⁸, Anders Jerkstrand¹¹, Erkki Kankare²², Rubina Kotak¹¹, Laurent Le Guillou², Giorgos Leloudas^{23,24}, Peter Lundqvist²³, Kate Maguire¹, Ilan Manulis²⁵, Steven J. Margheim²⁶, Seppo Mattila²², Justyn R. Maund¹¹, Paolo A. Mazzali⁸, Matt McCrum¹¹, Ryan McKinnon³, Matt Nicholl¹¹, Reynald Pain², Joe Polishaw¹¹, Maria Letizia Pumo¹², David Rabinowitz³, Emma Reilly¹¹, Cristina Romero-Cañizales^{5,6}, Richard Scalzo¹³, Brian Schmidt¹³, Steve Schulze^{5,6}, Stuart Sim¹¹, Jesper Sollerman²³, Giacomo Terreran^{11,12}, Massimo Turatto¹², Emma Walker³, Nicholas A. Walton¹⁹, Fang Yuan¹³, Luca Zampieri¹²

¹ESO, ²CNRS-IN2P3, ³Yale Univ., ⁴Sapienza Univ. Roma, ⁵PUC, ⁶Millennium Center for Supernova

Science, ⁷SSI, Boulder, ⁸Liverpool John Moores Univ. ⁹INAF – Obs. Capodimonte, ¹⁰Univ. Andrés Bello, ¹¹Queen's Univ. Belfast, ¹²INAF Obs. Padova, ¹³RSAA, ANU, ¹⁴OATS–INAF, ¹⁵IAP, ¹⁶ICE, Bellaterra, ¹⁷Univ. de Chile, ¹⁸MPA, ¹⁹IoA, Cambridge, ²⁰Univ. Oxford Astrophys., ²¹INAF – Obs. Roma, ²²FINCA, ²³Stockholm Univ., ²⁴Dark Cosmology Centre, ²⁵Weizmann Institute of Science, ²⁶Gemini

PESSTO, which began in April 2012 as one of two ESO public spectroscopic surveys, uses the EFOSC2 and SOFI instruments on the New Technology Telescope during ten nights a month for nine months of the year. Transients for PESSTO follow-up are provided by dedicated large-field 1–2-metre telescope imaging surveys. In its first year PESSTO classified 263 optical transients, publicly released the reduced spectra within 12 hours of the end of the night and identified 33 supernovae (SNe) for dedicated follow-up campaigns. Nine papers have been published or submitted on the topics of supernova progenitors, the origins of type Ia SNe, the uncertain nature of faint optical transients and superluminous supernovae, and a definitive public dataset on a most intriguing supernova, the infamous SN2009ip.

The science goal of PESSTO¹ (Smartt et al., 2013) is to extend our knowledge of unusual and rare transient events that are now challenging our understanding of the two standard explosion mechanisms which have held for several decades: core-collapse and thermonuclear. For some supernovae we are unsure whether they are thermonuclear or core collapse in origin. Supernovae in the nearby Universe ($z < 0.05$) allow critical measurements to constrain the physics, such as progenitor detections and multi-wavelength (X-ray to radio) follow-up. This offers a powerful way to probe both the explosion mechanisms and shock physics. The first important data that PESSTO takes is a classification spectrum, which gives an immediate measurement of redshift and initial supernova type. These targets are prioritised for classification if they are nearby (within about 40 Mpc, e.g., Figure 1), are discovered shortly after explosion (within a few days), are intrinsically more luminous or fainter than the bulk of the canonical supernova population, have unexplained properties (such as pre-explosion outbursts) or are fast declining supernovae. The latter are difficult to find and follow-up in detail, as all currently running optical surveys have found.

PESSTO targets and strategy

To feed PESSTO, an alliance has been made with the two major wide-field southern

hemisphere surveys that have survey strategies that produce large numbers of young targets in PESSTO's sensitivity range ($\text{mag} < 20.5$). The La Silla QUEST survey searches for supernovae over 1000 square degrees on a 1–2 day cadence, providing PESSTO with 5–10 supernova candidates per night for classification. The rapid cadence allows for young objects to be identified for immediate follow-up and this has been the major feeder survey for PESSTO to date. The SkyMapper telescope is another powerful survey which has just started sky survey operations in earnest in September 2013 and promises a harvest of targets, and accompanying multi-colour light curves. The PESSTO science teams also scour the Catalina Sky Survey public discoveries, and, recently, the Panoramic Survey Telescope and Rapid Response System (Pan-STARRS1) survey discoveries for appropriate targets. PESSTO also welcomes early alerts from amateur supernova hunters who can inform us as quickly as possible when they find southern hemisphere and equatorial targets.

A critical component of PESSTO is communicating discovery and target details from all input surveys to ~ 120 science members, allowing them to comment, prioritise and ensure that the observers at the New Technology Telescope (NTT) get rapid and reliable information for the night's work. Speed is of the essence, as delays can lead to a scientifically critical epoch being missed. We have developed the PESSTO Marshall (based on input from Palomar Transient Factory [PTF] and Pan-STARRS1 software development) which assimilates all target information, displays interactive webpages and records comments, classifications and plans in a database. The Marshall talks to the La Silla QUEST, SkyMapper and Pan-STARRS1 databases directly, shares information and also pulls in publicly posted targets from the Catalina Sky Survey and amateur International Astronomical Union (IAU) posted targets. PESSTO developed a data reduction pipeline that allows a one command full reduction and calibration of spectra within seconds of data being taken. New classification spectra are publicly released within about 12 hours after the end of the night. These spectra are accompanied by an instant announcement to the Astronomer's Telegram, reporting target details and classifications.

The PESSTO observing team is typically made up of two observers at La Silla, and one or two people acting as a support team in Europe or Chile who take over the data release and telegram posting at the end of the Chilean night. This gives an excellent opportunity for students to be trained at the telescope in



Figure 1. The PESSTO image of SN2013ej in M74 (Valenti et al., 2013), taken with EFOSC2 on the NTT. The supernova is the bright object in the bottom left corner. This nearby SN had pre-explosion images of the galaxy, allowing a direct search for the progenitor star (ESO Picture of the Week, 2 September 2013).

making real decisions, communicating with a large science team, reducing data instantly and working out how to optimise the nights observing. PESSTO observing slots are allocated a year in advance and the younger scientists in the collaboration are keen to get this invaluable experience. PESSTO members coordinate observations with other facilities, such as the VLT, the Telescopio Nazionale Galileo (TNG), the William Herschel Telescope (WHT) and a host of 1–2-metre facilities for light-curve monitoring (e.g., Liverpool Telescope, Panchromatic Robotic Optical Monitoring and Polarimetry Telescopes [PROMPT], Small and Moderate Aperture Research Telescope System [SMARTS], Las Cumbres Observatory Global Telescope [LCOGT]).

PESSTO first-year science highlights

A successful first year of PESSTO led to the identification of 33 supernovae as scientifically interesting for detailed follow-up, and work on these is either complete or in preparation by team members. The highlight of the year was the spectacular rise in luminosity of a supernova known as SN2009ip. A transient was first discovered in 2009 in NGC 7259, which turned out to be the giant outburst of a star in the luminous blue variable stage. Although it was labelled a supernova and given the IAU name, it had not catastrophically exploded, but returned to a state of restless variability during the next three years. The star was monitored frequently (Pastorello et al., 2013) before a spectacular double peaked rise to supernova-like luminosities in August and

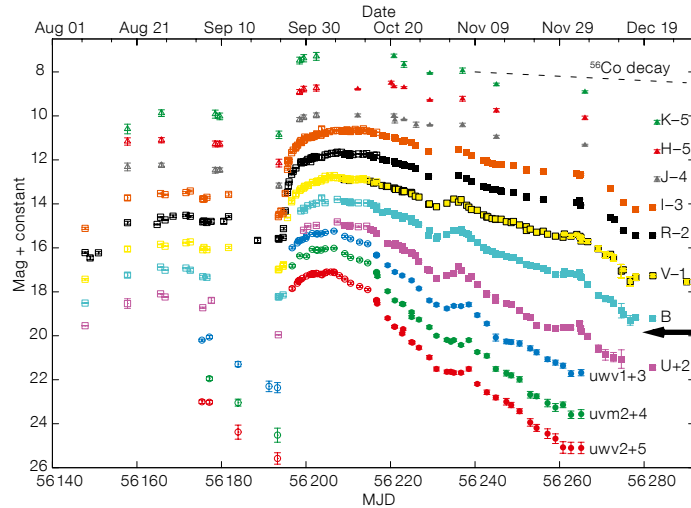
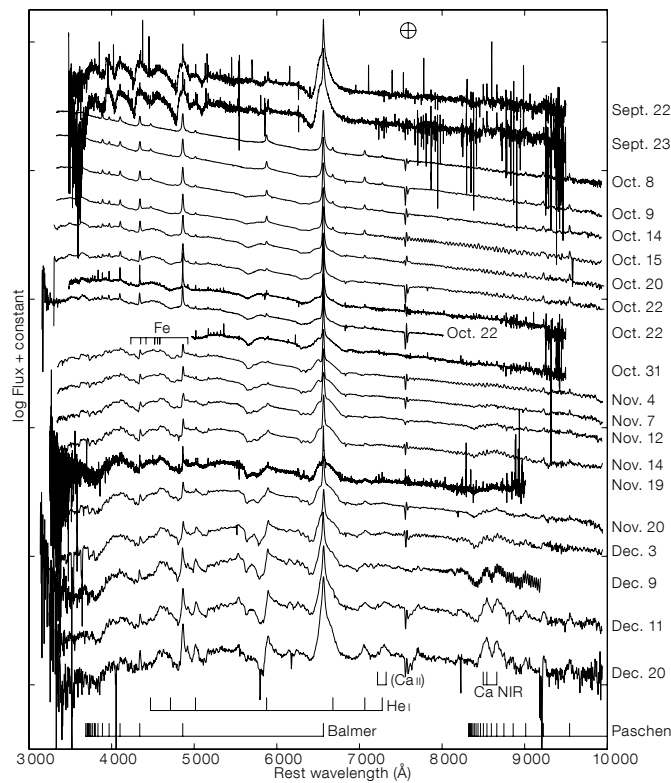


Figure 2. PESSTO light curve (upper) and spectral sequence (lower) for SN2009ip (Fraser et al., 2013), showing the initial explosion or eruption in August 2012 and rapid rise to maximum in September 2012. It is still not known if the star underwent core collapse.



September 2012 (Figure 2); it has been classified as a type “IIn” supernova, which means narrow hydrogen lines are visible. PESSTO monitored the outburst from the rise to peak until solar conjunction in 2013 and is now observing it during the second season (Fraser et al., 2013; Fraser et al., in prep).

This is the first time in history that a star has been monitored for years, photometrically and spectroscopically, before its explosion as a supernova. It is still not clear if the massive

progenitor star has actually undergone core collapse or if the observed luminosity is powered from colliding shells which were ejected by the star in eruptive phases, such as through the pulsational pair-instability process. It is certainly a “super”-nova simply from its observed luminosity and the similarity with other type IIn explosions at larger distances. This type of instability may be quite common for these events. PESSTO produced a public optical and near-infrared dataset for SN2009ip and continues to do so with the hope that the

second season data can detect (or set limits on) the nucleosynthetic products expected if core collapse occurred.

Other PESSTO highlights include a joint VLT X-shooter project for high resolution spectra of type Ia supernovae to look for interstellar absorption signatures that could shed light on the decades long progenitor system debate (Maguire et al., 2013). The detection of an excess of blue-shifted components led Maguire et al. to suggest that this is due to mass-loss signatures in the single degenerate scenario and that there are two distinct populations of normal, cosmologically useful SNe Ia. There are a growing number of supernovae for which we are struggling to explain their physical mechanisms and in many cases it is ambiguous whether or not a core collapse or thermonuclear explosion has occurred. One example is the group of faint type I supernovae, which, by definition, have no observable hydrogen or helium, but show conflicting signs of having a massive star or white dwarf origin. PESSTO studied SN2012hn, which is a faint type I supernova that lies 6 kpc from an E/SO host (Valenti et al., 2013a). There is no sign of star formation at its location, but spectra show strong oxygen, calcium and carbon lines after 150 days which are more indicative of nucleosynthesis in core-collapse supernovae (Figure 3).

Another supernova with an ambiguous origin is SN2012ca. Studies of this object, which build on previous work, show that distinguishing between the type Ia SNe and core collapse when there is interaction with circumstellar material is not easy (Inserra et al., 2013). These events are significant for determining how many physical channels could produce the cosmologically important type Ia SNe. The new class of superluminous supernovae has caught the attention of the community as the source of the luminosity is still not understood. PESSTO classified four of these in its first year at redshifts around $z = 0.2$ and the first detailed study was submitted by Benetti et al. (2013). These supernovae cannot be powered by ^{56}Ni , which is the mechanism powering normal type Ia and Ibc SNe as they decay too fast. Two models have emerged as candidates, magnetar-powered and shock breakout from a dense and extended circumstellar shell or dense wind. Future multi-wavelength observations of the nearest events are likely to be the best way to distinguish between the models. Finally PESSTO has studied very nearby (< 20 Mpc) supernovae to determine their progenitor origins through early and frequent spectroscopic monitoring combined with archive images of the progenitor explosion site (Maund et al., 2013; Childress et al., 2013; Valenti et al., 2013b).

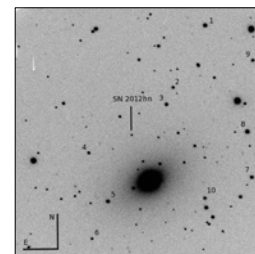
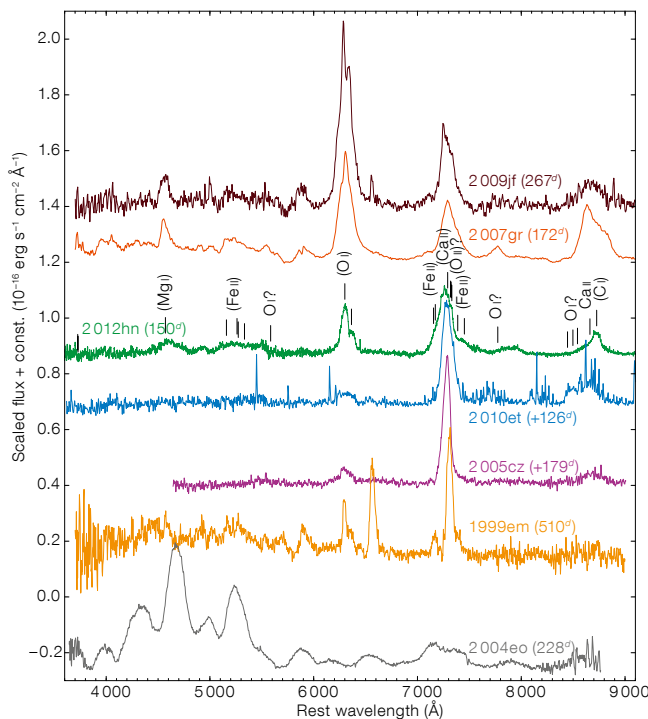


Figure 3. PESSTO image showing the position of the faint type I supernova 2012hn, at 6 kpc away from its host galaxy NGC 2272. Left: Nebular spectrum of SN2012hn (green) compared to other SNe. Prominent lines of forbidden O, Ca and Mg are visible, similar to those seen in core-collapse SNe, while the [Fe II] features typical of type Ia SNe are weak or missing; see Valenti et al. (2012a) for more details.

SSDR1 and outlook

PESSTO provides reduced classification spectra within 12–24 hours of the data being taken and releases these publicly through the Weizmann Interactive Supernova data REpository² (WiSeREP) and an Astronomer’s Telegram announcement. The final reduced data products which are now available as SSDR1 (Spectroscopic Survey Data Release 1) contain better reductions (telluric correction and fringe frame correction, more accurate flux calibration). All follow-up spectra with EFOSC2 and SOFI are available. We are also releasing all intermediate data products that may be useful to the community in the Italian Astronomical Archives (INAF IA2) in Trieste³. PESSTO releases 2D flux-calibrated and wavelength-calibrated frames as associated data products so that users can re-extract signal (either the transient or background galaxy) for objects with high levels of background contamination. In addition, all images taken with EFOSC2 and SOFI are reduced, astrometrically calibrated and photometrically calibrated (as far as the small fields will allow) within SSDR1.

On the technical side, the future outlook for PESSTO is to improve the absolute flux calibration of spectra (see Smartt et al., 2013) in SSDR2 and beyond. On the science side, PESSTO is trying to minimise the time between transient discoveries in the partner surveys and the first spectra being taken to

look for novel signatures of the explosion mechanisms that can constrain physical models and also to probe the parameter space of rapidly varying extragalactic transients. With a large spectroscopic survey sample, statistical studies of the transient population along with host galaxy properties will be possible. With all the major ESO community supernova groups on board, PESSTO has rapidly evolved into a prodigious science survey in its first year, with great promise for its future years.

References

- Benetti, S. et al. 2013, MNRAS, submitted, arXiv:1310.1311
- Childress, M. J. et al. 2013, ApJ, 770, 29
- Fraser, M. et al. 2013, MNRAS, 433, 1312
- Inserra, C. et al. 2013, MNRAS, in press, arXiv:1307.1791
- Maguire, K. et al. 2013, MNRAS, 436, 222
- Maund, J. R. et al. 2013, MNRAS, 431, 102
- Pastorello, A. et al. 2013, ApJ, 767, 1
- Smartt, S. J. et al. 2013, A&A, in prep.
- Valenti, S. et al. 2013a, MNRAS, in press, arXiv:1302.2983
- Valenti, S. et al. 2013b, MNRAS, in press, arXiv:1309.4269

Links

- ¹ PESSTO web page: <http://www.pessto.org>
- ² WiSeREP: <http://www.weizmann.ac.il/astrophysics/wiserep>
- ³ INAF IA2 data archive: <http://ia2.oats.inaf.it/>